Understanding the Lung Disposition of Inhaled Compounds using the Bronchial Epithelial Cell Culture Model Calu-3

Vijender Panduga MPharm

Thesis submitted to the University of Nottingham for the degree of Doctor of Philosophy

August 2018

Abstract

Understanding the biological processes that control pulmonary drug retention is essential for designing novel inhaled therapeutics with optimized target site exposure in the lungs. However, due to lack of suitable experimental methods drug disposition in the lungs following inhalation remains poorly characterized. Establishing human airway cell culture models for such investigations may help creating microenvironment of the lungs allowing to gain understanding of inhaled drug distribution in the lungs at a cellular and subcellular level. In this direction, the current thesis aimed at applying a physiologically relevant human bronchial epithelial cell model Calu-3, for improving understanding of the role of two biological factors, i.e., transporter proteins and lysosomal sequestration, on the pulmonary disposition of inhaled molecules.

Calu-3 cell layers grown under air-liquid interface culture conditions for 21 days were used for investigating inhaled drug uptake and permeability mechanisms. Lysosomal sequestration of inhaled molecules was assessed by measuring their cellular partition coefficient (K_p) in the presence of cytosol-lysosomal pH gradient disruptors. A cell-fractionation approach was also used for directly determining inhaled compound association with lysosomes. Lung retention following intra-tracheal administration in rats was determined for various molecules. Compound concentrations in *in vitro* and *in vivo* samples were quantified using liquid chromatography - tandem mass spectrometry.

With an objective to study the transporter-mediated cellular disposition, ipratropium bidirectional transport as well as accumulation and release studies were performed in Calu-3 layers in presence or absence of a range of transporter inhibitors. Ipratropium showed a polarized transport across Calu-3 layers with a significantly higher permeability (P_{app}) in the basolateral to apical direction than in opposite side. The presence of efficient carrier-mediated uptake and efflux mechanisms for ipratropium was evident on the apical side of the cell layers. Acting in concert, apical transporters seem to promote the ‘luminal recycling’ of the drug and due to limited flux across the basolateral side, ipratropium appeared to permeate the airway epithelium predominantly through paracellular diffusion. Thus, these results in Calu-3 layers were able

to reconcile conflicting absorption data in undifferentiated lung epithelial cells and in intact lungs previously reported for ipratropium.

Measurements of K_p in Calu-3 cells for monobasic, dibasic, quaternary and zwitterion molecules reflected their lung tissue affinity and were in agreement with unbound drug volume of distribution ($V_{u, lung}$) reported in a rat lung slice model. Further, inhaled drug uptake and permeability in Calu-3 layers following pH-gradient disruption demonstrated the role of lysosomal sequestration as a retention mechanism across the airway epithelium. Finally, the cellular disposition mechanisms of compounds investigated in Calu-3 cell model, i.e. permeability and lysosomal association successfully explained their lung retention *in vivo* in rats.

Overall, this work supports the application of the Calu-3 cell line for identifying compounds that are likely to be retained in the lung following pulmonary delivery, as an alternate to animal-based experiments. As Calu-3 model only represent cell types present in the bronchial epithelium, further studies with complex co-culture systems consisting of different cell types is advocated to simulate the complex lung physiology *in vitro* at the cellular level.

ACKNOWLEDGEMENTS

I am profoundly grateful to my supervisor, Dr Cynthia Bosquillon, for providing the opportunity to pursue my PhD studies. Her words of encouragement, enthusiasm and patience have always been great help during the time of laboratory work and writing of this thesis.

I would also like to thank Dr Michael J Stocks, for his supervision, scientific inputs and for providing novel chemical moieties synthesised in his lab along with their *in vivo* lung absorption data generated elsewhere.

I gratefully acknowledge the vice-chancellor's scholarship from the University of Nottingham. Without this support, it would have been difficult for me to undertake my PhD.

Many thanks also to my internal assessor, Dr Pavel Gershkovich for his valuable comments on my work which helped to improve and extend my research ideas. I am very thankful to Dr Catherine Ortori and Dr Sarmad Sarir for their assistance during LC-MS/MS method development and analysis.

I would like to express my gratitude to Ms Erhel Bodiou for her support towards validating Calu-3 model for the purpose of lysosomal sequestration studies. I also greatly appreciate Mr Ali Alazzo for his help with investigations using confocal microscopy. I also thank current and previous members of the cell culture lab, Dr Richard Argent, Dr Almulathanon Ammar, Dr Emanuela Cingolani, Dr Robert Cavanagh, Dr Rosa Catania, Elhuni Ibteisam, and Alali Muqdam for their friendship and support provided over the period of my PhD studies.

My sincere thanks to Dr Richard Weaver, director, XenoGesis Ltd and Dr Manfred Ismair, chief scientific officer, XenoGesis Ltd, for their participation in scientific discussions. I am deeply grateful to Rina Mistry, research scientist, XenoGesis Ltd, for her bioanalytical support for *in vivo* lung absorption studies.

A very special thanks to my wife Sravanthi Bellamgari, who made this possible for me through constant support, sacrifices and encouragement. Finally, I would like to dedicate this thesis to the memory of my mother, Suguna Panduga and my grandmother, Rambai Nerella who played an immense role in my life.

1. INTRODUCTION 1
1.1. Lung anatomy and physiology 4
1.2. Factors affecting the disposition of inhaled therapeutics in the lungs .. 6
1.2.1. Non-absorptive clearance mechanisms 6
1.2.1.1. Mucocliliary clearance 6
1.2.1.2. Metabolism 6
1.2.2. Absorptive clearance mechanisms 7
1.2.3. Physicochemical properties of molecules 8
1.2.4. Tissue binding and intracellular sequestration 9
1.2.5. Drug transporters 10
1.2.5.1. ABC transporter family 11
1.2.5.2. SLC transporter family 13
1.3. Experimental methods for studying the disposition of inhaled drugs in the lungs 18
1.3.1. *In vivo* whole animal models 18
1.3.2. *Ex vivo* models 20
1.3.3. *In vitro* models 22
1.3.3.1. Precision-cut Lung Slice Model 22
1.3.3.2. Cell culture models 22
1.3.3.3. 16HBE14o- 23
1.3.3.4. Calu-3 24
1.3.4. Other strategies for an improved understanding of inhaled drug disposition in the lungs 25
1.3.4.1. Imaging techniques 25
1.3.4.2. Transfected cell lines 27
1.3.4.3. Knockout models 27
1.4. Summary 29
1.5. Aims and Objectives of this PhD 29
2. MATERIALS AND METHODS 31
2.1. Materials 31
2.2. Methods 35
2.2.1. Cell culture 35
2.2.2. Trans-epithelial electrical resistance (TEER) measurements 36
2.2.3. Drug transport studies 36
2.2.4. Drug uptake studies 38

2.2.5. Drug release studies 38
2.2.6. Bioanalysis 39
2.2.6.1. *In vitro* study samples 39
2.2.6.2. *In vivo* study samples 39
2.2.7. Lysosomal sequestration studies 40
2.2.7.1. Confocal microscopy 40
2.2.7.2. Quantitation of LysoTracker™ Green accumulation in Calu-3 cells 41
2.2.8. Cellular partition coefficient (K_p) 42
2.2.9. Isolation of lysosomes from Calu-3 cells and quantification of lysosome associated concentrations 43
2.2.10. Unbound fraction of compounds in Calu-3 cell lysates 45
2.2.11. Lung retention of compounds, *in vivo* 45
2.2.12. Cytotoxicity assessment 46
2.2.13. Total protein quantitation 46
2.2.14. Statistical analysis 47
3. CELLULAR DISPOSITION OF ANTICHOLINERGIC BRONCHODILATORS - ROLE OF DRUG TRANSPORTERS 48
3.1. Introduction 48
3.2. Aims 50
3.3. Results 51
3.3.1. Barrier properties of Calu-3 layers 51
3.3.2. Drug transport studies 54
3.3.3. Uptake studies 59
3.3.4. Drug release studies 61
3.3.5. Effect of organic cations on FITC-dextran permeability 63
3.4. Discussion 64
3.5. Conclusion 70
4. APPLICATION OF CALU-3 CELLS FOR LYSOSOMAL SEQUESTRATION STUDIES 71
4.1. Introduction 71
4.2. Aims 73
4.3. Results 74
4.3.1. Suitability of Calu-3 cells for lysosomal sequestration studies – Confocal microscopy 74
4.3.2. Quantification of LTG sequestration in Calu-3 cells 77
4.3.2.1. Optimisation of LTG concentration and incubation time 77

4.3.2.2.Effect of cytosol-lysosomal pH gradient disruptors on LTG accumulation 78
4.3.2.3.Effect of various compounds on LTG accumulation 80
4.3.3. Isolation of lysosomes from Calu-3 cells 83
4.4. Discussion 86
4.5. Conclusion 89
5. UNDERSTANDING THE ROLE OF LYSOSOMAL SEQUESTRATION IN THE CELLULAR DISPOSITION OF INHALED COMPOUNDS. 90
5.1. Introduction 90
5.2. Aims 92
5.3. Results 93
5.3.1. Cellular partition coefficient (K_p) 93
5.3.2. Unbound fraction of compounds in Calu-3 cell lysate 97
5.3.3. Quantification of lysosomal associated compound concentrations ... 98
5.3.4. Cellular retention and permeability of compounds in Calu-3 layers. 101
5.3.5. Effect of bafilomycin A1 on cellular retention and permeability of compounds in Calu-3 layers 101
5.3.5.1.Effect of bafilomycin A1 in the absorptive direction 102
5.3.5.2.Effect of bafilomycin A1 in the secretion direction 103
5.3.5.3.Effect of bafilomycin A1 on the efflux ratio of various molecules.... 104
5.3.6. Influence of structural modification on intracellular accumulation, permeability and lung retention 108
5.4. Discussion 114
5.5. Conclusion 118
6. GENERAL DISCUSSION 120
6.1. Conclusions 123

Appendix A. Chromatographic conditions, calibration curve range and lower limit of quantitation (LLOQ) for various compounds 124

Appendix B. Effect of various compounds on Calu-3 cell viability. 125

Appendix C. Calibration curve generated using known concentrations of bovine serum albumin for determining the total protein concentrations of cell lysates collected from inserts of a 12-well Transwells® plate and 24-well tissue culture plate. 126

Appendix D. Multiple reaction monitoring (MRM) transitions, cone voltage and collision energy for all the compounds 127

Appendix E. Representative calibration curve of formoterol 128

Appendix F. Representative calibration curve of DS81 128

Appendix G. Representative calibration curve of indacaterol 129

Appendix H. Representative calibration curve of imipramine 129

Appendix I. Representative calibration curve of ipratropium 130

Appendix J. Representative calibration curve of salmeterol 130

Appendix K. Representative calibration curve of DS12 131

Appendix L. Representative calibration curve of DS13 131

Appendix M. Representative calibration curve of DS86 132

Appendix N. Representative calibration curve of tiotropium 132

Appendix O. Representative calibration curve of glycopyrronium 133

Appendix P. Representative calibration curve of salbutamol 133

Appendix Q. Stability of compounds in Hank's balanced salt solution (pH 7.4) following storage in a freezer (- 20^{o}C) for 7 days. 134

Appendix R. Expression of OCT\OCTN transporter genes in Calu-3 cells assessed using semi-quantitative PCR 134

References 135

PAPERS DISCUSSED

This thesis is based on the following papers,

1. Panduga V, Stocks MJ, Bosquillon C. Ipratropium is 'luminally recycled' by an inter-play between apical uptake and efflux transporters in Calu-3 bronchial epithelial cell layers. Int J Pharm. 532: 328-336, (2017).
2. Panduga V, Erhel Bodiou, Richard Weaver, Stocks MJ, Bosquillon C. Cellular and subcellular distribution in bronchial epithelial cells influence the lung retention properties of inhaled drugs. (Manuscript under preparation)

LIST OF TABLES

Table 2-1. Chemical structures, molecular weight, predicted LogP (cLogP) and pKa (cpKa) for various compounds 32

Table 5-1. Effect of bafilomycin A1 on the efflux ratio of inhaled compounds in Calu-3 layers 112

Table 5-2. Coefficient of apparent permeability (P_{app}) across Calu-3 layers, lysosomal accumulation and lung absorption half-lives in rats for DS12, DS13, DS81 and DS86. 113

LIST OF FIGURES

Figure 1-1. Inhalational drug delivery for local or systemic effects 4

Figure 1-2. Schematic representation of cell types across the airway epithelium 5

Figure 1-3. Factors influencing the fate of inhaled particles in both central and peripheral airways 8

Figure 1-4. Mechanisms of inhaled drug absorption across the airway epithelial membrane 10

Figure 1-5. Predicted secondary structure for organic cation transporter 1 (OCT1) 15

Figure 3-1. TEER profiles for Calu-3 layers 52

Figure 3-2. Permeability characteristics of paracellular (FITC-dextran) and transcellular (metaprolol) markers across Calu-3 layers 53

Figure 3-3. Permeability of anticholinergic bronchodilators across Calu-3 layers. 55

Figure 3-4. Concentration-dependent permeability of ipratropium across Calu-3 layers. 56

Figure 3-5. Effect of various transporter inhibitors on the permeability of ipratropium across the Calu-3 layers. 58

Figure 3-6. Uptake of ipratropium across the Calu-3 layers. 60

Figure 3-7. Release of pre-loaded ipratropium from Calu-3 layers. 62

Figure 3-8. Permeability of FITC-Dextran across Calu-3 layers in presence of various organic cations 63

Figure 3-9. Schematic representation of ‘luminal recycling’ of inhaled organic cation, ipratropium involving various transporter proteins. 67

Figure 4-1. Confocal microscopic images of Calu-3 cells treated with LysoTracker™ Green. 75

Figure 4-2. Confocal microscopic images of Calu-3 cells treated with LysoTracker™ Green in presence of various inhaled compounds 76

Figure 4-3. Time and concentration-dependent accumulation of LysoTracker™ Green (LTG) in Calu-3 cell. 77

Figure 4-4. LysoTracker™ Green accumulation in Calu-3 cells under various incubation conditions. 79

Figure 4-5. LysoTracker™ Green (LTG) accumulation in Calu-3 cells in the presence of compounds representing various chemical classes 81

Figure 4-6. LysoTracker™ Green accumulation in Calu-3 cells in the presence of various inhaled compounds representing various chemical classes. 82

Figure 4-7. Recovery of acid phosphatase activity in various supernatant fractions following ultracentrifugation of cell lysate. 84

Figure 4-8. Imipramine concentrations associated with lysosomes 85

Figure 5-1 Cellular partition coefficient (K_p) of various compounds in Calu-3 cells. 95

Figure 5-2. Cellular partition coefficient (K_p) for compounds in Calu-3 cells in the presence of cytosol-lysosomal pH gradient disruptors. 96

Figure 5-3. Relationship between cLogP and unbound fraction (f_u) of compounds in Calu-3 cell homogenate 98

Figure 5-4. Lysosomal associated concentrations of various compounds. 100

Figure 5-5. TEER values across Calu-3 layers following their incubations with HBSS alone (control) or HBSS containing bafilomycin A1. 102

Figure 5-6. Cellular retention of various compounds in Calu-3 layers in the presence or absence of bafilomycin A1 (Bfm A1). 105

Figure 5-7. Permeability of various compounds in Calu-3 layers in the presence or absence of bafilomycin A1 (Bfm A1). 106

Figure 5-8. Fold-change in the permeability of inhaled compounds across Calu-3 cell layers in the presence of bafilomycin A1. 107

Figure 5-9. Comparative cellular partition coefficient (K_p) of basic (DS12 & DS81) and their quaternary pairs (DS13 & DS86) in Calu-3 cells. 110

Figure 5-10. Percentage of administered dose remaining in the lungs at various time points for various novel compounds in male SD rats following intratracheal administration. 111

LIST OF ABBREVIATIONS

A-B	apical to basolateral
ABC	ATP binding cassette
ALI	air-liquid interface
ATP	adenosine-5’-triphosphate
B-A	basolateral to apical
BCRP	breast cancer resistance protein
BSA	bovine serum albumin
COPD	chronic obstructive pulmonary disease
DMEM	Dulbecco’s modified Eagle’s medium
DMSO	dimethyl sulphoxide
FBS	fetal bovine serum
FITC	fluorescein isothiocyanate
HBSS	Hank’s balanced salt solution
HEK	human embryonic kidney
HPLC	high-performance liquid chromatography
LC-MS/MS	liquid chromatography – tandem mass spectrometry
MDCK	Madin-Darby Canine Kidney
MDR	multi drug resistant protein
MRP	multi drug resistance associated protein
OAT	organic anion transporter
OATP	organic anion transporting polypeptide
OCT	organic cation transporter
OCTN	organic cation/carnitine transporter
P_{app}	apparent permeability

PBS	phosphate buffered saline
PCR	polymerase chain reaction
P-gp	p-glycoprotein
qPCR	quantitative polymerase chain reaction (real-time PCR)
SLC	solute linked carrier
TEER	transepithelial electrical resistance
Triton X-100	t-ocylphenoxypolyethoxyethanol

Chapter One

1. Introduction

Inhaling medicines has been practiced for more than 3500 years for treating respiratory ailments based on the concept of 'local drug delivery for local action' (Hickey 2013; Stein and Thiel 2017). Successful management of various respiratory diseases such as asthma, chronic obstructive lung disease (COPD), cystic fibrosis and lung infections through inhalation demonstrates its ability to deliver drug molecules directly to the site of action (Hickey 2013). Also, advances in inhalational formulation and drug delivery technologies facilitate delivering complex molecules, beyond lungs for diseases affecting the heart (pulmonary arterial hypertension, PAH), the brain (Parkinson's, migraine and epilepsy) and diabetes mellitus (Figure 1-1) (de Kruijf and Ehrhardt 2017).

For locally acting drugs, inhalation results in better therapeutic indices through achieving higher local lung tissue concentrations with lower systemic exposure (Backman et al. 2014). However, as respiratory diseases continue to be one of the leading causes of morality worldwide, a tremendous opportunity for developing novel and disease modifying therapeutics exists (Barnes et al. 2015). For instance, currently used therapeutics for COPD could not halt the progression of the disease; inhaled corticosteroids are effective only in managing mild-moderate asthma and there exists a severe unmet medical need for novel therapeutics for treating corticosteroid-insensitive inflammation in patients with severe asthma. Furthermore, there is a great need for designing inhaled anti-infective agents for viral, bacterial and fungal infections of the lungs, with suitable properties for achieving high lung retention (Strong et al. 2018).

In contrast to the increasing medical need, the development of innovative inhaled therapies for respiratory diseases is inadequate and suffers from a higher attrition rate in comparison to other delivery routes (Barnes et al. 2015). One of the barriers for developing inhaled therapeutics is hypothesised to be

the lack of understanding of drug distribution in the lungs following their deposition in airways (Backstrom et al. 2018). While excellent progress has been made with respect to inhalational devices and formulations for effective drug delivery, consequent interaction of inhaled therapeutics with luminal components of the lungs is poorly understood (Ehrhardt 2017). This is primarily due to a lack of suitable experimental methods which allow delineating the various mechanisms of lung disposition. For instance, the traditional inhalational drug development process consists of various pre-clinical and clinical investigations with a major focus on ensuring safety and efficacy of investigational molecules (Backman et al. 2017). Drug concentrations available for pharmacological action in the lungs is determined by various factors such as dissolution in lung fluids, mucociliary clearance, absorptive clearance into the systemic circulation, interaction with transporter proteins, and affinity for lung tissues such as non-specific binding and sequestration in sub-cellular organelles (Cooper, Ferguson, and Grime 2012). However, as lung disposition of inhaled therapeutics has historically been characterised based on total lung concentrations or their appearance in the blood circulation, the fate of drug molecules within the lung tissues and the effect of molecular properties on cellular disposition in airways remain elusive (Cooper, Ferguson, and Grime 2012). Optimising compound properties for high lung retention without understanding local drug distribution at the target site could lead to a lack of efficacy (Perry et al. 2017).

Drug exposure at the target site in quantities sufficient for eliciting a pharmacological activity for a desired period of time is one of the essential requirements for the successful development of drug molecules. Various research strategies such as the ‘Three Pillars of Survival’ and ‘5R frame work’ included ‘establishing target site exposure’ as one of the key determinants in decision making for progression of molecules. In cases where measuring drug exposure at the target site is not feasible for practical and ethical reasons and the target site is separated by physiological barriers such as the blood-air barrier, it is essential to demonstrate the ability of therapeutics to cross these barriers (Cook et al. 2014; Morgan et al. 2018; Morgan et al. 2012). Also studying drug distribution and disposition at the cellular level is essential for

understanding how drug molecules reach their target site. In addition, various mechanisms affecting target site exposure is considered highly valuable as this information could facilitate designing novel molecules with better and optimised exposure (Hann and Simpson 2014).

In vitro epithelial cell models have been recognised as valuable tools for modelling biological barriers and allow, as opposed to *in vivo* models, investigating the role of molecular mechanisms affecting drug disposition in a less complex environment (Schneider et al. 2013). In contrast to the area of oral drug delivery where human epithelial colorectal adenocarcinoma cell line, Caco-2 is considered as a gold standard for studying drug absorption, no *in vitro* airway epithelial model has been agreed upon as a standard model for inhalational drug disposition studies (Ehrhardt 2017). As the airway epithelium is considered to be the primary barrier for the absorption of inhaled molecules, various airway cell cultures models are in place for characterising their permeability (Forbes et al. 2015). The use of specialised cell culture inserts such as Transwells® allows to mimic the *in vivo* physiological situation, such as air-liquid interface (ALI) for pulmonary models, where cells remain submerged in cell culture medium basally while being exposed to the atmosphere, apically (Marshall et al. 2015; Sakolish et al. 2016). For instance under such conditions, Calu-3, a bronchial adenocarcinoma cell line resembled the bronchial epithelium in terms of cell structure, secretory and barrier properties (Grainger et al. 2006). However, these models have predominantly been applied for studying the absorptive clearance of inhaled molecules and for establishing *in vitro* to *in vivo* correlations (Forbes et al. 2015; Mathia et al. 2002). Their suitability for studying non-specific binding, transporter-mediated uptake and lysosomal sequestration as lung tissue retention mechanisms has not yet been reported and various investigations presented here are aimed in that direction. These efforts are in the spirit of the 3R (replace, refine and reduce) principle and validation of human airway *in vitro* model for lung disposition studies would allow reductions in the labour intensive animal experiments and avoid interspecies differences.

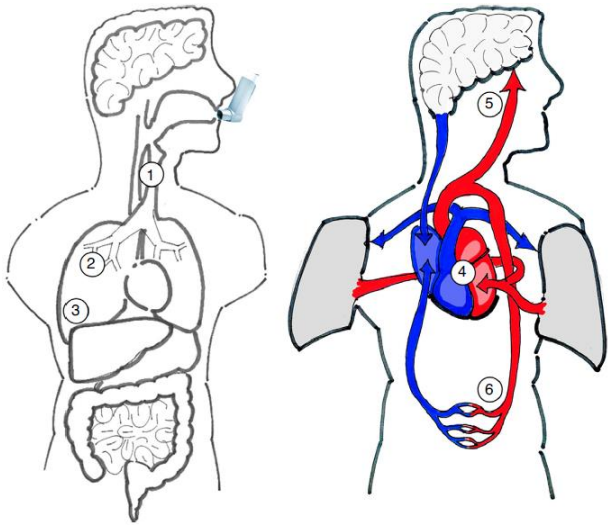


Figure 1-1. Inhalational drug delivery for local or systemic effects

Inhalation is well-established for delivering therapeutic molecules across the airways for local lung diseases (1, 2 and 3) such as asthma, COPD and inflammation. Large surface area of the airways and low drug metabolising enzymes facilitate delivering small and large molecules through inhalation to major organs such as brain and heart and for the management of various systemic conditions such as diabetes (4, 5 and 6). Image taken from de Kruijf and Ehrhardt, 2017 with permission from the publisher.

1.1. Lung anatomy and physiology

The human respiratory system is characterised by an inverted tree structure, in which airways repeatedly bifurcates for about 23 times between the trachea and the alveolar sacs, and is situated within the space of the chest cavity (Hastedt et al. 2016). The respiratory tract is broadly divided into two components: the conducting and respiratory zones, according to their functional role. The conducting airways, represented by the trachea, bronchi, bronchioles and terminal bronchioles, are responsible for the conditioning of inspired air (Liu et al. 2013). The respiratory bronchioles, alveolar ducts and alveolar sacs constitute the respiratory zone, where oxygenation of blood takes place with the removal of carbon dioxide. The alveolar region and respiratory bronchioles receive the entire cardiac output through the pulmonary circulation, while the systemic circulation supplies blood to larger airways which receive only 1% of the cardiac output (Upton and Doolette 1999).

The composition of airway epithelia across the respiratory tract show regional differences in terms of cell type, structure and functional role (Figure 1-2) (Klein et al. 2011). For instance, the epithelium of conducting airways consists of

various metabolically active cells which are covered with a thick (>50 µm) mucus layer while the alveolar epithelium forms a very thin (< 1 µm) barrier between the alveolus and blood circulation (Darquenne et al. 2016). Based on their ultrastructural, functional and biochemical properties, airway epithelial cells could be categorised as of a basal, ciliary or secretory type (Knight and Holgate 2003).

With ~ 300 cilia/cell, ciliated epithelial cells are the major cell type of the tracheal region and represent 50% of airway epithelial cells (de Souza Carvalho, Daum, and Lehr 2014; Klein et al. 2011). Goblet or mucous cells are responsible for secreting a sufficient amount of mucus with optimal viscoelasticity properties. Basal cells are present throughout the airway epithelium and the number of basal cells decrease with airway size. Basal cells are considered to play an important role in generating mucous and ciliary cells of the airway epithelium (Knight and Holgate 2003). Cellular components of the alveolar region include, type-I cells, type-II cells and macrophages. Type-I cells are flat and thin which occupy ~ 90% of the alveolar region and are responsible for gas exchanges, while type-II cells are involved in the secretion of pulmonary surfactant (de Souza Carvalho, Daum, and Lehr 2014).

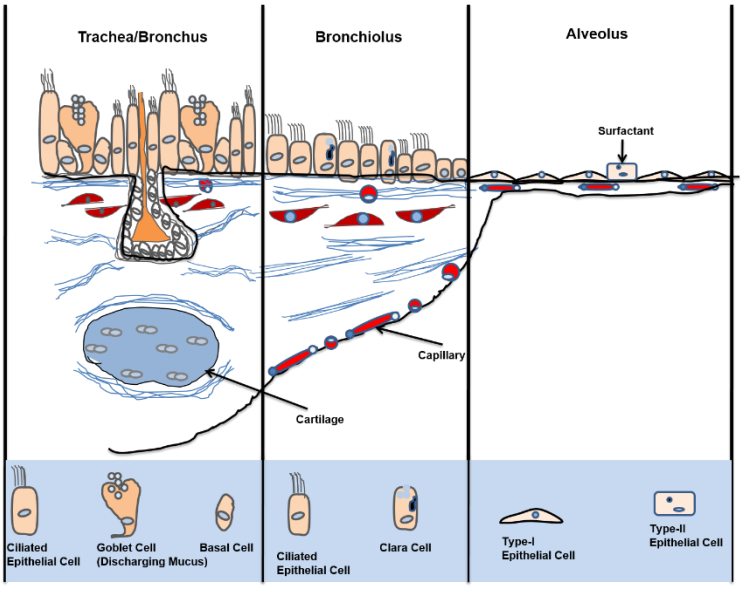


Figure 1-2. Schematic representation of cell types across the airway epithelium

The airway epithelial layer shows region specific cell types and changes from a pseudostratified layer in the bronchial region to cuboidal cells in the

bronchiolus and finally to a thin squamous epithelium in the alveolus. Image taken from Klein et al. 2011 with permission from the publisher.

1.2. Factors affecting the disposition of inhaled therapeutics in the lungs

Handheld devices such as pressurised metered-dose inhaler (pMDI), dry powder inhaler (DPI) or soft mist nebulizer are used for delivering a fixed dose of drug to the airways. Inhaled particles, depending on the location of their deposition in airways, are subjected to various non-absorptive and absorptive clearance mechanisms (Backman et al. 2014; Ruge, Kirch, and Lehr 2013).

1.2.1. Non-absorptive clearance mechanisms

1.2.1.1. Mucocliliary clearance

The conducting region of the respiratory tract acts as a physical defence system, in which repeated branching of airways form a ‘sifting zone’ where the large particles (> 10 µm in size) are captured due to impaction. Together with cilia, the mucus secreted by the submucosal glands and goblet cells of the upper and lower airways constitute the mucociliary clearance mechanism (Figure 1-3) (Ruge, Kirch, and Lehr 2013). Mucus is responsible for trapping or absorbing particulates or gases, respectively. Cilia with a beating frequency of 1,000 to 1,500 cycles/minute move the particulate containing mucus towards pharynx for swallowing or expectoration (Hastedt et al. 2016).

As a result of the mucociliary clearance mechanism, most of the particles deposited in the trachea and/or the initial bronchial region of the respiratory tract are cleared with a half-life of 30 minutes. However, clearance half-lives for particles deposited in the deeper airways range in hours, where the mucociliary mechanism is absent. Those particulates which enter the alveolar region of airways, after escaping the first line of defence, will be subjected to cellular defence mechanisms mediated by alveolar macrophages(Harada and Repine 1985).

1.2.1.2. Metabolism

Drug metabolising enzyme belonging to CYP1, CYP2 and CYP3 families are responsible for Phase I reactions which increases the hydrophilicity of

xenobiotics by introducing various functional groups. These reactions are in general followed by Phase II metabolic reactions facilitating conjugation with glucuronic acid, glutathione, acetylation, methylation or sulfation. CYP enzymes are considered to provide an additional line of defence and contribute towards non-absorptive clearance, through detoxification of inhaled xenobiotics (Bo Olsson 2011; Somers et al. 2007). Most common CYP isoforms expressed in the lung include CYP1B1, CYP2B6, CYP2E1, CYP3A5 and CYP1A1 (Ding and Kaminsky 2003). In comparison with CYP enzymes, less information is available regarding phase II enzymes in the lungs. The lungs were found to show similar expression and activity of sulfotransferases as that of the liver, while an intermediate activity was detected for esterases and epoxide hydrolases (Somers et al. 2007).

Various lung diseases such as lung cancer and COPD are associated with exposure to inhalational toxicants, including tobacco smoke. Catalytic enzymes belonging to CYP families could activate and enhance the deleterious effect of these inhalational toxicants (Hukkanen et al. 2002). However, comparatively lower levels of CYP enzymes are found to be expressed in the lungs than in the liver and intestine (Bo Olsson 2011; Somers et al. 2007). The low metabolic activity in the lungs is reflected by a rapid and complete absorption of small molecules following their administration into the lungs (Brown and Schanker 1983; Patton 1996; Tronde, Norden, Jeppsson, et al. 2003). It is also utilised for a pro-drug approach as demonstrated in the case of ciclesonide and beclomethasone dipropionate. Inhalation of these pro-drugs is followed by a slow release of their corresponding active form in the lungs leading to an extension of their duration of action (Mukker, Singh, and Derendorf 2016; van den Brink et al. 2008). The differences in the metabolic activity between the lungs and the systemic circulation has also been targeted for achieving higher concentrations in the lung with minimal blood exposure (Bo Olsson 2011).

1.2.2. Absorptive clearance mechanisms

Inhaled particles interact with various lung luminal components including the surfactant layer, the epithelial lining fluid, the epithelium and its basement, the

interstitium and the endothelium. Of all these, the epithelial cell membrane is considered to pose a significant barrier for the permeation of molecules across the air-blood barrier (Bo Olsson 2011). The permeability characteristics of inhaled compounds across the airway epithelium determine their rate of disappearance from the lungs through absorptive clearance (Backman et al. 2017). Rapid absorption into the systemic circulation may subject inhaled molecules to a quicker elimination through kidneys and liver, shortening their duration of local or systemic pharmacological action (Patton and Byron 2007). Understanding the various factors affecting drug absorption across the lung epithelium may aid in designing molecules with longer lung retention and hence extend their duration of action.

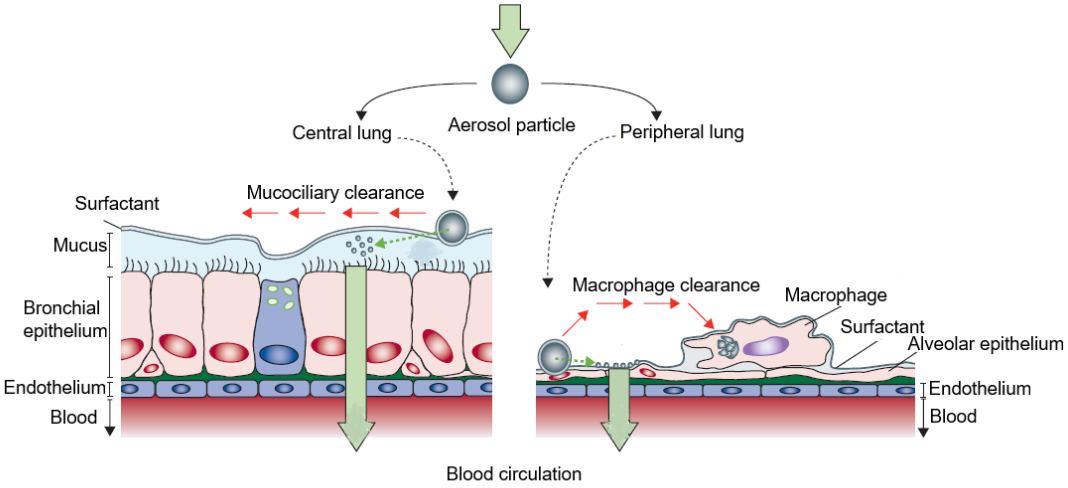


Figure 1-3. Factors influencing the fate of inhaled particles in both central and peripheral airways

Following deposition, aerosol particles come in contact with airway fluids and get dissolved. Depending on their physicochemical properties, molecules get absorbed into the systemic circulation. Undissolved aerosol particles may be subjected to either mucociliary or macrophage clearance. Image taken from Ruge, Kirch, and Lehr 2013 with permission from the publisher.

1.2.3. Physicochemical properties of molecules

Respiratory drugs are characterised by their lower lipophilicity and higher polar surface area, hydrogen bonding capacity, and molecular weight in comparison with their oral counterparts (Ritchie, Luscombe, and Macdonald 2009).

These physicochemical properties influence their mode of transport across the airway epithelial barrier i.e. through para-cellular and/or transcellular

mechanisms (Figure 1-4) (Salomon and Ehrhardt 2012). Lipid soluble molecules cross epithelial barriers using the transcellular pathway, due to their inherent ability to traverse the lipid bilayers of cellular membranes. In general, lipophilic compounds show rapid absorption from the lungs with a half-life ($t_{1/2}$ ~ time taken for the absorption of 50% of the administered dose) of around 1 minute in rats following intra-tracheal administration (Brown and Schanker 1983; Patton, Fishburn, and Weers 2004). In contrast, lipid-insoluble compounds show a slower absorption from the lungs with absorption $t_{1/2}$ of about 60 minutes. Hydrophilic molecules cannot diffuse through lipid membranes and hence make use of aqueous pores of the inter-cellular junctions for crossing the airway epithelium, which represents the para-cellular pathway (Patton, Fishburn, and Weers 2004). However, a higher absorption from the rat lungs (50 and 17% of administered dose within 1h) than the small intestine (~2% of the administered dose) for lipid insoluble mannitol and inulin suggests a lower tightness of the airway epithelium than that in the gastro-intestinal tract (Schanker 1978). On the other hand, various transporter proteins expressed on cell membranes may influence the trans-epithelial permeability of both moderately hydrophobic and hydrophilic molecules through facilitating their entry and/or exit into and out of cells, respectively (Wagner, Hu, and Wang 2016).

1.2.4. Tissue binding and intracellular sequestration

Binding to tissue components, specifically or non-specifically and sequestration in intracellular organelles such as mitochondria and/or lysosomes could attribute ‘lung tissue affinity’ for inhaled compounds. These factors lower the free drug available for absorptive or metabolic clearance and thus enhance their tissue retention (Backman et al. 2017). Also, lipid membranes could work as ‘cellular depot’ for various compounds with moderate and high lipid solubility and increase their lung tissue accumulation following inhalation (Anderson, Linden, and Rabe 1994; Lombardi, Cuenoud, and Kramer 2009). Comparatively basic compounds achieve higher lung tissue retention than acidic and neutral compounds, which could be attributed

to sequestration in acidic lysosomal compartments due to an ion trapping phenomenon (Cooper, Ferguson, and Grime 2012).

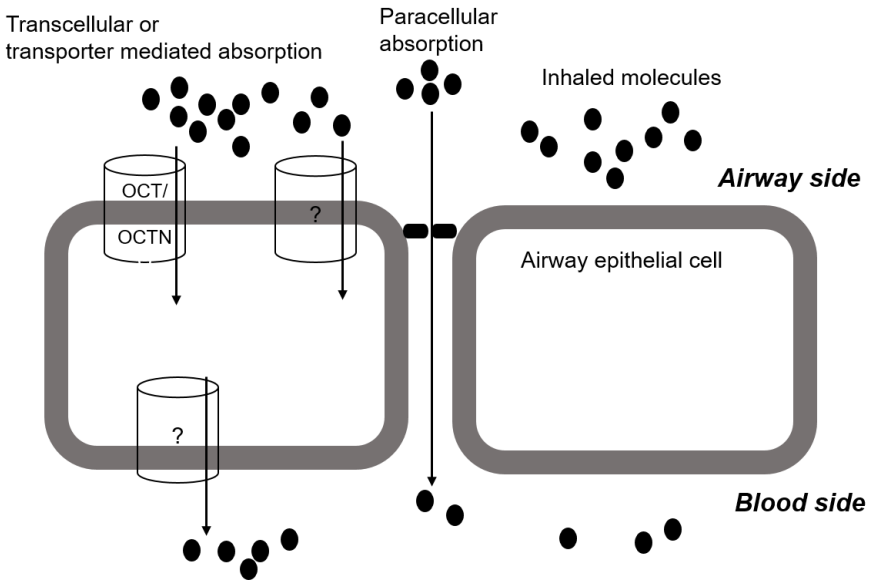


Figure 1-4. Mechanisms of inhaled drug absorption across the airway epithelial membrane

Inhaled molecules, depending on their physicochemical properties, permeate the airway epithelial membrane either transcellularly or through the paracellular route. Various transporter proteins (e.g., organic cation transporters (OCT) or organic cation/carnitine transporters (OCTN) may facilitate cell uptake and/or permeability of various organic cations across the airway epithelium which are otherwise intrinsically poorly permeable due to their charge at physiological pH. Image was adapted from Salomon and Ehrhardt, 2012 with permission from the publisher.

1.2.5. Drug transporters

Transporters are specialised membrane proteins whose major function is to control the movement of molecules into and out of cells (Xiong et al. 2015). Approximately 10% of the human genome encodes for transporter proteins, reflecting their importance in managing various cellular functions (Hediger et al. 2013). These transporter proteins are expressed on cells of various organs with barrier function such as intestine, brain, liver, kidney and placenta (You and Morris 2006). The lungs were found to express the highest transporter related gene levels after the liver and kidney (Bleasby et al. 2006).

Physiologically, transporters work as gatekeepers of cellular membranes and facilitate influx and efflux of nutrients or endogenous substrates including sugars, amino acids, peptides, and nucleotides (Cesar-Razquin et al. 2015;

You and Morris 2006). Transporters could interact with various drug molecules, depending on their structural similarity with the endogenous substrates. This could lead to altered drug disposition across biological barriers affecting target tissue exposure, and efficacy of therapeutic molecules (You and Morris 2006).

At the mechanistic and molecular level, these transporters are categorised within either the ABC (ATP-Binding cassette) or SLC (solute carrier) transporter families (You and Morris 2006). ABC transporter proteins with ATP-binding domain, utilise ATP hydrolysis as a source of energy for transporting molecules across membranes. Solute carrier (SLC) transporters, which transport substrates based on their electrochemical potential difference, are classified as facilitated transporters (You and Morris 2006). Transporters belonging to both the SLC and ABC super families are shown to be expressed in the lungs (Bosquillon 2010). Both transporter expression along the airway tract and their functionality i.e. uptake (influx/bidirectional), or efflux could influence local drug distribution including exposure to submucosal target sites, residence time in the lungs and also modulate lung absorption into the systemic circulation (Gumbleton et al. 2011).

1.2.5.1. ABC transporter family

ABC transporters are characterised by their ability to use energy from ATP hydrolysis for pumping various substrates across biological barriers against a concentration gradient (Higgins 1992). Based on their sequence homology, ABC transporters have been categorised into seven families, ABCA to ABCG (Xiong et al. 2015). Immunohistochemical staining studies in lung tissues suggest that bronchial and bronchiolar epithelial surfaces express three of the ABC transporter sub families, ABCB1 (multidrug resistance protein, MDR1/p-glycoprotein, P-gp), ABCC1 (multidrug resistance related protein, MRP1) and ABCG2 (breast cancer resistance protein, BCRP) (Scheffer et al. 2002). Reverse transcription polymerase chain reaction (RT-PCR) studies also confirm the presence of ABC-transporters in lung tissues including the trachea (Langmann et al. 2003).

Typical ABC transporter functional units make use of four membrane-associated core domains, two transmembrane domains (TMDs) and two nucleotide binding domains (NBDs). TMDs are highly hydrophobic with six membrane-spanning α-helices and are hypothesised to form the substrate binding site (Higgins 1992; Linton 2007). NBDs, also referred as ATP-binding domains with characteristic Walker A and B motifs, are responsible for the coupling of ATP-binding and hydrolysis providing energy for the translocation of substrates (Higgins 1992; Linton 2007).

Most of the P-gp substrates are amphipathic, and relatively hydrophobic molecules which are uncharged or weakly basic molecules, even though acidic compounds are also transported. The substrates include both large and small molecules, linear and cyclic peptides along with ionophores (Schinkel and Jonker 2003; You and Morris 2006). In contrast to P-gp, MRP1 transporter substrates include conjugated or unconjugated organic anions (Schinkel and Jonker 2003; You and Morris 2006).

Based on their inherent ability to efflux substrates from cells, ABC transporters proteins are assumed to be involved in protecting lung cells from various environmental pollutants in addition to other protective mechanisms in the upper and lower airways (Leslie, Deeley, and Cole 2005; Nickel et al. 2016). The protective role of ABC transporters against respiratory distress was also demonstrated in various ABC-knockout mice (Chai, Ammit, and Gelissen 2017). Even though the precise function of P-gp in the lungs is not yet fully understood, their apical expression on the epithelium suggests a role in translocation of substrates from the interstitium into the luminal side (van der Deen et al. 2005). MRP1 transporter protein could be involved in transporting substrates into the interstitial space (Scheffer et al. 2002). Since MRP1 preferentially transports a proinflammatory cysteinyl leukotriene LTC4, these transporter proteins role in various respiratory diseases with inflammatory component such as asthma requires further investigation (Scheffer et al. 2002).

1.2.5.2. SLC transporter family

SLC transporters constitute the largest group of membrane proteins and second only to G-Protein coupled receptors in the human genome, with around 52 gene families consisting of 400 transporter genes (Cesar-Razquin et al. 2015; Rives, Javitch, and Wickenden 2017). Due to their ability to influence drug disposition, the SLC22 transporter family has attracted a lot of interest and is one of the best studied among SLC transporters (Nigam 2018). With transporter sub-families for organic cations (OCTs), organic cations and zwitterions (OCTNs) and organic anions (OATs), the SLC22 gene family is responsible for the homeostasis of these ions through facilitating their cellular uptake, distribution and elimination.

Organic cation transporter 1 (OCT1), the first member of this family, was cloned and characterised by Grundemann et al., using functional expression cloning in Xenopus oocytes (Grundemann et al. 1994). Studies in oocytes expressing rOct1 demonstrated that ^{14}C-TEA uptake was potential-dependent, pH-independent and inhibited by the presence of organic cation of various molecular structures (Grundemann et al. 1994). Subsequently, other members of the organic cation transporter family, rat OCT2 (rOct2) (Okuda et al. 1996), human OCT1 (Zhang et al. 1997), human OCT2 (Gorboulev et al. 1997; Grundemann et al. 1998) and rat OCT3 (rOct3) (Kekuda et al. 1998) were cloned and characterised in terms of their expression and functional properties. Membrane depolarisation or the presence of an outward-driven concentration gradient could lead to OCT-mediated efflux of organic cations (Koepsell, Lips, and Volk 2007; Volk 2014).

A cDNA has been cloned for a novel organic cation transporter, OCTN1 from human fetal liver. Using ^{14}C-TEA as a substrate OCTN1 mediated organic cation transport was found to be pH-dependent, saturable and susceptible to the presence of metabolic-inhibitors (Tamai et al. 1997). Also, studies in Xenopus oocytes and HEK293 cells transiently expressed with OCTN1 demonstrated cation exchange mechanism for the bidirectional transport of organic cations (Yabuuchi et al. 1999). A lower affinity towards OCTN1 was shown for zwitterion carnitine when compared with organic cation TEA (Wu et al. 2000). In contrast, OCTN2 with about 75.8% similarity with human OCTN1,

showed a higher affinity for carnitine than organic cations. While OCTN2 mediated carnitine uptake was increased in a sodium-dependent manner, no such dependence was seen for organic cation transport (Tamai et al. 1998; Wu et al. 1999). These indicate that OCTN2 operate as a Na^+ - carnitine co-transporter as well as Na^+- independent transporter for organic cations (Koepsell, Lips, and Volk 2007; Volk 2014).

Gene expression studies using microarray indicate high transcript levels (50-75% quartile) for both OCTN1 and OCNT2 in human lung tissues while transcript levels of OCT1 and OCT3 transporters fell within the 25-50% expression quartile and a low expression (0-25% quartile) was seen for OCT2 (Bleasby et al. 2006). Quantitative RT-PCR studies indicate lower mRNA expression levels of OCT1 and OCT3 on airway epithelial cells in comparison to human liver and kidney tissue samples, while mRNA expression was undetectable for OCT2. Also, higher mRNA expression was seen for OCTN1 and OCTN2 in airway epithelial cells, with airway epithelial cells showing higher OCTN1 immune reactivity than alveolar epithelial cells (Horvath et al. 2007). Immunohistochemistry studies indicate apical expression of OCT1-3 transporter proteins in bronchial epithelial cells of mouse, rat and human (Kummer et al. 2006; Lips et al. 2007; Lips et al. 2005). Other transporter proteins belonging to the SLC family such as PEPT2 (SLC15A2) and ENT1 (SLC29A1) were shown to be expressed in the lungs, while no levels were seen for OAT (SLC22A6) and those of OCT2 (SLC22A2) (Lena Gustavsson 2016). Expression of multidrug and toxin extrusion protein 1 (MATE1) is also confirmed on the apical side of bronchial and bronchiolar cells (Berg et al. 2018). Among transporters present in the lung, the OCTs are the most investigated proteins in terms of their functional role in the lungs (Salomon and Ehrhardt 2012).

Amino acid sequence and hydropathy plot analysis predict a 12 - transmembrane domain (TMD) containing secondary structure for OCT/OCTNs with an amino and carboxy termini on the cytoplasmic side (Figure 1-5) (You and Morris 2006). These transporters are also characterised by a large extracellular loop and an intracellular loop between TMDs 1 and 2 and TMDs 6 and 7, respectively. The large extracellular loop consist of

conserved cysteine, which form disulfide bridges and play an important role in membrane trafficking whereas the transport function of SLC22 transporters is regulated by protein kinases present on phosphorylation sites on the intracellular loop (Volk 2014). The fourth and tenth transmembrane domains are assumed to play an important role in substrate recognition by the transporter proteins (Schinkel and Jonker 2003; You and Morris 2006).

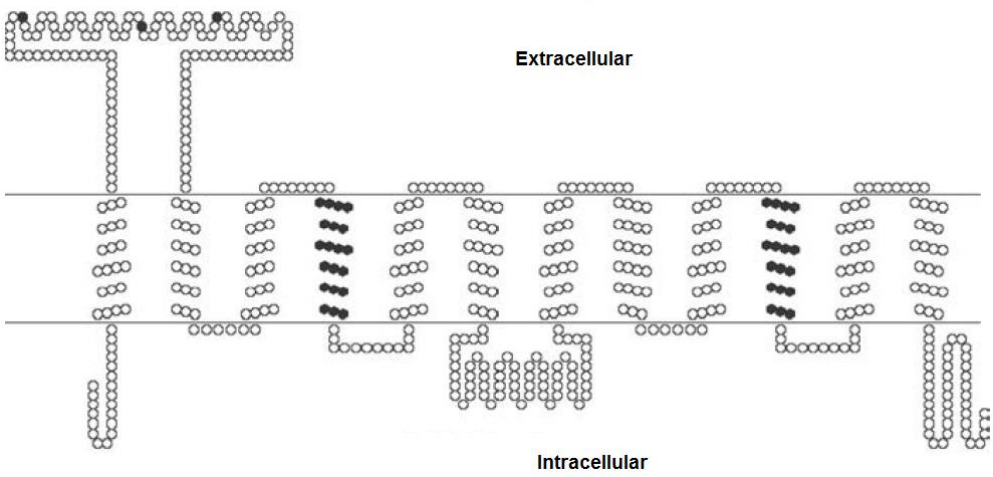


Figure 1-5. Predicted secondary structure for organic cation transporter 1 (OCT1)

Organic cation transporters are predicted to have a 12 transmembrane domains (TMDs) structure with a large extracellular loop containing N-glycosylation sites between TMDs 1 and 2. A large intracellular loop between TMDs 6 and 7 is predicted to have phosphorylation sites. Both TMD4 and TMD10 contribute towards substrate recognition by OCTs. Image taken from You and Morris, 2006 with permission from the publisher.

Transporters belonging to OCT or OCTN subgroups are characterised by their similar mechanism of drug transport and substrate specificities. Individual compounds working as substrates for one subtype transporter could be substrates and/or inhibitors of transporters of the other subgroup (Koepsell 2013). However, their shared substrates and tissue distribution pattern makes it difficult to assign specific roles for each transporter protein within subgroups of the SLC22 transporter family (Volk 2014). In general, substrates of OCT include organic cations and weak bases which are positively charged at physiological pH (Koepsell, Lips, and Volk 2007). However, positive charge is not an essential attribute for an OCT substrate, as non-charged compounds such as cimetidine at alkaline pH, could also be transported by OCTs. In addition to organic cations, OCTN1 transports zwitterions such as

ergothioneine and L- carnitine. On the other hand, L-carnitine and acetyl-L-carnitine are preferred substrates of OCTN2 while some of the organic cations such as tetraethylammonium (TEA), and choline could also be transported (Koepsell, Lips, and Volk 2007). The model cationic compound, 1-methyl-4-phenylpyridinium (MPP^+) is taken up efficiently by all subtypes of OCT subtypes and shows comparable Michaelis-Menten K_m values (Koepsell, Lips, and Volk 2007). While the other cation substrate, tetraethylammonium (TEA) shows lower affinity (higher K_m) towards the OCT3 subtype than the OCT1 and OCT2 subtypes. Even though certain cations (decynium-22, tetrapentylammonium and disprocynium), non-charged compounds (corticosterone, and β-estradiol) and anions (probenecid and α-ketoglutarate) are not substrates of OCT transporters, these compounds inhibit OCT mediated transport (Koepsell, Lips, and Volk 2007). Substrates of OCT show species differences in terms of their affinity and transport mechanism. For instance, a substrate of OCT in one species could be a non-transported inhibitor of OCT in other species. This is exemplified by tetrabutylammonium which is a substrate of hOCT1 and rabbit OCT1 but a non-transported inhibitor of rat OCT1 and mouse OCT1. OCT transported substrates also show a mutual inhibition, either in a competitive or non-competitive manner (Koepsell, Lips, and Volk 2007).

Various organic cations manage essential functions in the lungs including fluid homeostasis, neurotransmission, immune reactions and response to stress situations. These include neurotransmitters (acetylcholine, dopamine, epinephrine, histamine and serotonin), antioxidants (ergothioneine), and hormones (prostaglandin E2 and prostaglandin F2α). Due to their net positive charge at physiological pH, the above cations cannot permeate epithelial barriers and OCT/OCTNs facilitate their translocation within the lungs (Salomon and Ehrhardt 2012). For instance, luminal release of acetylcholine from the airway epithelium was shown to be mediated by organic cation transporters (OCT1/2) (Kummer et al. 2006; Lips et al. 2005). Likewise, OCT3 and/or OCT2 with their expression on basal cells of airway epithelium and on bronchial smooth muscle cells, are assumed to modulate the interstitial concentrations of various neurotransmitters such as histamine, serotonin and

dopamine (Koepsell, Lips, and Volk 2007). While OCTN1 is the primary transporter responsible for cellular transport of ergothioneine in response to oxidative stress, OCTN2 is essential for translocation of fatty acids in the mitochondria (Volk 2014).

An alternating-access mechanism was proposed to explain the transport of organic cations by OCT/OCTNs (Koepsell 2011). As per this model, transporter proteins undergo structural changes allowing interaction of substrates with the central binding site from either the cytoplasmic side or extracellular side (Quistgaard et al. 2016). Following binding of substrate to the transporter protein in outward – open mode, conformational changes induce the substrate-transporter complex to pass through a transient occluded state, before releasing the substrate onto the cytoplasmic side in inward-open mode of the transporter. The transporter could return to outward-open status either with an empty binding site or carrying a substrate from the cytosolic side for its translocation to the extracellular side (Volk 2014). Rapid inward-to-outward reorientation of the binding site of substrate-bound transporter protein compared to reorientation of an empty transporter, could lead to trans-stimulation of its carrier function (Koepsell 2011). Structural changes associated with OCTs during transport include movement of the six N-terminal TMD against the six C-terminal TBD, where a hinge domain in TMD 11 is found to be crucial for this movement (Koepsell 2011). At higher substrate concentrations, electroneutral cation exchange was proposed as a major OCT mediated transport mechanism (Koepsell 2011).

Currently inhaled therapeutics such as mast cell stabilisers and bronchodilators which include β2-agonists and antimuscarinic agents are permanently charged, zwitterions or carry a net positive charge. Due to their physicochemical properties, permeability across airway epithelium for accessing their therapeutic target site i.e. smooth muscle cells could be limited. Carrier mediated transport facilitated by OCT/OCTNs could be anticipated for these inhaled therapeutics in the lungs (Salomon and Ehrhardt 2012).

1.3. Experimental methods for studying the disposition of inhaled drugs in the lungs

Understanding the various factors affecting drug concentrations in the lungs is of paramount importance for the discovery and development of novel inhaled therapeutics (Cooper, Ferguson, and Grime 2012). While various procedures are well-established for assessing aerosol particle size distribution for effective drug deposition in the lungs, characterising lung disposition of inhaled particles post-deposition still remains a challenging task (Sakagami 2006). In order to delineate the various mechanisms affecting lung disposition, a variety of experimental models are available (Liu et al. 2013). These models include *in vivo*, *in vitro* and *ex vivo* approaches,

In vivo - inhaled compound deposition, distribution and retention are studied in the lungs along with the rate and extent of inhaled compound absorption into the systemic circulation.

Ex vivo - isolated perfused lung allows investigating the ability of compounds to cross epithelial barrier in intact lungs.

In vitro - understanding of various mechanisms of drug transport and permeability at the cellular level is typically studied using airway epithelial cell models

1.3.1. *In vivo* whole animal models

In vivo studies allow measuring compound concentrations in the lungs and in blood/plasma, representing target organ and systemic exposure, respectively. These studies facilitate the understanding of the pharmacokinetics of inhaled compounds and help optimising their pharmacological response (Cooper, Ferguson, and Grime 2012). Large animals such as rabbits, sheep, dogs and monkeys find major applications when formulation and /or device efficiency is assessed together with inhalational pharmacokinetics (Sakagami 2006). Most frequently, small rodents such as rats and guinea pigs are employed for studying lung disposition of inhaled compounds, as they require lower amounts of test compounds due to their small size (Liu et al. 2013).

For studying lung disposition, intra-tracheal (IT) instillation is one of the most extensively used techniques which allows a known amount of compound to be administered in the trachea. The typical experimental protocol involves placing rodents in a supine position, following anaesthesia, on a board tilted at an angle of 45 degrees. With the help of a small animal laryngoscope, the trachea is located and the compound is administered either as a solution or suspension after inserting a cannula in the trachea (Hendrickx et al. 2017). Alternatively, an invasive procedure is used where the trachea is exposed following a small surgical procedure in anesthetised animals and a cannula is inserted between two cartilaginous rings (Fernandes and Vanbever 2009). The development of small animal aerosolizers or insufflators facilitated the administration of liquid or dry powder formulations through the IT route (Nahar et al. 2013).

Even though the IT route allows to control the dose administered and bypass nasal passages, it does not represent inhalational delivery in humans. This technique requires animals to be under anaesthesia and is also not suitable for repeated administration of compounds as insertion of the cannula may lead to inflammation in the trachea. Since the typical volume of instillation (~100 µL) is larger than rat epithelial lining fluid (45 – 55 µL), this procedure may lead to change in the lung physiology (Sakagami 2006). Even though relatively easy to use, small changes in the technique of IT administration could lead to changes in the site of drug deposition and consequently, the rate and extent of drug absorption from the lungs (Codrons et al. 2004).

To overcome the limitations of the intra-tracheal administration technique, various passive dose administration chambers are introduced which allow compound exposure to conscious animals through whole-body, nose only or head only exposure systems, mimicking physiological conditions. Whole body chambers require larger amounts of compound than other exposure systems and, compounds may get absorbed from other routes such as oral, and subcutaneous, in addition to inhalation. In comparison with whole body exposure systems, head only and nose only chambers facilitate delivering larger amounts of compounds. However, nose only or head only exposure systems require animals to be placed in individual holding tubes subjecting animal to stressful conditions (Nahar et al. 2013).

Following inhalation, drug disposition in the lungs are characterised based on either lung tissue concentration or through broncho-pulmonary lavage (Liu et al. 2013). Estimation of lung concentrations at various time points after dose administration allows to determine the percentage of dose remaining in the lungs and to calculate lung absorption rate constants. However, in such studies, information regarding local drug distribution in the lungs is lost due to the nature of sample processing such as homogenisation of whole lungs (Cooper, Ferguson, and Grime 2012). Modification of the study design involves collecting blood samples following IT administration of compounds to determine the rate and extent of lung absorption into the systemic circulation (Sakagami 2006). However, characterising the pharmacokinetics of inhaled compounds based on systemic plasma exposure requires highly sensitive analytical methods, as typical doses in rats range between 2-20 µmol/kg which is expected to achieve a maximum plasma concentration of 1-10 nM only (Cooper, Ferguson, and Grime 2012).

1.3.2. *Ex vivo* models

Isolated perfused lungs (IPL), maintained in an artificial environment mimicking *in vivo* situations provide an alternative animal model for studying airway to perfusate transfer of molecules following aerosol or intra-tracheal administration (Byron 1993). This system allows investigating various physiological processes affecting drug disposition within the lungs without the involvement of other systemic processes such as elimination or drug-redistribution. Even though human lung perfusions models have been attempted, isolated perfused rat lung (IPRL) system is the most commonly employed ex vivo model for characterising drug absorption and disposition of inhaled molecules (Nahar et al. 2013).

Briefly, following anaesthesia, tracheostomy is performed for surgical separation of lungs along with heart after cannulating the pulmonary artery and pulmonary vein. The lungs are suspended by the trachea in an artificial thoracic chamber maintained at 37^{o}C. Lung perfusion is maintained where the perfusion buffer enters and exits the lungs, through the pulmonary artery and vein, respectively. Following establishment of the IPL system, compounds are

administered in the trachea by instillation of liquids, nebulisation or dry powder insufflation. Outlet samples are collected from the pulmonary vein at various time points in order to measure and calculate the % of dose administered appearing in the perfusate (Fernandes and Vanbever 2009; Liu et al. 2013). Based on time-course profiles of administered molecule appearance in the perfusate, PS a parameter reflecting the product of the permeability coefficient (P) and surface area (S) is calculated. In addition, the absorption rate constant (K_a) and apparent half-lives ($t_{1/2}$) are typically calculated from these profiles (Sakagami 2006).

During the perfusion process various approaches are employed to check the viability of the lungs, such as visual inspection for oedema formation, or weight gain. Other methods of lung viability include measuring tidal volume, dynamic compliance and airway conductance along with perfusion flow at various time points. The conditions used in IPL studies vary in terms of presence or absence of ventilation, buffer collection in a single pass or recirculation of buffer and maintenance of lungs either in positive or negative pressure etc. (Fernandes and Vanbever 2009).

A good IPRL- *in vivo* correlations in terms of drug absorption in the lungs was obtained suggestive of the suitability of this model (Bosquillon et al. 2017). With structural integrity and luminal cellular composition (macrophages, epithelial and endothelial cells) maintained, this model also facilitates studying the effect of particle size on deposition and disposition of inhaled molecules in the lungs (Tronde, Norden, Jeppsson, et al. 2003). However, in the IPRL model the lungs maintain their physiologically optimal conditions only for 2 - 3h. The IPRL model could underestimate the absorption of molecules which show good absorption from the airways, as the bronchial circulation is severed during the surgical procedure. Complicated surgical procedures which demand technical skills, not amenable for high throughput and expensive to establish could limit the applicability of this model (Fernandes and Vanbever 2009). In addition, studying the role of active transport mechanisms in overall permeability across the airway epithelium or the contribution of individual cell types in lung drug disposition cannot be delineated in the IPL model (Sakagami 2006).

1.3.3. *In vitro* models

1.3.3.1. Precision-cut Lung Slice Model

Organ slices are considered as an appropriate *in vitro* model which retain the architecture of tissues of origin and facilitate studying drug retention, metabolism and interactions at an individual organ level (de Kanter et al. 2002; Graaf, Groothuis, and Olinga 2007). The typical procedure for preparing organ slices includes removal of the organ of interest from anaesthetised experimental animals and transferring it to an ice-cold buffer. Following slicing with commercially available organ slicer, the organ slices are incubated with buffer containing test compounds at 37^{o}C (de Kanter et al. 2002). The use of lung slice models for metabolic, toxicological and histopathological evaluation of compounds is well-established (De Kanter et al. 1999; Fisher et al. 1994; Le Prieur et al. 2000; Monteil et al. 1999; Wijeweera et al. 2001). Recently, lung slice models have also been applied to determine the distribution volumes and mechanism of lung retention, including lysosomal sequestration, of inhaled therapeutics in the lungs (Backstrom, Boger, et al. 2016; Backstrom, Lundqvist, et al. 2016).

1.3.3.2. Cell culture models

The application of *in vitro* cell culture models is well-established for understanding the fate of inhaled therapeutics in the lungs including drug uptake, binding, permeability, mechanism (s) of drug transport, metabolism and toxicity (Forbes and Ehrhardt 2005). Compared to *in vivo* studies, *in vitro* models are advantageous in terms of ethical issues, provide control over study conditions including compound exposure time and sample collection, and a known area of epithelial cell layer exposed to compounds (Liu et al. 2013). Since columnar and alveolar type I cells (AT-I) in the airways and alveolar region, respectively, occupy the majority of the lung epithelial surface area, *in vitro* models based on these region specific cell types are considered more appropriate. In addition to representing the cellular composition of the airway epithelium, the ability to form tight junctions as reflected by a high transepithelial electrical resistance (TEER) is one of the essential criteria for developing lung cells as an *in vitro* epithelial model (Forbes 2000).

Currently, there are a variety of *in vitro* respiratory cell culture models consisting of both continuous and primary cells. Primary cell cultures closely resemble the *in vivo* situations and may be considered as ideal *in vitro* systems for drug delivery applications in the lungs. However, these cell models are limited by their lower isolation yield, require time-consuming procedures, and show donor-to-donor variation (Liu et al. 2013). Also primary cells of human lung origin form monolayers with a limited lifetime and it is difficult to obtain high TEER values (Fernandes and Vanbever 2009). On the other hand, due to their ability to grow continuously, human lung epithelial cells of either cancerous origin or transformed cells find major applications in the area of inhalational drug delivery and toxicity testing (Sakagami 2006).

Among continuous cell cultures, Calu-3 and 16HBE14o- epithelial models of airway origin have been identified as suitable models for drug absorption studies in the lungs (Forbes et al. 2015; Forbes 2000). These cell lines are well-characterised in terms of their tight junctional properties, metabolic and transporter protein expression profiles. In contrast, applications of alveolar epithelium origin cell lines such as A549 and TT1 are limited to toxicological evaluation as these models fail to form tight junctions and hence are not suitable for drug transport experiments (Haghi et al. 2014).

1.3.3.3. 16HBE14o-

The 16HBE14o- cell line was developed following transformation of bronchial epithelial cells collected from a one-year old male heart-lung transplant patient. Immunocytochemical and functional studies confirmed the presence of various drug transporter proteins including P-gp, lung resistance-related protein and Caveolae-1 (Ehrhardt et al. 2003). 16HBE14o- cell lines have been utilised for understanding mechanisms of drug transport (Forbes and Lansley 1998; Forbes 2000) and for developing correlations between *in vitro – ex vivo* lung models in terms of compound permeability across the lung epithelium (Bosquillon et al. 2017). However, 16HBE14o- cells were found not to produce mucus, thus are not representative of the native bronchial epithelium (Forbes 2000).

1.3.3.4. Calu-3

Calu-3 is a bronchial adenocarcinoma cell line obtained from a 25-year-old Caucasian male, is commercially available from the American Type Culture Collection (ATCC) and is one of the well-established airway epithelial cell lines in the area of pulmonary drug delivery (Forbes 2000). These cells are readily available, form tight junctions and demonstrate suitable barrier properties, allowing permeability studies when grown on porous membranes under air-liquid interface conditions (ALI) (Foster et al. 2000; Min et al. 2016; Nichols et al. 2014). Calu-3 cells were shown to have airway epithelial cell features including cilia and mucus, in addition to various transporter and metabolic systems when grown at an air-liquid interface (Florea et al. 2003; Hutter et al. 2014). Histological and histochemical evaluations performed on Calu-3 cells following culturing at ALI, established the formation of a pseudostratified columnar epithelium. Also, under these conditions, Calu-3 cells differentiated into mucus secreting goblet cells, presented microvilli, and showed expression of occludin and E-cadherin, i.e., TJ and adherens junction proteins, respectively (Kreft et al. 2015). Expression and functional properties of transporters relevant for inhalational drug delivery such as OCT1, OCT3, OCTN1 and OCTN2 is extensively investigated in Calu-3 cells using their marker substrates and standard inhaled compounds (Ingoglia et al. 2015; Mukherjee, Pritchard, and Bosquillon 2012). An excellent correlation was also found between permeability coefficients of various molecules with diverse physicochemical properties in Calu-3 layers and lung absorption rate constants in rats *in vivo* as well as in an *ex vivo* lung perfusion model (Bosquillon et al. 2017; Mathia et al. 2002).

However, there are certain limitations associated with these models as expected with most of the *in vitro* epithelial models. In contrast to a complex lung environment with approximately 40 different cell types, for instance, Calu-3 cells only represent cell types present in the bronchial epithelium without any interaction with other cell types which may influence the disposition of inhaled molecules (Kaur and Dufour 2012). Further studies with complex co-culture systems consisting of different cell types is advocated in order to simulate the complex lung physiology in vitro at the cellular level (Haghi et al. 2010).

Also, none of the current *in vitro* airway epithelial models are able to incorporate changes in surface area and drug-epithelial interactions associated with stretching caused by the inhalation process (Haghi et al. 2010).

1.3.4. Other strategies for an improved understanding of inhaled drug disposition in the lungs

1.3.4.1. Imaging techniques

Imaging studies facilitate characterising drug availability, retention and distribution in target organs including the functional role of transporter proteins in drug disposition, noninvasively (Kusuhara 2013). For the purpose of imaging transporter-mediated processes *in vivo,* both single photon emission computed tomography (SPECT) and positron emission tomography (PET) employ radiotracers, while magnetic resonance imaging (MRI) make use of gadolinium complex (Kusuhara 2013; Tournier, Stieger, and Langer 2018). Due to their non-invasive nature, these methods allow the collection of experimental data at various time points from the same subject under identical experimental conditions, thus avoiding inter-subject variability (Tournier, Stieger, and Langer 2018).

Compared to other techniques, PET offers advantage of introducing isotopes such as ^{11}C, ^{13}N, ^{15}O and ^{18}F, into the structures of drug molecules and thus visualise their distribution in organs (Dolovich and Labiris 2004; Kusuhara 2013). For instance, PET imaging was employed for investigating the functional role of organic cation transporters (OCT) and organic anion-transporting polypeptide (OATPs) using their substrates ^{11}C sulpiride and ^{11}C Dehydropravastatin, respectively (Ijuin et al. 2012; Kaneko et al. 2018; Takano et al. 2017). In addition, various preclinical and clinical investigations demonstrated the utility of PET for assessing transporter-mediated drug-drug interactions involving major transport proteins including P-gp, BCRP, OATP, MRP and MATEs (Langer 2016). However, the application of PET is limited by short half-lives of its probe substrates (20-110 minutes) along with the requirement of specialised facilities and personnel (Mann, Han, and Eyal 2016). SPECT is gaining more popularity as its probe technetium-99m (^{99m}Tc) offers

a long half-life (~6 hours) and is easy to obtain with generator systems (Mann, Han, and Eyal 2016).

Both PET and SPECT allow assessing pulmonary disposition of inhaled radiopharmaceuticals and thus could be applied for studying the functional role of lung transporters using radiolabelled substrates of various transporter proteins (Dolovich and Labiris 2004; Tournier, Stieger, and Langer 2018). However currently, only a few studies were attempted focussing on pulmonary transporters. These include, for instance, applying PET technique for understanding the role of mouse Mrp1 in the accumulation of its substrates in the lungs following systemic administration (Okamura et al. 2013). Also, the expression and functional role of multi-drug resistance proteins (MDR1/MRP1) in human lung was imaged using SPEC (Mohan et al. 2016; Ruparelia et al. 2008). Thus, there is an enormous opportunity for understanding inhaled drug disposition and the role of pulmonary drug transporters with the application of imaging approaches. The use of these imaging techniques is, however, limited by the non-specificity of various transporter probe substrates. Additional information from genetic knockout models and/or use of transporter inhibitors could be employed as a supportive evidence for identifying the transporter under investigation (Mann, Han, and Eyal 2016).

Imaging mass spectrometry (IMS), which is a relatively new, highly sensitive and label-free technique, has the ability of simultaneous detection of many molecules and their metabolites along with their spatial localisation in a given tissue section (Aichler and Walch 2015; Mann, Han, and Eyal 2016). For IMS, three ionisation methods are used, namely electrospray ionisation (ESI), secondary ion mass spectrometry (SIMS) and matrix-assisted laser desorption/ionisation (MALDI) (Rubakhin et al. 2005). The distribution of compounds in the lungs has been previously investigated using IMS, including for demonstrating the epithelial and sub-epithelial localisation of inhaled broncholdilators (Backstrom et al. 2018; Marko-Varga et al. 2011; Matsumoto et al. 2017 ; Prideaux et al. 2011). However IMS could not be easily applied *in vivo* and requires extensive sample processing (Mann, Han, and Eyal 2016; Rubakhin et al. 2005).

1.3.4.2. Transfected cell lines

Various cultured cell lines such as Madin-Darby canine kidney (MDCK), LLC-PK1, HEK293 or CHO cells with stable or transient expression of various recombinant transporters are used for investigating drug-transporter interactions (Giacomini et al. 2010). These transfected cell systems with defined human uptake and efflux transporter proteins allow understanding the coordinated action of transporter proteins in the overall cellular disposition of molecules (Cui, Konig, and Keppler 2001; Taghikhani, Fromm, and Konig 2017). For instance, the functional interplay between OCT1/OCT2 mediated uptake and efflux by MATE1 transporters in the renal secretion of organic cations such as metformin and ipratropium were investigated using single or double transfected MDCK cells (Konig et al. 2011). The involvement of multiple transporters or transporter-enzyme interactions in the hepatic disposition of molecules were experimentally demonstrated with the help of triple or quadruple - transfected MDCK cell lines (Fahrmayr et al. 2012; Kopplow et al. 2005).

However, variable expression of endogenous transporter proteins in wild type and transfected cell lines could confound the data interpretation with respect to the role of various drug transporters (Goh et al. 2002; Kuteykin-Teplyakov et al. 2010). This limitation has recently been overcome in a new MDCK cell line model with knocking down of endogenous MDR1, which could be used as an alternate *in vitro* model for investigating the role of efflux transporter proteins in drug disposition (Karlgren et al. 2017; Simoff et al. 2016).

Since most of the inhaled molecules are well-recognised substrates of SLC transporters (Hendrickx et al. 2013; Nakamura et al. 2010; Nakanishi et al. 2013; Salomon et al. 2015), multi-transfected MDCK cell lines with lung specific transporter proteins may allow delineating uptake and efflux mechanisms involved in their lung disposition.

1.3.4.3. Knockout models

Transporter gene-knockout models have been applied successfully to understand the physiological functions of transporter proteins and transporter-mediated drug disposition (Giacomini et al. 2010). For instance, Mdr1a$^{-/-}$ and

Bcrp$^{-/-}$/ Mdr1a$^{-/-}$/ Mdr1b$^{-/-}$ mice were utilised to illustrate the protective roles of P-gp and BCRP proteins, respectively, across the blood-brain barrier (Polli et al. 2009; Schinkel et al. 1994).

A variety of commercialised knockout models are predominantly being used as custom gene-knockout rodent models may lead to inter-laboratory phenotypic differences due to changes in diet, housing conditions, sex and strain (Zamek-Gliszczynski et al. 2013). Also introduction of humanised transporter animal models helped to overcome the issues related to inter-species differences in terms of extrapolating transporter activities to human (Choo and Salphati 2018; Scheer et al. 2012; Scheer et al. 2013; van de Steeg et al. 2012). These models were effectively utilised to investigate OATP- and OCT/MATE-mediated hepatic drug distribution and renal excretion, respectively (Higgins, Bedwell, and Zamek-Gliszczynski 2012; Tsuda et al. 2009; van de Steeg et al. 2012).

In comparison with their application for understanding drug disposition in major organs such as brain, liver, kidney and intestine, transporter-gene knockout models have been underutilised for investigating the role of pulmonary drug transporters in inhaled drug absorption. For instance, the main application of these models has been limited to the study of P-gp role in the absorption of compounds from the lungs (Al-Jayyoussi et al. 2013; Manford et al. 2008; Price et al. 2017). Thus, the use of transporter-gene knockout models, especially of the SLC22 family such as OCT1, OCT3 and MATE1/2 has a potential for improving our understanding of the role of these transporters in lung absorption of inhaled molecules. Also, transporter knocked down *in vitro* epithelial cell layers such as Caco-2 have been applied for studying the role of transporter proteins in order to overcome the limitations associated with chemical inhibitors (Li et al. 2011). Such investigations, using transporter knocked down lung epithelial model Calu-3 could facilitate identifying the contribution of various transporter proteins in the overall cellular disposition of inhaled molecules. However, the use of transporter-gene knockout models is associated with a number of limitations including the potential for up or downregulation of other transporter proteins following knock down of the transporter under investigation (Zamek-Gliszczynski et al. 2013). Hence it is

essential to understand the presence of such compensatory mechanisms for a meaningful interpretation of results obtained from knockout models.

1.4. Summary

Even though inhalational drug delivery is well-established for the management of local diseases such as asthma and COPD, drug disposition in the lungs is poorly understood. Existing experimental methods characterise lung disposition of inhaled molecules either by monitoring their appearance in blood circulation or measuring total tissue levels. Various tissue affinity factors such as lysosomal sequestration and drug transporter proteins could influence local lung concentrations of inhaled therapeutics through altering their intracellular accumulation. However, very few systemic attempts to understand the contribution of these factors in the tissue retention of inhaled molecules have been reported. Consequently, inhaled drug disposition in the lungs at the cellular level is poorly understood. Application of *in vitro* airway epithelial models may facilitate studying permeability mechanisms of inhaled compounds across the airway epithelium and also help to characterise the cellular retention mechanisms including lysosomal sequestration. A better understanding of these factors could lead to designing molecules with optimised pharmacokinetic properties in the lungs following inhalation.

1.5. Aims and Objectives of this PhD

This thesis focuses on applying the human bronchial airway epithelial model Calu-3 for better understanding the mechanisms controlling the permeability of inhaled compounds across the lung epithelium, as well as their retention in the lung tissue, including the role of drug transporter proteins and lysosomal sequestration.

Drug permeability and uptake characteristics of ipratropium, a permanently charged short acting anticholinergic bronchodilator, were investigated in the first results chapter. For these investigations Calu-3 cells were grown on porous membranes under air-liquid interface (ALI) culture conditions for 21 days. Even though ipratropium is a well-recognised substrate of Organic Cation Transporters (OCT), their contribution in its trafficking across the

bronchial epithelium is not yet clearly understood. While various *in vitro* uptake studies in undifferentiated cells suggested transporter-mediated ipratropium absorption, *ex vivo* lung perfusion studies indicate a paracellular diffusion as a major lung absorption mechanism. The results presented in this chapter fill this existing gap and highlights the concerted action of uptake and efflux transporter mechanisms in managing local lung concentrations of ipratropium.

In the next chapter, the suitability of Calu-3 cells for measuring lysosomal association of inhaled compounds was assessed for the first time. The presence of functional lysosomes was verified, and a cell fractionation approach was applied for isolating lysosomes from Calu-3 cells in order to measure lysosomal association of compounds. While the experimental techniques employed in this chapter such as florescence microscopy and cell fractionation are well-established in the literature (Duvvuri, Feng, et al. 2004; Duvvuri and Krise 2005; Ufuk et al. 2015), these investigations are essential for validating the Calu-3 model for lysosomal sequestration studies.

In the final chapter, lysosomal sequestration of inhaled compounds was characterised by measuring their cellular partition coefficient (K_p) in Calu-3 cells and retention across Calu-3 layers in the presence or absence of cytosol-lysosomal pH gradient disruptors. Lysosomes were isolated from compound treated Calu-3 cells using cell fractionation approach for directly measuring lysosomal sequestration of inhaled compounds. Lung retention was determined for molecules following intra-tracheal administration in rats and their retention mechanisms were explained based on permeability characteristics and cellular accumulation of compounds in Calu-3 model. This is the first report where the cellular disposition of inhaled therapeutics is presented using an *in vitro* airway epithelial model in Calu-3 cells. Also, in contrast to previous qualitative reports, lysosomal association of inhaled molecules is demonstrated quantitatively and its influence on retention in the airway epithelium is also presented for the first time. This novel application of *in vitro* airway epithelial model may fasten screening of inhaled compounds for their lung retention potential and lower the animal - based experiments for this purpose.

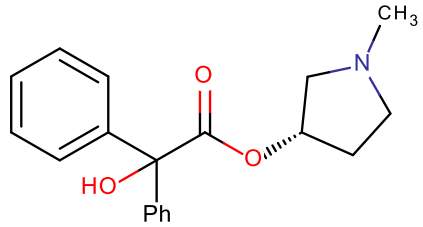
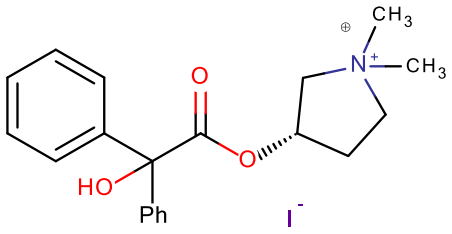
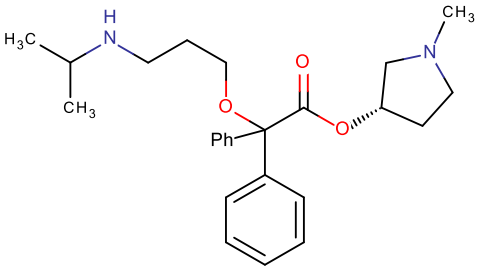
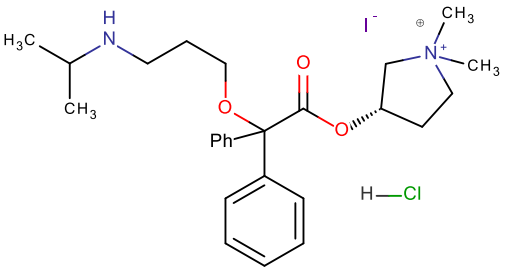
Chapter Two

2. Materials and Methods

2.1. Materials

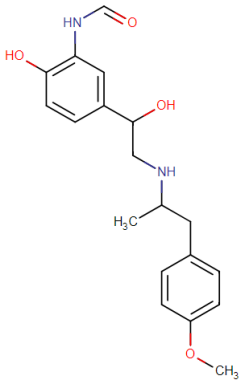
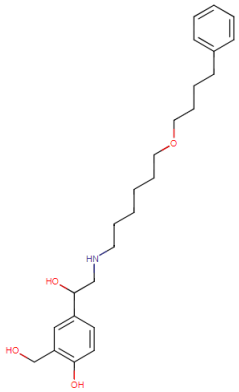
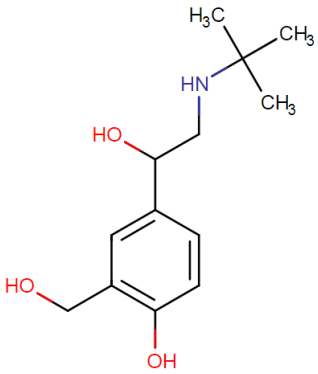
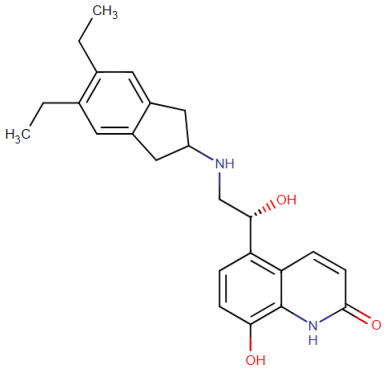
Human bronchial adenocarcinoma cells, Calu-3 cells were procured from the American Type Culture Collection (Rockville, MD, USA) and used between passage numbers 30 and 40. Polycarbonate Transwell® insert (12 well, with 0.4 µm pore size and a surface area of 1.12 cm^2) and cell culture flasks (25 and 75 cm^2) were obtained from Corning Costar (Kennebunk, US). LysoTracker™ Green DND-26 and Bafilomycin A1 were purchased from Alfa Aesar (Ward Hill, MA) and ThermoFisher Scientific (UK), respectively. Indacaterol was obtained from Insight Biotechnology Ltd (Wembley, UK). Lysosomal Enrichment Kit was obtained from ThermoFisher Scientific, UK. Rapid Equilibrium Dialysis devices were procured from Sigma-Aldrich (Poole, UK). All the other cell culture reagents and chemicals were procured from Sigma-Aldrich (Poole, UK). HPLC grade solvents for LC-MS/MS analysis were purchased from Fisher Scientific UK. (Loughborough, UK). The DS12, DS13, DS81 and DS86 compounds were obtained from Dr Michael J Stocks laboratory, Division of Biomolecular Science and Medicinal Chemistry, University of Nottingham, Nottingham (UK). The chemical structures and physicochemical properties of inhaled drugs and investigational compounds used in this study are compiled in the *Table 2-1*.

Table 2-1. Chemical structures, molecular weight, predicted LogP (cLogP) and pKa (cpKa) [a] for various compounds

DS12  Molecular weight: 311.09 clogP: 2.67 cpKa: 7.8	**DS13**  Molecular weight: 453.32 clogP: - 1.59 cpKa: -
DS81  Molecular weight: 410.22 clogP: 3.78 cpKa: 7.8, 10.5	**DS86**  Molecular weight: 460.68 clogP: - 0.38 cpKa: 10.47

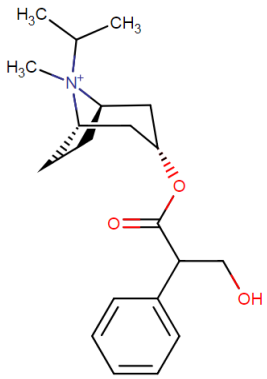
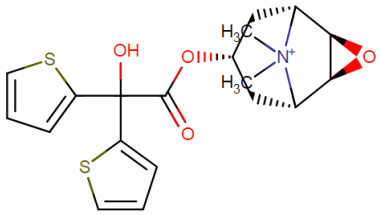
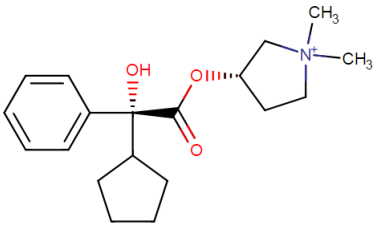
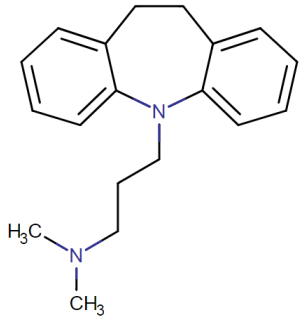
[a] cLogP and cpKa were obtained using MarvinSketch (14.8.4.0)

Table 2.1. Continued...

Formoterol  Molecular weight: 344.4 clogP: 1.91 cpKa: 8.61, 9.81	**Salmeterol**  Molecular weight: 415.6 clogP: 3.82 cpKa: 10.12, 9.4
Salbutamol  Molecular weight: 239.3 clogP: 0.44 cpKa: 10.12, 9.4	**Indacaterol**  Molecular weight: 392.5 clogP: 3.31 cpKa: 8.51, 9.71

Structures and physicochemical properties were obtained from www.drugbank.ca

Table 2.1. Continued...

Ipratropium  Molecular weight: 332.46 clogP: - 1.8 cpKa: -	**Tiotropium**  Molecular weight: 392.5 clogP: - 1.8 cpKa: -
Glycopyrronium  Molecular weight: 318.4 clogP: - 1.2 cpKa: -	**Imipramine**  Molecular weight: 280.4 clogP: 4.53 cpKa: 9.2

Structures and physicochemical properties were obtained from www.drugbank.ca

2.2. Methods

2.2.1. Cell culture

Calu-3 cells were cultured in Dulbecco's modified Eagle's medium / Ham's F12 nutrient mixture (DMEM: F12) 1:1 supplemented with 10% v/v of foetal bovine serum (FBS, non USA origin and sterile filtered), 1% v/v of penicillin-streptomycin antibiotic solution, 1% v/v of 2 mM L-glutamine and 1% v/v of non-essential amino acids. They were maintained in a humidified incubator at 37^{o}C under 5% CO_2 environment in 75 cm^2 tissue culture flasks with replacement of medium every other day. Upon reaching confluency (80-90%), Calu-3 cells were washed with 10 mL of pre-warmed sterile PBS and subjected to trypsinisation with the addition of pre-warmed 0.25% v/v trypsin-EDTA mixture (5 mL). Upon visual confirmation of cell detachment, 8 mL of media was added to neutralise the action of trypsin and the resulting cell suspension was centrifuged at 800 rpm for 5 minutes. The cell pellet was suspended in fresh medium and the cell suspension was transferred to a new flask using a split ratio of 1:5.

The trypan blue exclusion method was used to count the number of viable cells. For this, 100 µL of cell suspension was mixed with an equal volume of 0.5% w/v trypan blue. A 10 µL of this mixture was placed on a haemocytometer and cells were counted in outer squares while excluding dead cells which had accumulated the trypan blue dye. The number of viable cells counted were averaged and used for determining the cell seeding density into multi-well tissue culture plates or into Transwells® (12-wells, pore size - 0.4 µm; surface area - 1.12 cm^2). For drug permeability and transport studies, Calu-3 cells were seeded at a density of 1 x 10^5 cells/cm^2 on Transwells®. After 24 h of incubation under submerged conditions in a humidified incubator at 37^{o}C under 5% CO_2, they were raised in air-liquid interface culture conditions by aspirating the medium from both the apical and basolateral chambers and adding 500 µL of medium in the basolateral chamber only. Thereafter, the cell culture medium was replaced every other day until day 21 post seeding when the differentiated cell layers were used for experimentation.

2.2.2. Trans-epithelial electrical resistance (TEER) measurements

Formation of tight junctions across Calu-3 layers was assessed on alternate days before changing the medium by measuring the TEER. For this, 500 and 1500 µL of medium were added to the apical and basolateral side, respectively, and the cell layers were incubated for 30 minutes in a humidified incubator at 37ºC under 5% CO_2. An EVOM meter with chopstick electrodes (World Precision Instruments, Stevenage, UK) was used for measuring the TEER after sterilising the electrodes with 70% v/v industrial methylated spirit (IMS). TEER values obtained in Transwells® without cells were measured and subtracted from readings obtained from wells with cells. TEER values were normalised to per unit surface area of the Transwells® insert membrane. Only cell layers exhibiting TEER values greater than 500 ohm.cm^2 were selected for experimentation. Data obtained in layers which had maintained a TEER value above this threshold at the end of the experiment were considered for analysis.

2.2.3. Drug transport studies

The transport of molecules was measured in both apical to basolateral (absorptive, *a-b*) and basolateral to apical (secretion, *b-a*) directions across Calu-3 cell layers which had been maintained under ALI for 21 days. Stocks of various compounds were prepared by dissolving solids in dimethyl sulfoxide (DMSO) and test solutions were prepared by diluting stock solutions in Hank's Balanced Salt Solution (HBSS) such that the final DMSO concentration was less than 1% v/v.

For *a-b* experiments, 0.55 mL of HBSS containing the test compound (10 µM) was added into the apical (donor) chamber of the Transwells® and the study was initiated by adding 1.5 mL of blank HBSS to the basolateral (receiver) chamber. For *b-a* experiments, 1.55 mL of HBSS with the test compound was placed in the basolateral (donor) compartment and the study was initiated by adding 0.5 mL of blank HBSS on the apical (receiver) side of the layers. A 0.05 mL sample was collected from the donor compartments for determination of

the initial concentration and the Transwell® plate was placed on an orbital shaker (60 rpm) inside a humidified incubator at 37ºC under 5% CO_2. Appearance of drug in the receiver compartments was monitored by collecting 0.3 mL or 0.1 mL samples for *a-b* and *b-a* experiments, respectively, after 0.5, 1, 2 and 4 h. At each time point, samples were replaced with an equal volume of blank HBSS. At the end of the experiment, 0.05 mL was collected from the donor compartments and all the study samples were stored at -20ºC until analysis by LC-MS/MS. FITC-dextran (Average molecular weight~4000) was used as a paracellular permeability marker. For this molecule, the fluorescence intensity of the samples was measured using a multimode microplate reader Spark® 10M (Tecan) at an excitation and emission wavelengths of 485 and 535nm, respectively, and converted into FITC-dextran concentrations using a standard curve.

For investigating the role of transporters in drug cellular disposition, Calu-3 layers were pre-incubated with HBSS containing one of the transporter inhibitors (1-methyl-4-phenylpyridinium, MPP^+ - 500 µM, tetraethylammonium, TEA - 5 mM, L-carnitine - 1 mM, probenecid-100 µM or verapamil-100 µM), for 30 minutes. Each experiment was initiated by co-incubating the donor side of the cell layers with the test compound and one transporter inhibitor in HBSS and adding HBSS containing the inhibitor in the receiver compartment. Thus, transporter inhibitor is present at same concentration in both donor and receiver compartments. After each sample collection, the volume collected from receiver compartment was replaced with HBSS containing the inhibitor in order to maintain a constant inhibitor concentration throughout the experiment.

Permeability data were obtained from at least three layers and the apparent permeability coefficient (P_{app}) was calculated using the equation below.

$$P_{app} = \frac{J}{A \times C_0}$$

Where:

- J is the flux of molecules across the cell layers (moles/sec)
- A is the surface area of the Transwell® insert membrane in cm^2

- C_0 is the initial concentration of the compound in the donor chamber (moles/mL)

2.2.4. Drug uptake studies

The role of drug transporters in the cell uptake of test molecules was investigated at 10 µM after exposure from either the apical or basolateral sides of the Calu-3 cell layers maintained under ALI conditions. The incubation and experimental conditions were similar as those described above except that the drug solution was withdrawn from the donor compartment at various time points and the cell layers were quickly washed with cold PBS (4^{o}C), three times. The layers were excised from the Transwells® and collected into 1.5 mL tubes. Cells were lysed with the addition of chilled methanol containing the internal standard. The cell lysates were vortexed, centrifuged at 10,000 rpm for 10 minutes at 4^{o}C and the supernatant collected were stored at -20^{o}C until analysis.

For inhibitory experiments, the layers were subjected to 30 minutes of pre-incubation with MPP^+ - 500 µM, TEA - 5 mM, L-carnitine - 100 µM or probenecid - 100 µM. The cell layers were then exposed to compound (10 µM) under investigation in presence of one of the inhibitors in the donor compartment while HBSS containing the inhibitor was placed in the receiver compartment. Cell uptake in the presence of inhibitors was expressed as a percentage of drug accumulation in control conditions.

2.2.5. Drug release studies

Drug release from cell layers pre-loaded with the test compounds (10 µM) from either the apical or basolateral side was investigated with blank HBSS in contralateral compartment. After 45 minutes of incubation, the compound solution and HBSS was aspirated from the donor and receiver compartment, respectively. The cell layers were given a quick wash with cold PBS, three times. They were then exposed to 500 µL HBSS with or without inhibitors (MPP^+- 500 µM, TEA - 5 mM or Probenecid – 100 µM) from both the apical and basolateral sides. The release of the accumulated compound was studied by collecting 50 µL of sample from both compartments over a period of 2 h. Each sample was replaced with 50 µL of either blank or inhibitor containing

HBSS. The effect of inhibitors on drug release was presented as % of drug release in comparison to the control group.

2.2.6. Bioanalysis

2.2.6.1. *In vitro* study samples

The study samples (50 µL) were processed with the addition of 150 µL of chilled methanol containing 5 nM of the internal standard (tolbutamide for metaprolol, ipratropium for tiotropium and salbutamol, and glycopyrronium for all other compounds). The samples were vortexed and centrifuged at 10,000 rpm for 10 minutes at 4^{o}C. The resulting supernatant was mixed with 0.1% v/v formic acid (1:1 v/v) and 10 µL of this was injected into the Quattro Ultima triple-quadrupole mass spectrometer (Micromass, UK) interfaced via an electrospray ionization probe with Agilent (1100 Series, Agilent Technologies) HPLC system.

Standard working stocks of various compounds were prepared in methanol and a 12 - point calibration curve (CC) was prepared in HBSS. Sample quantitation was achieved by fitting curves to a weighted linear regression (1/concentration or 1/concentration^{2}). Quality control (QC) samples prepared in blank HBSS were interspersed between study samples to monitor batch performance. Batch acceptance was set at within ± 20 % of the nominal concentration for each standard and QC sample.

Chromatographic separation was achieved using a mobile phase consisting of methanol: water with 0.1% v/v formic acid. The flow rate was set at 0.3 mL/min. The sample temperature was kept at 4^{o}C, and the column temperature was set at 40^{o}C. Details of chromatographic conditions, calibration curve range, and lower limit of quantitation (LLOQ) were mentioned in Appendix A.

2.2.6.2. *In vivo* study samples

These samples were analysed at XenoGesis Ltd, BioCity Nottingham, UK. Lung homogenates (50 µL) were precipitated with the addition of methanol (200 µL) containing the internal standard (tolbutamide – 10 nM). The samples were mixed on a Bio Shake for 2 minutes at 2000 rpm. The samples were then centrifuged at 10,000 rpm for 20 minutes at 4^{o}C and the supernatant was

injected into the LC-MS/MS system. Standards and quality control samples were processed in a similar manner after spiking compound stocks prepared in methanol into blank matrices. Batch acceptance was set at within ± 20 % of the nominal concentration for each standard and QC sample.

For both *in vitro* and *in vivo* study samples, analytes were detected in the positive ionization mode and data acquisition was carried out by using multiple reaction monitoring. Instrument control and data acquisition were performed by MassLynx software packages (version 4.1). Data processing and analysis were performed using the QuanLynx software. LC-MS/MS details and representative calibration curves of various compounds are presented in the Appendix D and Appendices E - P, respectively. Stability in HBSS was confirmed for compounds following their storage in – 20^{o}C for 7 days (Appendix Q), which was the study samples storage condition before subjecting them for LC-MS/MS analysis.

2.2.7. Lysosomal sequestration studies

2.2.7.1. Confocal microscopy

LysoTracker^{TM} Green (LTG) accumulation in Calu-3 cells, alone or in the presence of various molecules, was qualitatively assessed using confocal laser scanning microscopy as described previously (Ufuk et al. 2015). LTG incubations were also performed in the presence of known cytosol - lysosomal pH gradient disruptors, bafilomycin A1, monensin or NH_4Cl.

Clear bottom Ibidi 8-well chambers were seeded with 0.2 mL of Calu-3 cell suspension (0.5 × 10^5 cells/mL). Cells were allowed to attach to the surface by incubating the chambers in a humidified incubator at 37^{o}C under 5% CO_2. LTG (100 nM) solution was prepared alone (control) and in combination with known cytosol - lysosomal pH gradient disruptors or test molecules in HBSS, such that the DMSO concentration in the final solution was < 1% v/v. For NH_4Cl, bafilomycin A1 and monensin, the concentration in the incubation mixture was maintained at 10 mM, 100 nM and 20 µM, respectively. Test molecules were included at 10 µM and consisted of representative examples of quaternary, dibasic, and zwitterionic molecules. Imipramine (10 µM) was included as a

representative of cationic amphiphilic drug (CAD), which was showed previously to lower the fluorescence of LTG (Ufuk et al. 2015).

On reaching suitable confluency, Calu-3 wells were washed with 200 µL of warm HBSS and were treated with LTG alone or LTG with known cytosol - lysosomal pH gradient disruptors or test molecules and incubated for 1 hour at 37ºC in a humidified incubator under 5% CO_2, with protection from light exposure. At the end of the incubation, the LTG solution was removed and cells were washed 3 times with cold HBSS. Cells were treated with FluoroBrite DMEM media (Gibco® FluoroBrite™, ThermoFisher Scientific, UK) and subjected to confocal laser scanning microscopy. LTG accumulation in Calu-3 cells were visualised using a Zeiss LSM 510 confocal laser microscope (Jena, Germany) with a Plan-Neofluar 10×/0.3 NA (numerical aperture) water immersion objective and helium/neon laser. Zeiss LSM Image Browser (version 3, 5, 0, 359) was used for processing the images.

2.2.7.2. Quantitation of LysoTracker™ Green accumulation in Calu-3 cells

The LTG fluorescence intensity in Calu-3 cells was measured upon co-incubation with various compounds, as reported previously with minor modifications (Kazmi et al. 2013). For this, collagen-coated 96-well microtiter plates were seeded with 100 µL of Calu-3 cell suspension (3.2× 10^5 cells/mL) and managed in a humidified incubator at 37ºC under 5% CO_2 for 48 hours. Before the experiment, the media was removed, and cells were washed with 100 µL of warm HBSS solution. LTG solutions (100 nM) were prepared alone or in combination with various compounds or known cytosol-lysosomal pH gradient disruptors as mentioned above. Also, the effect of incubation conditions on LTG sequestration, such as co-incubation only, pre- and co-incubation pre-incubation only was tested with cytosol-lysosomal pH gradient disruptors or imipramine. For co-incubation only group, Calu-3 cells were incubated with solutions containing both, LTG and pH gradient disruptors. While for pre- and co-incubation conditions, Calu-3 cells were pre-incubated with pH gradient disruptors for 30 minutes, before continuing incubations with solutions containing both, LTG and pH gradient disruptor for another 30

minutes. For pre-incubation only group, solution containing pH gradient disruptor was withdrawn from Calu-3 cells following 30 minutes of exposure, cells were washed with HBSS and incubations with solutions with LTG only were continued for 30 minutes.

Compounds from each chemical class were tested at 5 different concentrations (3.125 to 50 µM; for imipramine – 6.25 to 200 µM) for evaluating their concentration dependent effect on LTG fluorescence intensity. After addition of LTG containing solutions, the cells were incubated in quadruplicate for 30 minutes in a humidified incubator at 37^{o}C under 5% CO_2. Post incubation, solutions were removed, and the cells were washed three times with cold-HBSS. The cells were treated with chilled acetonitrile and the samples were then subjected to fluorescence measurement at an excitation and emission wavelengths of 470 and 520 nm respectively, using a multimode microplate reader Spark® 10M (Tecan). Cells treated only with HBSS were included to measure the background fluorescence and subtract it from that of LTG and compound treated cells. Reduction in fluorescence by the various compounds is reported as % of fluorescence in cells exposed to LTG alone.

2.2.8. Cellular partition coefficient (K_p)

The uptake of various compounds in undifferentiated Calu-3 cells was investigated at 5 µM. Incubations were also performed in the presence of bafilomycin A1 (100 nM) or monensin (20 µM). Imipramine was included as a positive control, for which cellular accumulation has been well characterised in various cell types (Ufuk et al. 2017; Ufuk et al. 2015).

Cell culture treated 24-well plates, were seeded with 0.5 mL of Calu-3 cell suspension (3.2× 10^5 cells/mL) and incubated for 3 days in a humidified incubator at 37^{o}C under 5% CO_2. Cell growth media was removed from the wells and Calu-3 cells were washed with warm HBSS. Uptake studies were initiated with the addition of a 0.5 mL of drug containing HBSS solution and plates were incubated on an orbital shaker (60 rpm) at 37^{o}C in a 95% air, 5% CO_2 environment. The experiment was conducted in quadruplicate. At various time points post incubation, i.e. 2, 5, 10, 15, 30, 45, 60 and 120 minutes, a buffer sample (100 µL) was collected from each well for determination of the

extracellular concentration and diluted appropriately using blank HBSS. The cell uptake was terminated by discarding the remaining drug solution and washing cells quickly with cold PBS three times. The cells were then lysed with the addition of 200 µL of ice-cold methanol. Both the buffer and cell lysate samples were matrix matched and stored at -20^{o}C until LC-MS/MS analysis.

The ratio (K_p) of total compound concentration in cell lysate (C_{cell}) and media (C_{media}) was calculated at various time points as mentioned below,

$$K_p = \frac{\text{Concentration in cells } (C_{cell})}{\text{Concentration in buffer } (C_{buffer})}$$

C_{cell} was calculated by dividing the total amount of compound measured in cells with the cell volume.

The cell volume was calculated using the protein concentration based on a reported value of 8.4 µL/mg protein for Calu-3 cells (Ingoglia et al. 2016). The protein concentration was measured using Coomassie (Bradford) protein assay reagent as mentioned in section 2.2.13.

2.2.9. Isolation of lysosomes from Calu-3 cells and quantification of lysosome associated concentrations

Calu-3 cells were grown in 25 cm^2 cell culture flasks for 6-7 days (~90% confluency) in a humidified incubator at 37^{o}C under 5% CO_2. Test solutions were prepared in HBSS alone or in combination with pH disruptors as mentioned in experimental details for LysoTracker^{TM} studies.

Upon reaching confluency, Calu-3 cells were washed with warm HBSS and incubated with compound containing solutions for 1 hour. Following this, cells were washed three times with cold HBSS and treated with 0.5 mL of Accutase® to detach the cell layers. The cell suspension was collected on ice by adding 1.5 mL of cold PBS and centrifuged at 800 g for 2 minutes at 4^{o}C. The resulting cell pellet was processed using Lysosomal Enrichment Kit (ThermoFisher Scientific, UK) as per the manufacturer's instructions, to generate a post-nuclear supernatant (referred as total cell lysate now onwards). A portion of

this supernatant (100 µL) was preserved for measuring the % of compound in total cell lysate and determining the % of lysosome recovery in the various isolated lysosomal fractions.

A discontinuous density gradient was prepared (30, 27, 23, 20 and 17% v/v) by mixing the gradient dilution buffer with 60% of OptiPrep™ medium and layered in ultracentrifuge tubes in descending concentrations. Total cell lysates were placed on top of the density gradient after mixing with the OptiPrep™ medium and were subjected to ultracentrifugation at 145,000g for 2 hours at 4°C.The resulting supernatant was collected into individual tubes as 1 mL fractions and kept on ice. To reduce the concentration of OptiPrep™ medium in the final lysosomal fractions, an equal volume of cold PBS was added to the tubes and these were centrifuged at 18000 g for 30 minutes at 4°C. The supernatant was removed, and the final lysosomal pellet was reconstituted in 150 µL of PBS. Compound concentrations in total cell lysate and lysosomal fractions were measured using LC-MS/MS.

The recovery of lysosomes in supernatant fractions was determined by measuring the activity of acid phosphatase, a lysosomal specific enzyme, using a commercially available kit (Sigma-Aldrich, UK). Various components of the assay such as substrate solution, stop solution and standard solutions were prepared according to the manufacturer's instructions. In brief, 50 µL of supernatant samples or total cell lysate was mixed with an equal volume of substrate solution and incubated at 37°C for 15 minutes. The reaction was terminated by adding the stop solution (200 µL) and the absorbance of the final mixture was measured at 405 nm. The absorbance of a standard solution was also measured in order to calculate the acid phosphatase activity in unknown samples as mentioned below,

Acid phosphatase activity (units/mL) =

$$\frac{\{\text{Absorbance}_{(\text{sample})} - \text{Absorbance}_{(\text{blank})}\} \times 0.05 \times 0.3}{\{\text{Absorbance}_{(\text{standard})}\} \times \text{incubation time (min)} \times V_{enz}}$$

0.05 = concentration (µmole/mL) of 4-nitrophenol in the standard solution

0.3 = total assay volume (mL)

V_{enz} = volume of enzyme sample added to the assay in mL

The recovery of lysosomes in various supernatant fractions was calculated as % of the acid phosphatase activity recovered in the fractions in comparison with that in the corresponding total cell lysate.

2.2.10. Unbound fraction of compounds in Calu-3 cell lysates

The binding of compounds to total cell lysates of Calu-3 cells was measured using Rapid Equilibrium Dialysis devices, as per the manufacturer's instructions.

Briefly, Calu-3 cell lysate (150 µL) mixed with the test compound (5 µM) and blank HBSS (350 µL) was transferred to the homogenate and buffer chambers, respectively. The samples were dialysed at 37^{o}C for 4 hours at 60 rpm. At the end of the experiment, equal volumes were collected from both chambers, samples were matrix matched and stored at -20^{o}C until LC-MS/MS analysis.

The unbound fraction in homogenate ($f_{u,\,hom}$) was determined as,

$$f_{u,hom} = \frac{\text{Concentration in buffer } (C_{buffer})}{\text{Concentration in homogenate } (C_{homogenate})}$$

2.2.11. Lung retention of compounds, *in vivo*

Animal experiments were conducted in accordance with UK Home Office regulations under the Animals (Scientific Procedures) Act 1986. These studies were conducted at Saretius Ltd, Science and Technology Centre, University of Reading, UK. Compound retention in rat lungs following intratracheal instillation was assessed as described previously (Backstrom, Boger, et al. 2016), with minor modifications. Briefly, male CD rats (225-250g) were anaesthetised using isoflurane (Merial Animal Health Ltd, UK) and placed on a board angled at 45 degrees. Compounds were solubilised in PBS and introduced into the trachea at a dose of 1 mL/kg using a customised cannula. In order to reduce the usage of animals, all four compounds (DS12, DS13,

DS81 and DS86) were mixed to give a final dose strength of 0.2 mg/ml except for DS12 (0.1 mg/mL, due to solubility limitation). At various time points (0.167, 0.5, 1, 3, 5, 8, 24 and 48h post dosing), animals were sacrificed using a schedule 1 method (CO_2). Lungs were collected, homogenised in PBS (1:3 w/v) and stored at -20^oC until analysis using LC-MS/MS. The resulting lung concentrations were plotted against time and the lung absorption half-life ($t_{1/2}$) was calculated using the terminal portion of the curve.

2.2.12. Cytotoxicity assessment

CellTitre 96® AQueous One Solution Reagent (Promega, Madison, WI) containing a tetrazolium compound (MTS) and an electron coupling phenazine ethosulfate was used to assess the metabolic activity of cells following incubation of Calu-3 cells with various compounds. Collagen-coated 96-well microtiter plates seeded with 100 µL of Calu-3 cell suspension (3.2×10^5 cells/mL) and incubated at 37^oC in a humidified incubator at 37^oC under 5% CO_2 for 48 hours. Calu-3 cells were incubated with various compounds in quadruplicate and incubated for 30 minutes. Each compound was tested for its effect on cell metabolic activity using the highest concentration employed in the various assays. Under similar conditions, cells treated with 0.6% v/v Triton X-100 were included as a positive control. Following incubation with the test compounds, a 20 µL of the MTS containing reagent was added to the wells and incubated for 3 hours in a humidified incubator at 37^oC under 5% CO_2. At the end of the incubation, the formation of a soluble formazan product, indicator of metabolically active cells, was measured at 490 nm using multimode microplate reader Spark® 10M (Tecan). The absorbance between compound treated and untreated cells (control) was compared to assess the effect of various compounds on Calu-3 cell metabolic activity. None of the test or standard compounds included in various investigations in the current study affected Calu-3 cell viability (Appendix B).

2.2.13. Total protein quantitation

Cell lysates (5 µL) collected either from Transwells® inserts or tissue culture well plates were mixed with 250 µL of Coomassie (Bradford) Protein Assay reagent (Thermo Scientific™). The resulting solution was mixed for 30 seconds

and incubated at room temperature for 10 minutes. At the end of the incubation period, the absorbance was measured at 595 nm with a multimode microplate reader Spark® 10M (Tecan). Standard solutions were prepared by dissolving bovine serum albumin in milli-Q water. The blank corrected absorbance of the various standard solutions was plotted against their respective concentration (100 – 1500 µg/mL) to obtain a standard curve. The protein concentrations of blank corrected unknown samples were determined using the standard curve (Appendix C).

2.2.14. Statistical analysis

The results are presented as mean ± standard deviation (n = 3 - 4). GraphPad Prism version 7 was used for statistical analysis. The normal distribution of initial transport and uptake data consisting of $n > 5$ was confirmed by testing for normality with Prism and thereafter, assumed for all data sets with $n < 5$. Unpaired t-test was used to compare two groups and ANOVA with Dunnett's multiple comparison test was used for more than 2 groups. A p value < 0.05 or < 0.01 or < 0.001 or < 0.0001 was considered as indicative of statistical significance and represented with an asterix * or ** or *** or ****, respectively.

Chapter Three

3. Cellular disposition of anticholinergic bronchodilators - Role of drug transporters

3.1. Introduction

Anticholinergic bronchodilators are the first line therapeutic agents in the pharmacological management of Chronic Obstructive Pulmonary Disease (COPD) (GOLD 2018). In order to maximise local drug concentrations in the lung with reduced systemic exposure, these drugs are administered by inhalation. Although their quaternary ammonium structure renders these molecules too polar to cross biological barriers, their engagement with the drug target on airway smooth muscles and their rapid absorption (Ensing et al. 1989; Hohlfeld et al. 2014; Leusch et al. 2001) (T_{max} ~ 5 minutes) following inhalation demonstrate their ability to cross the lung epithelial barrier. However, the absorption mechanism, i.e., drug transporter-mediated vs passive diffusion is not entirely clear.

The lungs express a range of transporters belonging to both the ATP-binding cassette (ABC) and solute carrier (SLC) families (Bleasby et al. 2006; Sakamoto et al. 2013). It has been hypothesised that polyspecific organic cation transporters and carnitine/cation transporter proteins (OCTs/OCTNs) belonging to the SLC22 superfamily of drug carriers, may play a role in the lung disposition of the anticholinergic bronchodilators (Koepsell, Lips, and Volk 2007). The short-acting ipratropium and the long-acting tiotropium are indeed recognised substrates for OCT1, OCT2 and OCTN2 while OCT3 only transports ipratropium and the OCTN1 subtype has a low affinity for both compounds (Hendrickx et al. 2013; Nakanishi et al. 2011; Nakanishi et al. 2013). Interactions between the more recently approved long-acting glycopyrronium and OCTs have not been systematically explored to date.

Nevertheless, OCT1 and OCT2 are known to transport the drug (Hendrickx et al. 2013).

In agreement with uptake experiments in OCT/OCTN transfected cells, it has been shown that both ipratropium and tiotropium are internalised by the human bronchial epithelial cell line BEAS-2B via an OCTN2-mediated mechanism (Nakamura et al. 2010). In addition, the transporter was also reported to be involved in the accumulation of the short-acting bronchodilator in the tracheal epithelium of mice *in vivo* (Nakanishi et al. 2013). More recently, a study in various lung epithelial cell lines highlighted the role of the OCT/OCTN carriers in the intracellular accumulation of ipratropium, with different subtypes playing a prominent role depending on the cell line (Al-Jayyoussi et al. 2015).

However, in contradiction with drug uptake data, the absorption of ipratropium in isolated perfused rat lungs (IPRL) following intra-tracheal delivery was unaffected by a pre-administration of a high concentration of the drug or of the OCT1-3 inhibitor MPP^+, suggesting it is primarily mediated by passive diffusion (Al-Jayyoussi et al. 2015). Drug uptake studies in undifferentiated lung cells and absorption measurement in intact lungs therefore led to contradictory conclusions regarding the role of drug transporters in the transepithelial permeability of anticholinergic bronchodilators.

Due to their low intrinsic permeability across cell membranes, charged molecules may exploit uptake and efflux transporters to enter or exit the cells, respectively (Proctor et al. 2016). To unravel the role of transporters in the permeability of drug molecules across biological barriers, epithelial monolayer systems are considered invaluable. For instance, the potential impact of carrier-mediated transport on the oral bioavailability of various cationic molecules was demonstrated in intestinal Caco-2 monolayers (Bourdet and Thakker 2006; Han et al. 2015). However, to date, no such systematic investigation has been undertaken with inhaled cationic anticholinergic bronchodilators in a permeability model that anatomically represents the lung epithelium.

Amongst available human airway in vitro models, the bronchial epithelial cell line Calu-3 is the most extensively used for investigating drug transport

characteristics (Forbes and Ehrhardt 2005; Ong, Traini, and Young 2013). When cultured at an air-liquid interface (ALI) on permeable supports, Calu-3 cells form tight layers that resemble the native bronchial epithelium (Grainger et al. 2006; Min et al. 2016) and are able to predict drug absorption in rat lungs (Mathia et al. 2002). Importantly, Calu-3 layers express the range of drug transporters found in normal human bronchial epithelial cell layers grown in similar conditions if maintained for 21 days at the ALI (Hutter et al. 2014). More specifically, the same OCT subtypes were present in both models, i.e., OCT1, OCT3, OCTN1 and OCTN2 with an OCT activity detected on the apical side of the Calu-3 layers (Mukherjee, Pritchard, and Bosquillon 2012). Furthermore, the functionality of OCT1, OCT3 and OCTN2 has also been confirmed in undifferentiated Calu-3 cells (Ingoglia et al. 2015, 2016).

However, Calu-3 cells showed time and passage number dependent barrier properties when managed under ALI conditions (Haghi et al. 2010). This was also reflected by a variety of TEER values (range - 300 to 2500 $\Omega.cm^2$) reported in the literature suggesting inter-lab variations in cell culture practices (Forbes and Ehrhardt 2005; Forbes 2000). Various cell culture conditions including seeding density, duration of culture, media composition, and membrane support were shown to influence cell morphology, tight junction formation and transporter expression in *in vitro* cell models of gastrointestinal tract as well (Behrens and Kissel 2003; Briske-Anderson, Finley, and Newman 1997). Hence in order to use the Calu-3 cell line for investigating drug disposition mechanisms, it is highly recommended to standardise this cell line in terms of its barrier properties (Forbes and Ehrhardt 2005; Gordon et al. 2015).

3.2. Aims

In this chapter, we hypothesized that investigating the permeability characteristics of the anticholinergic bronchodilators in differentiated ALI Calu-3 layers would clarify the role of the OCTs/OCTNs in their fate in the lungs. The barrier properties of the Calu-3 layers were first assessed in order to confirm their suitability for drug transport studies. Thus, the main objectives of these investigations included,

- Manage Calu-3 layers under ALI conditions using established procedures and demonstrate the formation of tight junctions by measuring the TEER and the permeability of paracellular and transcellular makers.
- Study the bi-directional transepithelial drug transport of anti-cholinergic bronchodilators across Calu-3 layers.
- Investigate the role of transporters in the cell uptake and permeability of ipratropium across Calu-3 layers.
- Study the intracellular accumulation and release of ipratropium in differentiated layers of Calu-3 in the presence or absence of various transporter inhibitors. This was to gain a deeper understanding of the involvement of drug transporters and their interplay in the drug disposition across the lung epithelial barrier.

3.3. Results

3.3.1. Barrier properties of Calu-3 layers

The measurement of TEER values was initiated from the 3rd day of seeding of cells in Transwells® and the values were recorded on every alternate day until the 21st day of post seeding. Calu-3 layers developed tight junctions as a function of time, reaching a TEER value of 1079 ± 191 Ω.cm^2 (mean ± SD, n=12) by day 7 of post-seeding on Transwells® (Figure 3-1). From day 14 onwards the electrical resistance values were stabilised and reached a steady state TEER values of 1412 ± 136 Ω.cm^2 by day 21 after seeding (Figure 3-1). These TEER values were comparable with earlier reports (Mathia et al. 2002) and suggested the presence of optimal electric properties. The apparent permeability (P_{app}) of FITC-dextran, a paracellular maker (FD-4, average molecular weight ~ 4000) and metoprolol, a passive transcellular permeability marker was measured across the Calu-3 layers, in both the absorptive (apical-basolateral, *a-b*) and secretion (basolateral-apical, *b-a*) directions. FD-4 showed a P_{app} value of 0.230 ± 0.079 and 0.197 ± 0.013 ×10^{-7} cm/sec in *a-b* and *b-a* directions, respectively (Figure 3-2, A). These values are found to be within 2-fold of reported P_{app} values for FD-4 in the literature (Mathia et al. 2002). Furthermore, metoprolol showed similar P_{app} in *a-b* and *b-a* directions

(9.88 ± 0.92 and 7.85 ± 1.51×10^{-6} cm/sec, respectively) (Figure 3-2, B).These results indicate Calu-3 formed tight junctions and differentiate compounds in terms of their permeability characteristics i.e. paracellular vs transcellular. These results along with previous investigations in our lab (Shemiss 2016, Appendix R; Hutter et al. 2014; Mukherjee, Pritchard, and Bosquillon 2012), where Calu-3 cells were validated in terms of expression of transporter proteins relevant for inhaled drug therapy such as OCT1, OCT3, OCTN1 and OCTN2, support using Calu-3 layers maintained for 21-days under ALI conditions for drug transport studies.

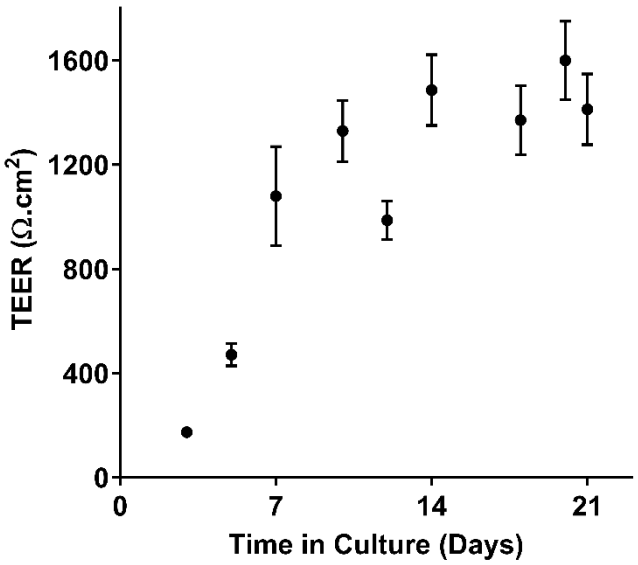
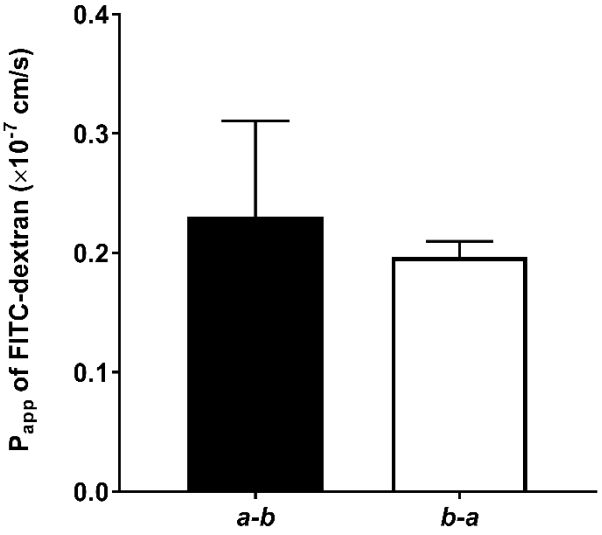


Figure 3-1. TEER profiles for Calu-3 layers

Calu-3 cells were seeded at a density of 1 × 10^5 cells/cm^2 and cultured on 12-well Transwell® inserts for 21 days under air-liquid interface culture conditions in a humidified incubator at 37°C under 5% CO_2. TEER values were measured across Calu-3 layers starting from day 3 of seeding until 21st day, using EVOM meter with chopstick electrodes. These values were normalised to the area of the Transwell® insert (1.12 cm^2) after adjusting for the resistance of the filter (~ 150 Ω. cm^2). Each data point is the mean ± SD of 12 Transwell® inserts from a single experiment.

A



B

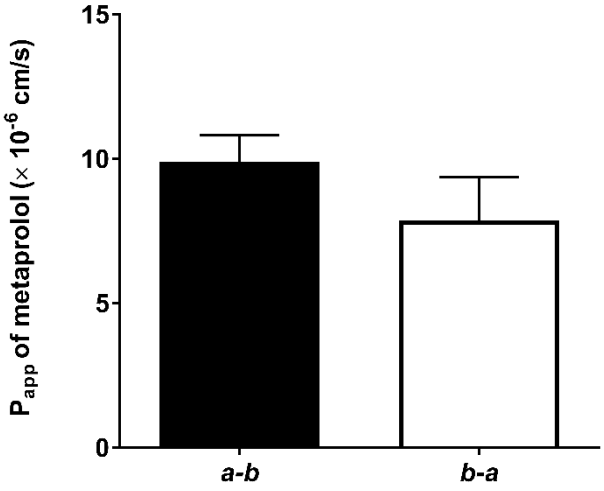


Figure 3-2. Permeability characteristics of paracellular (FITC-dextran) and transcellular (metaprolol) markers across Calu-3 layers

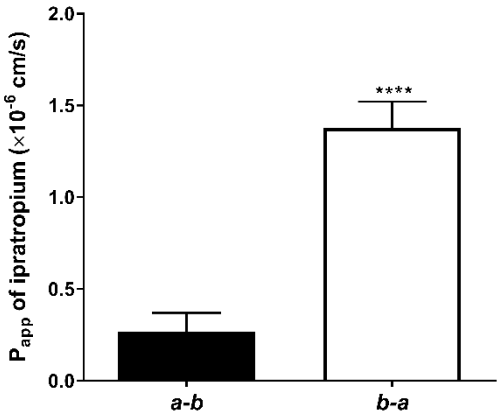
Calu-3 cells were seeded at a density of 1 × 10^5 cells/cm^2 on 12-well Transwell® inserts and cultured under air-liquid interface culture conditions in a humidified incubator at 37ºC under 5% CO_2. (A) The coefficient of apparent permeability (P_{app}) of FITC-Dextran (average molecular weight ~ 4000 Da, 0.5 mg/mL) was determined in the apical to basolateral (*a-b*) and basolateral to apical (*b-a*) direction across Calu-3 layers. For *a-b* study, data are represented as the mean ± SD of ten layers from three independent experiments; for *b-a,* data are represented as the mean ± SD of three layers from a single experiment. (B) The coefficient of apparent permeability (P_{app}) of metaprolol was determined at 10 µM in the *a-b* and *b-a* direction across Calu-3 layers. Data are represented as the mean ± SD of four layers from a single experiment.

3.3.2. Drug transport studies

The bi-directional permeability of the three anticholinergic bronchodilators ipratropium, tiotropium and glycopyrronium was measured in ALI Calu-3 layers at a concentration of 10 µM. A similar asymmetrical transport was observed for all anticholinergic drugs with, surprisingly, the P_{app} ($\times 10^{-6}$ cm/s) in the *b-a* direction found to be significantly higher than in the opposite direction: 1.38 ± 0.14 vs. 0.27 ± 0.10 for ipratropium; 1.19 ± 0.18 vs.0.22 ± 0.07 for tiotropium and 1.09 ± 0.1 vs 0.23 ± 0.06 for glycopyrronium, giving efflux ratios of 5.1, 5.4 and 4.7 respectively (Figure 3-3, A, Figure 3-3, B).

As a common mechanism of transepithelial transport was suspected for the three bronchodilators, the study was pursued with only ipratropium. Concentration dependent permeability measurements showed a trend towards a decrease in *a-b* transport with an increase in the apical donor concentration, the P_{app} value being significantly lower at 100 and 300 µM than at 10 µM (Figure 3-4, A). In contrast, increasing ipratropium basolateral concentration up to 300 µM had no effect on its secretory P_{app} (Figure 3-4, B).

A



B

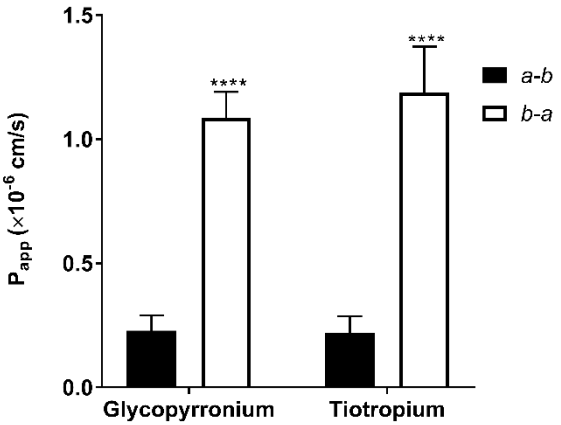
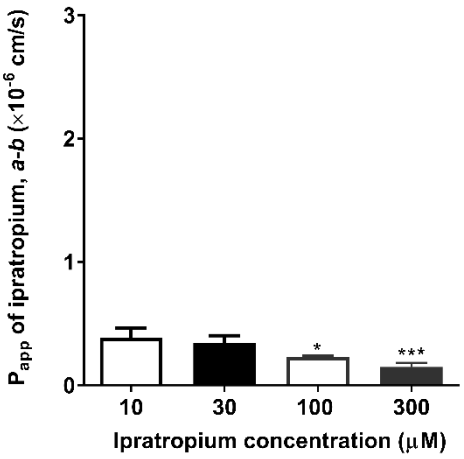


Figure 3-3. Permeability of anticholinergic bronchodilators across Calu-3 layers.

Calu-3 cells were seeded at a density of 1 × 10^5 cells/cm^2 and cultured at 37ºC under air-liquid interface culture conditions for 21 days on 12-well Transwell® inserts in a humidified incubator under 5% CO_2. (A) Coefficient of apparent permeability (P_{app}) of ipratropium measured in Calu-3 cell layers in the apical to basolateral (*a*-*b*) and basolateral to apical (*b*-*a*) direction at a concentration of 10 µM. Each data point represents mean ± SD of thirteen layers from four independent experiments. (B). Coefficient of apparent permeability (P_{app}) of glycopyrronium and tiotropium measured in Calu-3 cell layers in the apical to basolateral (*a*-*b*) and basolateral to apical (*b*-*a*) direction at a concentration of 10 µM. Data are presented as the mean ± SD of four layers from a single experiment. **** indicates a statistically significant higher permeability in the *b*-*a* than *a*-*b* direction ($p<0.0001$).

A



B

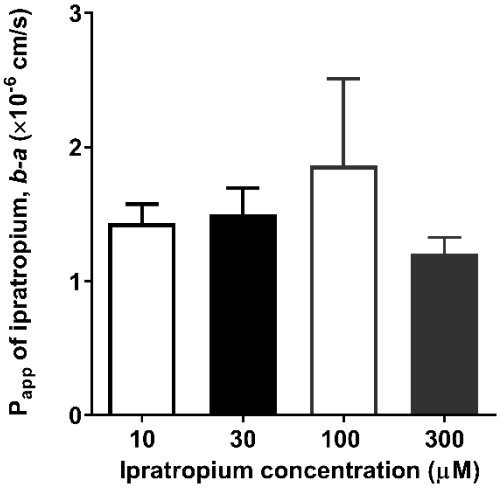


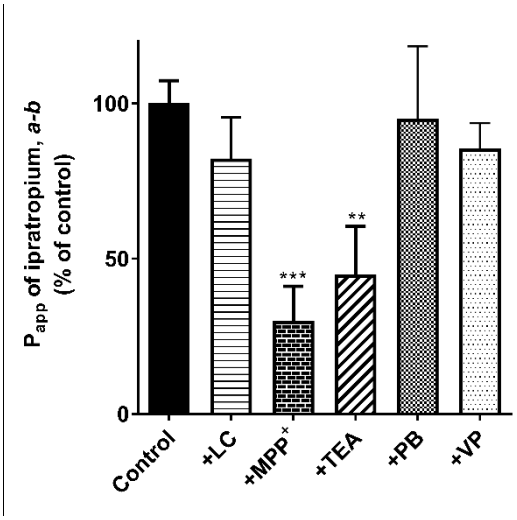
Figure 3-4. Concentration-dependent permeability of ipratropium across Calu-3 layers.

Calu-3 cells were seeded at a density of 1 × 10^5 cells/cm^2 and cultured for 21 days on 12-well Transwell® inserts under air-liquid interface culture conditions in a humidified incubator at 37°C under 5% CO_2. Coefficient of apparent permeability (P_{app}) of ipratropium measured over a range of concentrations (10 – 300 µM) in Calu-3 layers in the apical to basolateral direction, *a-b* (A) and in the basolateral to apical direction, *b-a* (B). Data are presented as mean ± SD of four layers from a single experiment. * indicates a statistically significant lower permeability than at a concentration of 10 µM (* $p<0.05$, *** $p<0.001$).

Ipratropium transport across Calu-3 ALI layers was subsequently studied in presence of a range of drug transporter inhibitors (Figure 3-5). MPP^+ is known to inhibit OCT1-3 without affecting the OCTNs while TEA interacts with all the OCT/OCTN family members (Koepsell, Lips, and Volk 2007). L-carnitine is a recognised inhibitor of the OCTN2 subtype and to a lesser extent of OCTN1 (Koepsell, Lips, and Volk 2007). Due to the apparent efflux observed, inhibitors of the ATP-binding cassette (ABC) family of transporters were also tested, although, to our knowledge, there is no indication in the literature that ipratropium might be one of their substrates. Verapamil is commonly used as a P-glycoprotein (P-gp) inhibitor (Keogh and Kunta 2006) but has also been shown to interfere with the activity of a range of drug transporters, including some of the multidrug resistance proteins (MRPs) (Zhou et al. 2008), multidrug and toxin extrusion (Cazzola et al.) transporters (Otsuka et al. 2005) and all the OCTs (Koepsell, Lips, and Volk 2007). Probenecid is known to inhibit the MRPs without affecting P-gp (Zhou et al. 2008) and although it also interacts with the Organic Anion Transporters (OATs) (Shitara, Sato, and Sugiyama 2005), our group has shown previously that these proteins are not expressed in Calu-3 ALI layers (Hutter et al. 2014).

MPP^+ significantly reduced ipratropium P_{app} in both the absorptive (*a*-*b*) and secretory directions (*b*-*a*), with a similar extent of reduction in permeability in both directions; i.e., ~30% of the control group (Figure 3-5, A and B). Co-incubation of ipratropium with TEA also caused a significant decrease in both P_{app}, supporting a possible role of OCTs in its broncho-epithelial permeability (Figure 3-5, A and B). However, in contrast to MPP^+, the decrease in permeability in the *b*-*a* direction was more pronounced than in the *a*-*b* direction with the P_{app} dropping to 23 or 45% of the control value, respectively (Figure 3-5, A and B). L-carnitine did not alter ipratropium transepithelial transport, ruling out an involvement of OCTN2 in the drug trafficking across the Calu-3 layers (Figure 3-5, A and B). Finally, when the permeability of ipratropium was assessed alongside verapamil or probenecid, both agents caused a significant decrease in its secretory transport without affecting the P_{app} in the *a*-*b* direction, thus abolishing the asymmetric transport observed in absence of inhibitors (Figure 3-5, A and B).

A



B

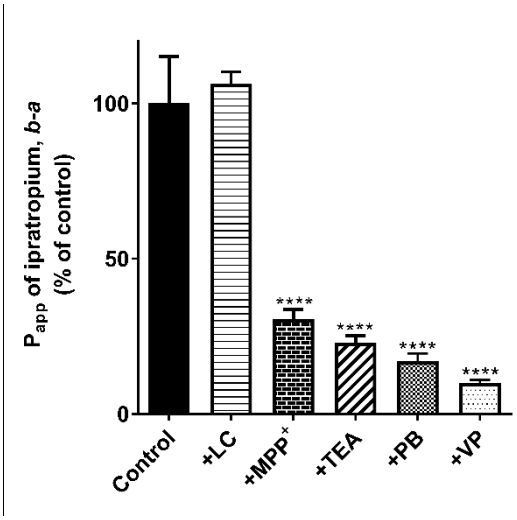


Figure 3-5. Effect of various transporter inhibitors on the permeability of ipratropium across the Calu-3 layers.

Calu-3 cells were seeded at a density of 1 × 10^5 cells/cm^2 and cultured for 21 days on 12-well Transwell® inserts under air-liquid interface culture conditions in a humidified incubator at 37°C under 5% CO_2. Coefficient of apparent permeability (P_{app}) of ipratropium measured at a concentration of 10 µM in the apical to basolateral, *a-b* (A) or the basolateral to apical, *b-a* (B) direction in 21 day old air-liquid interfaced Calu-3 layers in the presence and absence of various transporter inhibitors (L-carnitine, LC – 100 µM; 1-methyl-4-phenylpyridinium, MPP^+ - 500 µM; tetraethylammonium, TEA - 5 mM; probenecid, PB -100 µM; verapamil, VP - 100 µM). For studying the effect of various transporter inhibitors on P_{app} of ipratropium, respective inhibitor was added to both donor and receiver compartments. After each sample collection from the receiver compartment, equal volume of HBSS containing the respective inhibitor was added. Data are presented as mean ± SD of three

layers from a single experiment. * indicates a statistically significant lower permeability than in the control groups (** $p<0.01$, *** $p<0.001$ and **** $p<0.0001$).

3.3.3. Uptake studies

In order to gain a better understanding of the role of transporters in ipratropium trafficking across ALI Calu-3 layers, drug uptake measurements were undertaken in presence or absence of transporter inhibitors (Figure 3-6). As verapamil is known to interact with multiple transporter families, it was not tested as an inhibitor in those studies.

Ipratropium cell-associated concentration was quantified after apical or basolateral exposure over a period of 45 minutes. That was significantly higher when the drug had been added in the apical chamber (Figure 3-6, A and B) up to 15 minutes, likely as a consequence of carrier-mediated internalisation at the air interface. However, cell associated concentrations of ipratropium continued to decline post 20 minutes of incubation. In contrast, following exposure from basolateral side, ipratropium cell associated concentrations increased with incubation time and did not show signs of saturation (Figure 3-6, A and B).

Role of transporters in the uptake of ipratropium was investigated following its exposure from either apical or basolateral for a period of 5 minutes in the presence or absence of various transporter inhibitors. Both the apical and basolateral uptake of ipratropium by Calu-3 layers was significantly inhibited to ~50% of the control in presence of MPP^+ (Figure 3-6, C and D). On the other hand, TEA caused a dramatic reduction (~14 % of control) in ipratropium uptake from the apical side without affecting the uptake from the opposite side (Figure 3-6, C and D). Probenecid impact on ipratropium internalisation was intriguingly similar to that of TEA. Indeed, it largely inhibited the apical uptake (~10% of control) but had no effect on the internalisation from the opposite side (Figure 3-6, C and D). The effect of probenecid is in contradiction with its alleged interactions with an MRP transporter and indicates it interferes with the activity of an uptake transporter in Calu-3 layers.

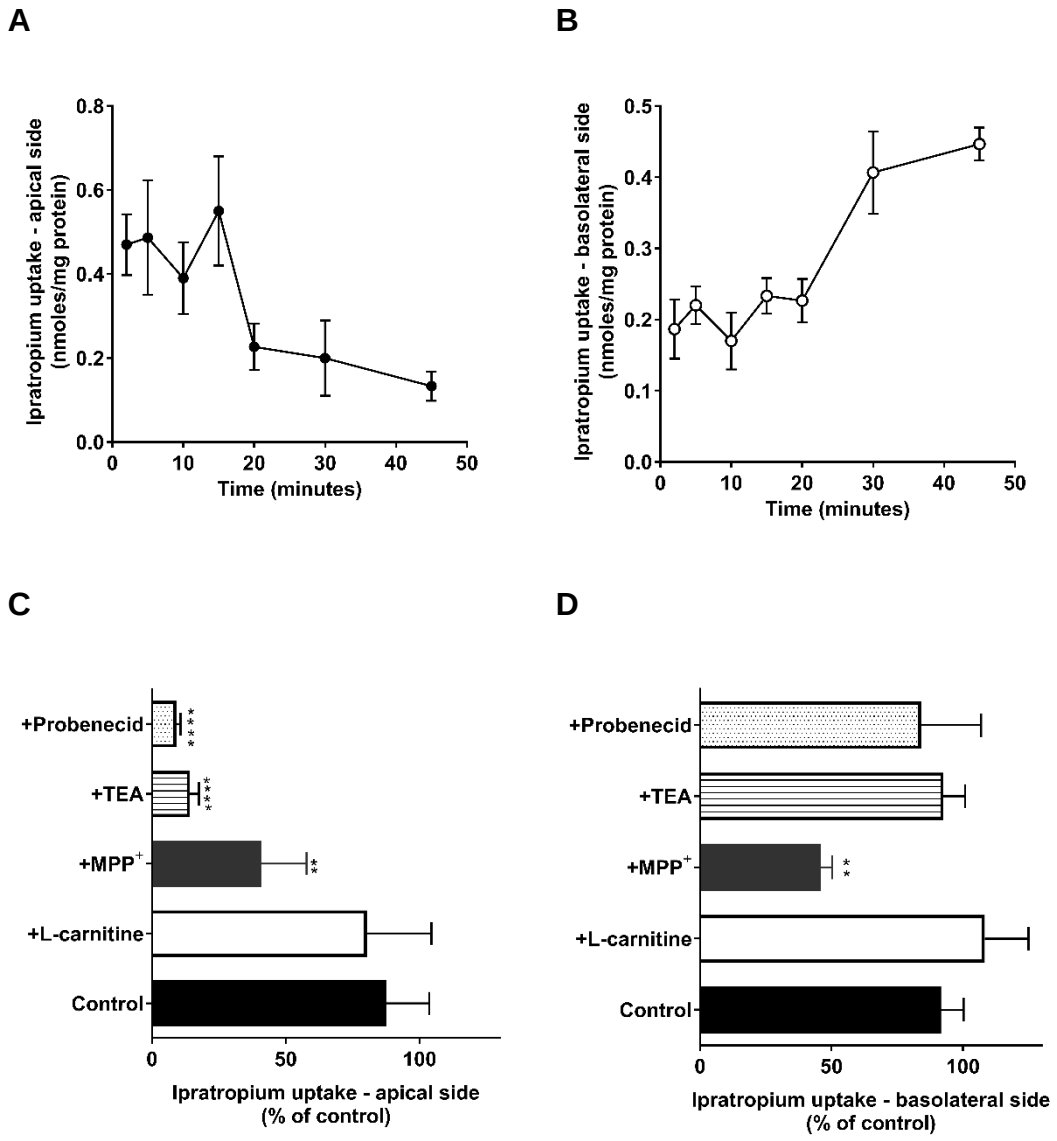


Figure 3-6. Uptake of ipratropium across the Calu-3 layers.

Calu-3 cells were seeded at a density of 1 × 10^5 cells/cm^2 and cultured for 21 days on 12-well Transwell® inserts under air-liquid interface culture conditions in a humidified incubator at 37ºC under 5% CO_2. Ipratropium uptake was measured at a concentration of 10 µM from the apical (A) or basolateral (B) side of 21-day old air-liquid interfaced Calu-3 layers over a period of 45 minutes. Ipratropium uptake was measured at a concentration of 10 µM from the apical (C) or basolateral (D) side of Calu-3 layers following co-incubation for 5 minutes in the presence of various transporter inhibitors (L-carnitine - 100 µM; 1-methyl-4-phenylpyridinium, MPP^+ - 500 µM; tetraethylammonium, TEA - 5 mM; probenecid - 100 µM). For testing the effect of various transporter inhibitors on the uptake of ipratropium, respective inhibitor was added to both donor and receiver compartments. Data are presented as mean ± SD of three layers from a single experiment. * indicates a statistically significant lower uptake than in the control groups (** $p<0.01$, **** $p<0.0001$).

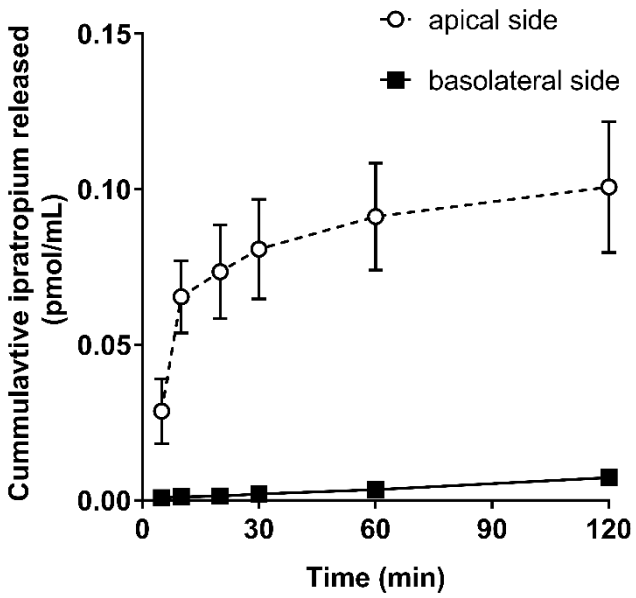
3.3.4. Drug release studies

The ability of ipratropium to be secreted across either membrane of Calu-3 cell layers was assessed following a 45 minute pre-loading from the apical side. Indeed, the drug concentrations in the basolateral compartment were below the quantification limit of the LC-MS/MS method after a 5 minute pre-exposure.

Ipratropium showed a preferential efflux into the apical compartment, the drug apical concentrations being ~ 13 - 60 times higher than in the basolateral chamber throughout the course of the study (Figure 3-7, A), which confirmed the presence of a secretory mechanism across the apical membrane of Calu-3 layers, as suggested by the bi-directional transport studies.

The mechanism behind the efficient secretion of ipratropium at the air-epithelium interface was further explored by monitoring its release into the apical compartment following a 5 minute apical pre-incubation in the presence of inhibitors. Both MPP^+ and TEA significantly reduced the release of intracellular ipratropium into the apical compartment to ~20 % of the control while probenecid caused a ~50% decrease (Figure 3-7, B). This showed that all three inhibitors impacted on transporters involved in both the uptake and release of ipratropium at the luminal side of the Calu-3 cell layers.

A



B

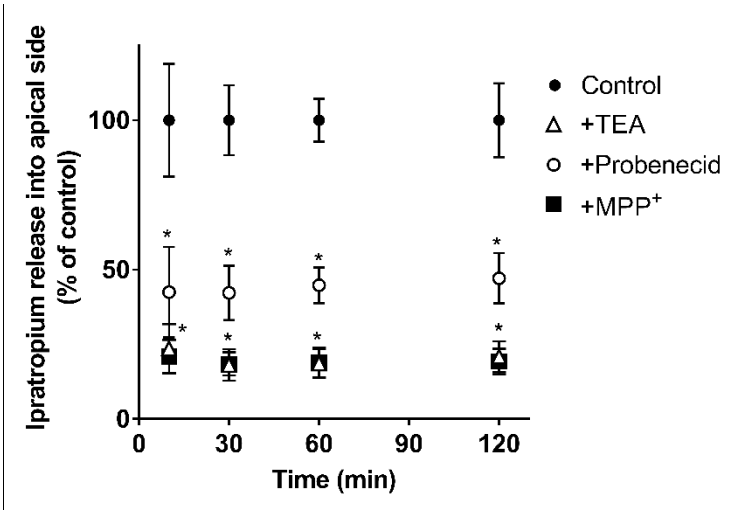


Figure 3-7. Release of pre-loaded ipratropium from Calu-3 layers.

Calu-3 cells were seeded at a density of 1 × 10^5 cells/cm^2 and cultured for 21 days on 12-well Transwell® inserts under air-liquid interface culture conditions in a humidified incubator at 37ºC under 5% CO_2. Release of ipratropium from 21 day old air-liquid interfaced Calu-3 layers into the Transwell® chambers was studied following an apical pre-loading at a concentration of 10 µM. (A) Cumulative ipratropium concentration released into the apical or basolateral chamber over time from Calu-3 layers pre-loaded with ipratropium for a period of 45 minutes. (B) Effect of various transporter inhibitors on the apical release of ipratropium following its pre-loading from the apical side for 5 minutes; (1-methyl-4-phenylpyridinium, MPP^+ - 500 µM; tetraethylammonium, TEA - 5 mM; probenecid - 100 µM). Data are presented as mean ± SD of four layers from a

single experiment. * indicates a statistically significant lower release as compared to the control ($p<0.0001$, represented as * in the graph for clarity).

3.3.5. Effect of organic cations on FITC-dextran permeability

Since it has been suggested organic cations might interact with the negatively charged tight junction proteins, potentially affecting paracellular diffusion (Lee and Thakker 1999), the permeability of FITC-dextran (average molecular weight ~ 4000) across Calu-3 layers was measured with or without ipratropium, TEA or MPP^+ in the test medium. The P_{app} of FITC-dextran was not altered by the presence of ipratropium or TEA but was significantly reduced by MPP^+ (Figure 3-8). This indicates the latest compound might alter the paracellular space and therefore, its impact on ipratropium permeability in the layers must be interpreted with caution. In contrast, TEA and concentration dependent effects on the drug transport can be confidently ascribed to transporter inhibition.

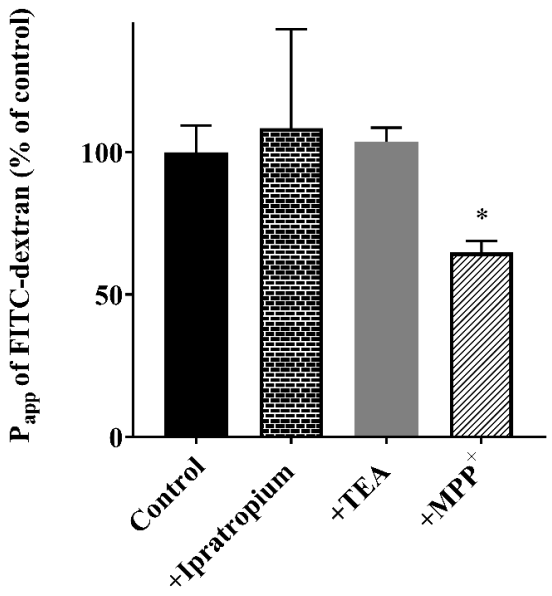


Figure 3-8. Permeability of FITC-Dextran across Calu-3 layers in presence of various organic cations

Calu-3 cells were seeded at a density of 1×10^5 cells/cm^2 and cultured for 21 days on 12-well Transwell® inserts under air-liquid interface culture conditions in a humidified incubator at 37°C under 5% CO_2. Coefficient of apparent permeability (P_{app}, as % of control) of FITC-dextran (average molecular weight ~ 4000 Da) was measured in the apical to basolateral direction (*a-b*) at a

concentration of 0.5 mg/mL in 21 day old Calu-3 layers in presence of the organic cations ipratropium - 300 µM, tetraethylammonium, TEA - 5 mM and 1-methyl-4-phenylpyridinium, MPP^+ - 500 µM. Data are presented as mean ± SD of three layers from a single experiment. * indicates a statistically significant lower permeability as compared to the control (* $p < 0.05$).

3.4. Discussion

The permeation pathway of anticholinergic bronchodilators across the absorption barrier in the lung remains controversial to date. Based on *in vitro* drug uptake studies in undifferentiated cells, it has been proposed OCT/OCTNs facilitate their transport across the airway epithelium (Nakamura et al. 2010). On the other hand, absorption studies in IRPL failed to demonstrate an involvement of the transporters, suggesting it is primarily driven by passive diffusion (Al-Jayyoussi et al. 2015). Given the importance of anticholinergic bronchodilators in the management of COPD, gaining further insight into the mechanisms by which they are processed by lung cells could help optimising their therapeutic benefits.

In this study, we used ALI human broncho-epithelial Calu-3 layers, a physiologically relevant *in vitro* model (Grainger et al. 2006; Min et al. 2016) of intermediate complexity between undifferentiated lung epithelial cells and intact lungs, with the aim to elucidate the role of drug transporters in the pulmonary disposition of inhaled anticholinergics. Expression for OCT1, OCT3, OCTN1 and OCTN2 transporters in the current batch of Calu-3 cells was confirmed by Dr Ligia Shemiss using semi-quantitative PCR studies (Shemiss 2016; Appendix R), as reported earlier from our lab (Mukherjee, Pritchard, and Bosquillon 2012). In the current study, a combination of transepithelial permeability and drug uptake/release measurements were performed in the layers, in presence or absence of drug transporter inhibitors. Our data highlights the existence of different drug transport mechanisms on the apical and basolateral surfaces of Calu-3 cells. It also reveals the absorption of anticholinergic bronchodilators across the bronchial epithelium is likely governed by a complex process involving an inter-play between paracellular passive diffusion and transporter mediated uptake/efflux across the apical cell membrane.

The three anticholinergic bronchodilators tested, i.e., ipratropium, tiotropium and glycopyrronium, exhibited a polarised transport across Calu-3 cell layers, with, unexpectedly, a higher permeability in the *b-a* direction (Figure 3-3). This implies the presence of a secretion mechanism across the layers that is more efficient than absorption processes facilitated by uptake transporters such as OCT/OCTNs. Permeability values were similar for the short acting bronchodilator, ipratropium and the long acting bronchodilators tiotropium and glycopyrronium, reflecting their similar pulmonary absorption profile in vivo (Leusch et al. 2001) and alluding to common disposition pathways across the epithelial barrier in the lung. Interestingly, a similar net secretion has been reported for the prototypical organic cation MPP^+ across Caco-2 layers (Bleasby, Chauhan, and Brown 2000), which suggests different epithelia might handle quaternized molecules in a similar manner.

Increasing ipratropium donor concentrations caused a significant reduction in its permeability in the *a-b* direction while *b-a* transport was unaffected over the range investigated (Figure 3-4). Similar saturable transport has been reported in the absorption direction for hydrophilic cations such as ranitidine and famotidine in the Caco-2 model (Lee and Thakker 1999). Based on cell uptake and permeability measurements over a concentration range, a three-compartment kinetic model was constructed for ranitidine for assessing the relative contribution of transcellular and paracellular pathways in its absorption across intestinal barrier. This model hypothesised a saturable paracellular pathway as the possible mechanism for the observed concentration-dependent permeability of hydrophilic cations (Bourdet, Pollack, and Thakker 2006). Hence, application of such mathematical models with cellular accumulation and permeability measurements of ipratropium may facilitate a better understanding of its absorption mechanisms across the airway epithelium. In the current study, the OCT inhibitors TEA and MPP^+ decreased the ipratropium absorptive transport while all inhibitors tested but L-carnitine limited its secretory permeability (Figure 3-5). It is noteworthy that the effect of MPP^+ on transepithelial transport must be interpreted with caution due to its impact on FITC-dextran permeability (Figure 3-8). These observations nevertheless demonstrated drug transporters play a significant role in

ipratropium asymmetric permeability across Calu-3 layers, although drug uptake and release studies were required to fully understand their contribution.

To account for a suspected high non-specific binding of the drug to cell membranes, ipratropium uptake in the layers was primarily evaluated in presence of inhibitors. However, uptake of ipratropium following exposure from apical or basolateral side over a period of 45 minutes indicated the presence of different uptake mechanisms across Calu-3 layers (Figure 3-6, A and B). While no saturable mechanisms were evident on the basolateral side (Figure 3-6, B), cell associated ipratropium concentrations decreased post 15 minutes of incubations from the apical side (Figure 3-6, A). These results from the apical side are unexpected and are in contradictory to earlier reports where organic cations showed a characteristic steady state uptake in airway epithelial cells (Ingoglia et al. 2015). It is worth noting that Calu-3 layers produce mucus on the apical side and binding of compounds to mucus proteins could influence their permeation as reported earlier, complicating data interpretation (Khanvilkar, Donovan, and Flanagan 2001; Murgia et al. 2018). Further investigations are mandatory to confirm this observation and to understand mechanisms involved across the apical side, preferably with radiolabelled compounds. Nevertheless, the higher cell-associated concentrations measured up to 15 minutes of luminal exposure of the cells to the drug alone as compared to those after a basolateral exposure pointed towards a more efficient transporter-mediated drug uptake from the apical side (Figure 3-6, A). This assumption was confirmed by the reduction in uptake observed in presence of TEA, MPP^+ and probenecid (Figure 3-6). Also, an extensive release of ipratropium in the apical chamber was measured post luminal loading of the cells with the drug which was, in addition, reduced by co-incubation with TEA, MPP+ and probenecid (Figure 3-7). This efficient apical efflux mechanism can explain why, despite a transporter facilitated uptake from the apical side, the *a-b* permeability of ipratropium across Calu-3 layers remains in the same range as that of low molecular weight paracellular markers such as mannitol or fluorescein (Forbes and Ehrhardt 2005).

A plausible hypothesis arising from our data is that, in the absorptive direction, ipratropium is unable to significantly permeate Calu-3 layers by the

transcellular route due to its incapacity to freely diffuse across biological membranes and the absence of an efficient efflux transporter on the basolateral side of the cells. Following transporter mediated uptake, the drug seemed to be shuttled back into the apical compartment, suggesting paracellular diffusion is the predominant process by which it permeates the epithelium (Figure 3-9). A similar 'luminal recycling' has been observed in the intestinal Caco-2 model with the antidiabetic drug metformin, which similarly to ipratropium, is a hydrophilic cation with a low membrane permeability (Proctor et al. 2016). This phenomenon has been proposed to contribute to the drug relatively high oral bioavailability by creating a sustained concentration gradient across the intestinal absorption barrier that enhances its diffusion by the paracellular route. Ipratropium diffusion across Calu-3 layers seems to be equally 'transporter enhanced' since saturation/inhibition of apical transporters resulted in a decrease in its absorptive transport (Figure 3-4, A). In contrast, ipratropium absorption in the IPRL was not influenced by a pre-administration of high concentrations of the drug or the OCT inhibitor MPP^+ twenty minutes before dosing (Al-Jayyoussi et al. 2015). This could be due to the small volume of lung fluid which, in the IPRL, maintains a high concentration gradient across the airway epithelium or to a rapid disappearance of the drug or inhibitor from the epithelium surface in the *ex vivo* model.

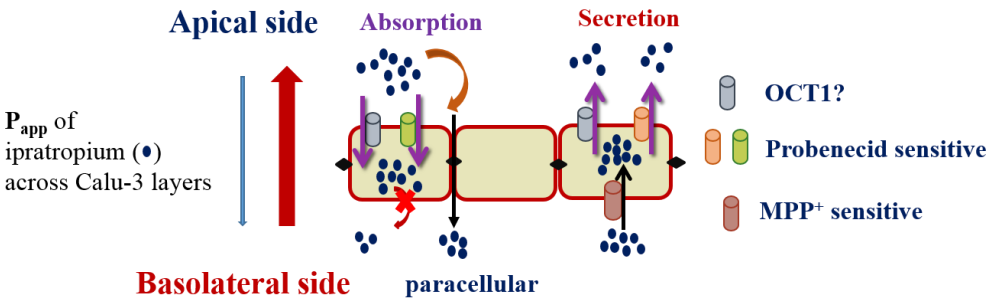


Figure 3-9. Schematic representation of 'luminal recycling' of inhaled organic cation, ipratropium involving various transporter proteins.

Cellular disposition studies of ipratropium in Calu-3 layers in presence or absence of various transporter inhibitors indicated efficient carrier- mediated uptake and release, while its transepithelial permeability was appeared to be limited by the lack of flux across the basolateral side. This could facilitate organic cations to cross airway epithelium through paracellular diffusion.

Importantly, Calu-3 layers provided a unique insight into the mechanism of drug transport from the blood circulation into the lung tissue, which is extremely challenging to investigate in a whole lung model. Ipratropium basolateral uptake was reduced by MPP^+ (Figure 3-6, C), while its *b-a* transport was independent of the concentration over the range studied (Figure 3-4, B), which suggests a low affinity transporter might facilitate its entry into the cells from the basolateral side. One or several efflux transporters apically expressed could then recognise the drug, allowing its translocation across the luminal cell membrane. Our data indicate that, in the secretory direction, the transcellular transport route is rendered possible for ipratropium thanks to the collaboration of drug transporters expressed on both sides of the cell layers. Due to their high OCT-mediated renal clearance (Ensing et al. 1989; Nakanishi et al. 2011; Turck et al. 2004), it is unlikely this process redistributes inhaled anticholinergics back into the lungs following their absorption into the bloodstream. However, such an inter-play between basolateral uptake transporters and apical efflux transporters might play a role in maintaining the pulmonary concentrations of other drug classes. It could also potentially be targeted to promote the accumulation of drugs in the lungs following their systemic administration.

Due to the complexity of the mechanisms controlling the disposition of ipratropium in Calu-3 cell layers and the non-specificity of the inhibitors, identifying the uptake and efflux transporters involved is extremely challenging. Nevertheless, studies with TEA, MPP^+ and L-carnitine support a role for an apically expressed OCT in the 'luminal recycling' of the drug. OCTs are indeed known to transport their substrates in both directions across the plasma membrane according to the concentration gradient (Koepsell, Lips, and Volk 2007). The most probable candidate would be OCT1. Although ipratropium is a substrate for all three OCTs (Hendrickx et al. 2013; Nakanishi et al. 2011; Nakanishi et al. 2013), OCT2 is not expressed in ALI Calu-3 layers (Mukherjee, Pritchard, and Bosquillon 2012) and the drug concentration tested (10 µM) is above its recently reported inhibitory concentration against OCT3 (Chen et al. 2017). In contrast, OCTN2 was reported to be the main transporter responsible for the intracellular accumulation of the drugs in the BEAS-2B cell line and

mice tracheal epithelial cells *in vivo*, likely because its expression is high in those cells in comparison to that of the OCTs (Nakamura et al. 2010; Nakanishi et al. 2013). Moreover, although OCTN2 was shown to be functional in undifferentiated Calu-3 cells (Ingoglia et al. 2016), it is unclear whether its activity is maintained when cells are cultured at an ALI.

The bidirectional ipratropium permeability data with/without inhibitors can nevertheless not be fully interpreted considering the sole activity of OCT1 on the luminal side of the cells. Inhibition studies with probenecid suggest the presence of an unknown uptake transporter together with an efflux transporter sensitive to the drug at the air-epithelium interface. Similarly, the MPP^+ sensitive basolateral uptake transporter remains to be unravelled. Intriguingly, although no data were presented, Koepsell et al noted in their 2007 review that probenecid inhibits the OCTs without being transported (Koepsell, Lips, and Volk 2007). The interactions of probenecid with transporters of organic cations need to be further investigated. Nevertheless, the unidentified apical transporters might potentially be members of the OCT or MATE families. Ipratropium has indeed very recently been recognised as a MATE substrate (Chen et al. 2017). Also, recent studies demonstrated the expression of MATE1 transporters on apical side of airway epithelial cells (Berg et al. 2018). These transporters have been reported to efflux cationic drugs across the apical membrane of hepatocytes and tubular renal cells (Muller et al. 2013). It is however currently unknown whether they are expressed in ALI Calu-3 layers.

Even though current investigations with various chemical inhibitors of transporters provided valuable mechanistic information on inhaled drug-transporter interactions, no individual transporter could be identified. This is one of the limitations of employing various inhibitors of transporter proteins which may cross-react with multiple transporters as noted previously (Wang et al. 2008). In addition, further investigations are required to establish the expression of various transporter proteins such as MATE in Calu-3 layers, which are shown to be present on the apical side of airway epithelial cells (Berg et al. 2018). These studies may help to further standardise the Calu-3 cell system for studying inhaled drug interactions with efflux transporters present in the lungs, in addition to uptake transporter such as OCTs.

3.5. Conclusion

In the current investigation, bidirectional transport and uptake studies in ALI Calu-3 layers were able to reconcile conflicting absorption data in undifferentiated lung epithelial cells and in intact lungs previously reported for the anticholinergic bronchodilators. The data confirm the absorption of ipratropium across the pulmonary barrier is unlikely to be significantly facilitated by drug transporters after pulmonary delivery. However, they highlight a potential role of both uptake and efflux transporters in modulating local drug concentrations in the lungs, which might have implications for the development of future inhaled drugs. In addition, this study showed that the use of simple yet anatomically relevant cell culture models of the airway epithelium is essential to gain understanding on the mechanisms controlling drug disposition in the lungs.

The data presented here thrown some novel insights into cellular disposition mechanisms relevant for inhalational molecules. These include the first demonstration of efficient cellular uptake and secretion mechanisms for anticholinergic bronchodilators across the apical side of bronchial epithelial cells with lack of flux across basolateral side.

However, one of the major limitations of the current investigations is the use of only a single passage of Calu-3 cells in the various uptake or permeability studies. Also, further investigations are required for identifying the driving force for transport of these molecules such as their dependence on extracellular pH, membrane potential and energy dependence which may strengthen the observations reported in the present study.

Chapter Four

4. Application of Calu-3 cells for lysosomal sequestration studies

4.1. Introduction

Many clinically important molecules including inhaled β_2 agonist bronchodilators are basic amines and these molecules have the propensity to accumulate in lysosomes (Kaufmann and Krise 2007). This phenomenon is referred as lysosomotropism, where basic amines upon permeating the lysosomal membrane in uncharged from, undergo ionisation due to low pH conditions and get entrapped due to low permeability of charged protonated forms (de Duve et al. 1974; MacIntyre and Cutler 1988). Lysosomal membrane bound ATP-dependent proton pump (vacuolar H^+ - ATPase) maintains the pH difference between the cytosol (pH~7.2) and the lysosome (pH~5.0) which is a driving force for the accumulation of basic compounds in lysosomes (Kornhuber et al. 2010). It was also demonstrated that highly lipophilic basic molecules, through increasing lysosomal pH and membrane permeability, lower the lysosomal accumulation of other basic amines (Kornhuber et al. 2010; Poole and Ohkuma 1981). These drug-drug interactions at lysosomal levels could potentially lead to altered target site as well as systemic concentrations of therapeutics (Daniel and Wojcikowski 1999; Daniel, Wojcikowski, and Palucha 2001).

Lysosomal sequestration is hypothesised to be one of the tissue retention mechanisms in the lungs for inhaled therapeutics (Boer 2003; Cooper, Ferguson, and Grime 2012). Currently, methods for evaluating lysosomal sequestration of inhaled molecules are predominantly based on rodent lung tissue models such as rat lung slices (Backstrom, Boger, et al. 2016; Backstrom, Lundqvist, et al. 2016). However, these tissue based models do not provide mechanistic understanding of lysosomal sequestration at the

airway epithelial cell level which is the first barrier encountered by inhaled molecules. Also, in a lung slice model, the cell types involved in the drug accumulation remain unknown. Moreover, there could be species differences in terms of tissue accumulation of compounds. Thus, there is a requirement for validating a human airway epithelial model for the purpose of studying lysosomal sequestration of inhaled therapeutics.

Calu-3, a sub-bronchial epithelial cell line is one of the most frequently used *in vitro* epithelial models for investigating the mechanisms underlying inhaled therapeutics interaction with lung epithelial membranes (Gordon et al. 2015; Hastedt et al. 2016; Ong, Traini, and Young 2013). However, in contrast to their predominant application for elucidating drug uptake and transport mechanisms, the suitability of Calu-3 cell model has not yet been explored for studying subcellular drug distribution of inhaled compounds. Lung cell models such as Calu-3, with their organ specific characteristics (Min et al. 2016) and transporter protein expression (Mukherjee, Pritchard, and Bosquillon 2012) could be appropriate *in vitro* model for characterising intracellular drug distribution of inhaled compounds, including lysosomal sequestration.

In general, the propensity of molecules to accumulate in lysosomes is studied by monitoring their interaction with a lysosome specific marker (Krise 2016). LysoTracker® dyes are frequently employed to qualitatively or semi-quantitatively assess the lysosomal sequestration of various compounds through microscopic techniques (Kazmi et al. 2013; Lemieux, Percival, and Falgueyret 2004). These fluorescent molecules readily permeate membranes and get entrapped inside the lysosomes due to their internal acidic pH. The role of the cytosolic - lysosomal pH gradient in the accumulation of lysosomotropic compounds including LTR is generally investigated using various lysosomal alkalinising agents (Assaraf 2015; Lemieux, Percival, and Falgueyret 2004). These agents include the Na/H^+ - ionophore, monensin (Tapper and Sundler 1990), the vacuolar-type H^+-ATPase inhibitor, bafilomycin A1 (Yoshimori et al. 1991), or NH_4CL, which raises lysosomal pH (Kornhuber et al. 2010). Similarly, compounds which accumulate in lysosomes and increase lysosomal pH are expected to lower the fluorescence intensity of LTR and these compounds are labelled as lysosomotropic (Kaufmann and

Krise 2007; Marceau, Roy, and Bouthillier 2014). This approach, for instance, was employed to study the lysosomal accumulation potential of various compounds using immortalized hepatocytes (Fa2N-4) (Kazmi et al. 2013) and the rat macrophage cell line, NR8383 (Ufuk et al. 2015).

In contrast to LTR based approaches, quantitative methods involve isolation of lysosomes using differential centrifugation from compound treated cells and estimate compound concentrations within these organelle fractions using advanced analytical techniques such as LC-MS/MS (Duvvuri, Feng, et al. 2004). Such quantitative information from these investigations could be valuable for developing mechanistic models which facilitate predicting lysosomal accumulation of various compounds based on their chemical properties (Assmus, Houston, and Galetin 2017; Zheng et al. 2011).

4.2. Aims

This chapter focuses on the characterisation of Calu-3 cells for the purpose of lysosomal sequestration studies. The specific objectives were to:

- Evaluate the suitability of Calu-3 cells for lysosomal sequestration studies using the lysosome specific fluorescent maker, LysoTracker® Green (LTG).
- Optimise the experimental conditions for high throughput screening of compound propensity to accumulate in Calu-3 lysosomes. Asses, qualitatively, lysosomal sequestration potential of inhaled compounds belonging to various chemical classes.
- Establish a cell fractionation approach for isolating lysosomes from the Calu-3 cells for the purpose of quantifying drug levels associated with lysosomes.

4.3. Results

4.3.1. Suitability of Calu-3 cells for lysosomal sequestration studies – Confocal microscopy

LTG sequestration was evaluated using confocal microscopy as an evidence for the presence of functional lysosomes in Calu-3 cells. Qualitative changes in the fluorescence intensity of LTG, upon co-incubation with imipramine, a known lysosomotropic basic compound or known cytosol-lysosomal pH gradient disruptors, (bafilomycin A1, and monensin) were also monitored.

Efficient sequestration of LTG was seen in Calu-3 cells (Figure 4-1, A), demonstrating the presence of active acidic organelles. The LTG fluorescence in Calu-3 cells was reduced in the presence of bafilomycin A1 and monensin (Figure 4-1, B and C respectively), confirming that LTG sequestration was facilitated by the pH gradient between cytosol and lysosomes.

Compounds which disrupt the cytosolic-lysosomal pH difference could be expected to alter the fluorescence intensity of LTG. For instance, the presence of imipramine and dibasic DS81 markedly lowered LTG fluorescence in comparison with the control (Figure 4-1, D and Figure 4-2, A). This could be attributed to the ability of these lipophilic basic amines to get entrapped in the lysosomes and alkalinise the lysosomal pH. On the other hand, the permanently charged ipratropium and zwitterion indacaterol failed to lower the fluorescence intensity of LTG, as expected from their physicochemical properties (Figure 4-2, B and C). These results indicated Calu-3 cells are a suitable model for lysosomal sequestration studies using LTG as a marker.

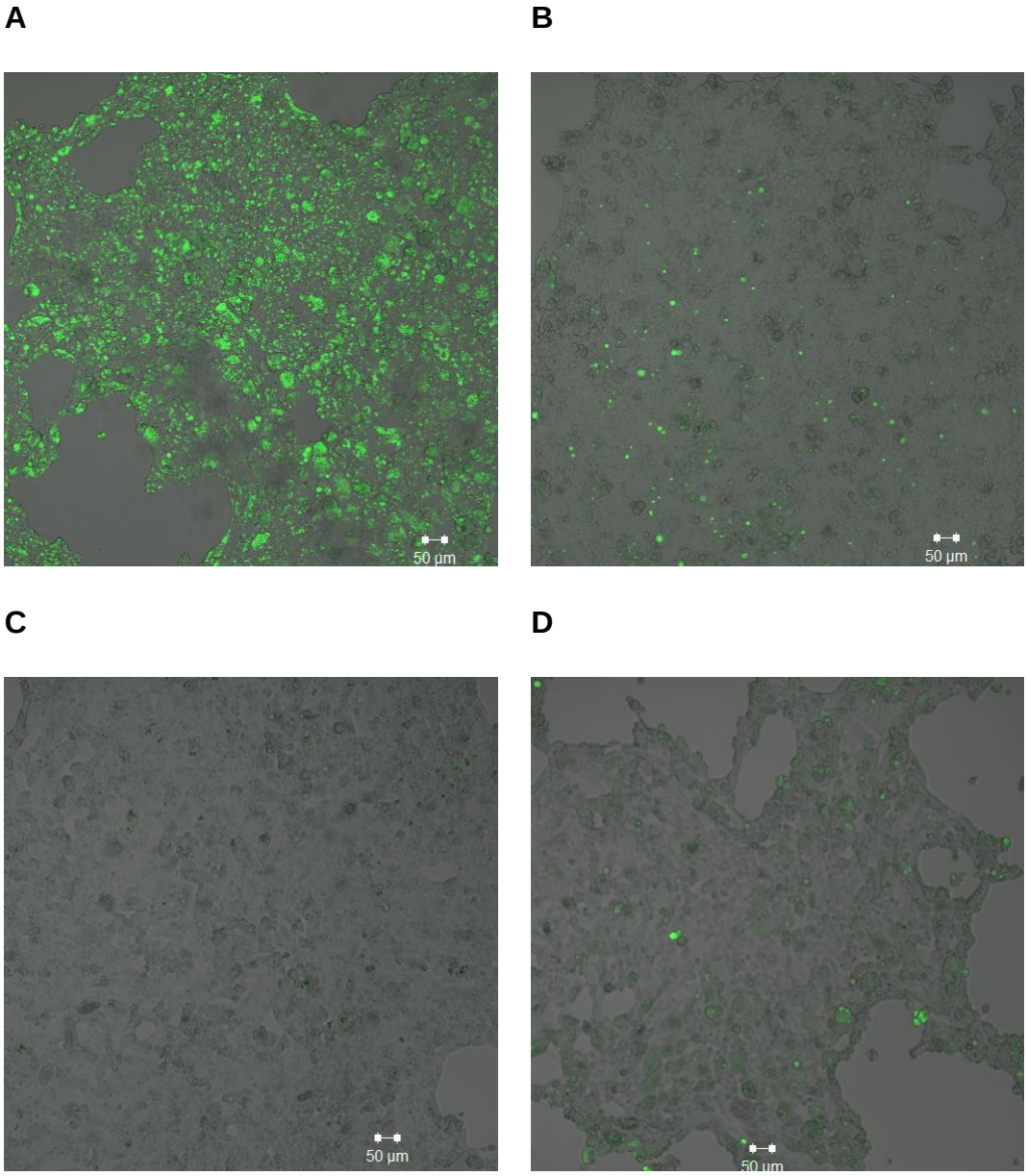


Figure 4-1. Confocal microscopic images of Calu-3 cells treated with LysoTracker™ Green.

Calu-3 cells (0.2 mL/chamber of 0.5×10^5 cells/mL) were added to clear bottom Ibidi 8-well chambers and grown for 36 hours in a humidified incubator at 37°C under 5% CO_2. LysoTracker™ Green accumulation in Calu-3 cells alone (A), or following co-incubation for 1 hour with bafilomycin A1 -100 nM (B), monensin-20 µM (C) or imipramine-10 µM (D), was monitored using confocal microscopy. Each image is a representative of images collected from four chambers per each condition.

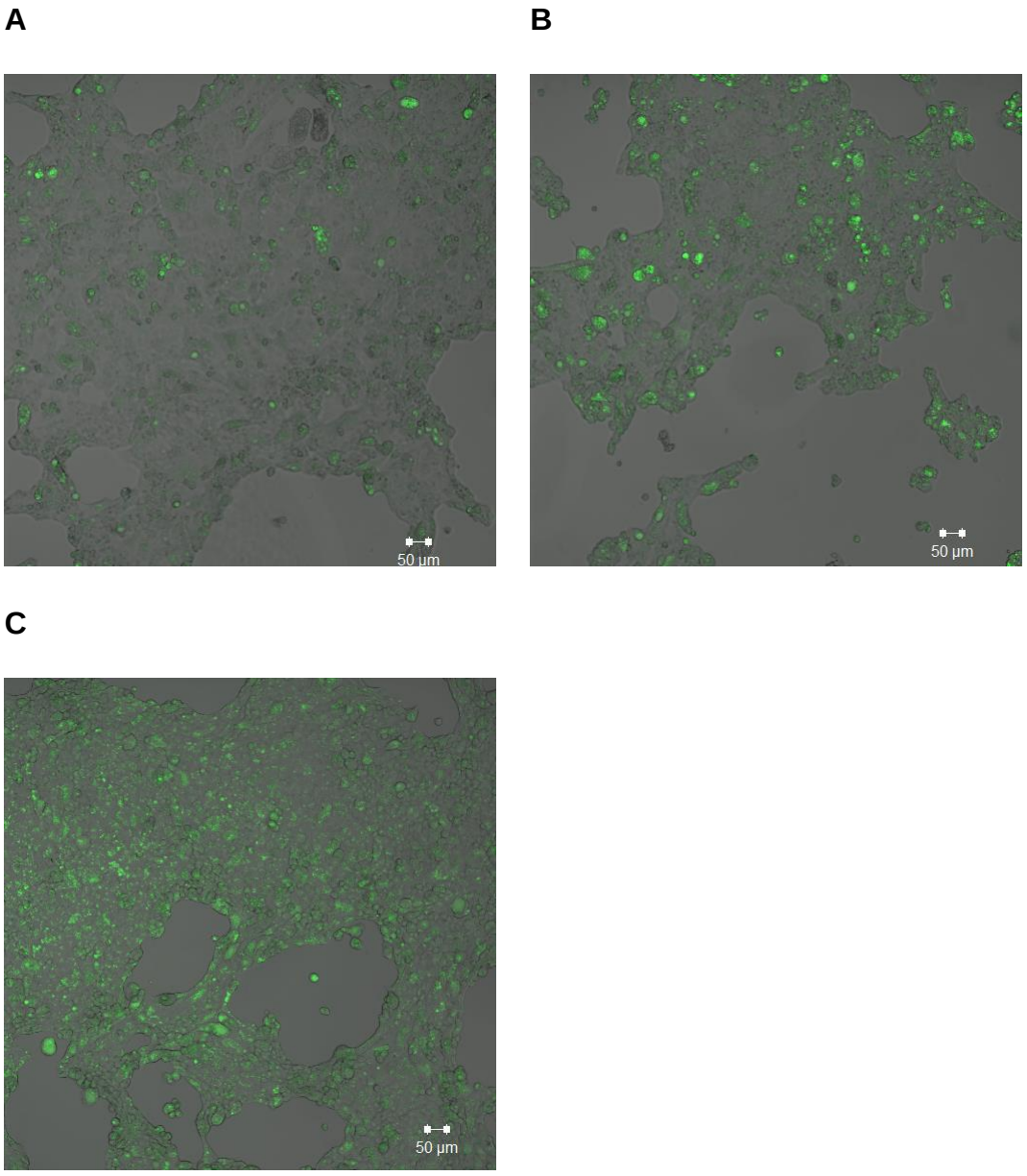


Figure 4-2. Confocal microscopic images of Calu-3 cells treated with LysoTracker™ Green in presence of various inhaled compounds

Calu-3 cells (0.2 mL/chamber of 0.5 × 105 cells/mL) were added to clear bottom Ibidi 8-well chambers and grown for 36 hours in a humidified incubator at 37°C under 5% CO_2. LysoTracker™ Green accumulation in Calu-3 cells was monitored using confocal microscopy following co-incubation for 1 hour with 10 µM of DS81(A), ipratropium (B) or indacaterol (C). Each image is a representative of images collected from four chambers per each condition.

4.3.2. Quantification of LTG sequestration in Calu-3 cells

4.3.2.1. Optimisation of LTG concentration and incubation time

The cell associated LTG fluorescence was quantified using a multimode microplate reader Spark® 10M (Tecan). Initial studies were performed to optimise the experimental conditions including incubation time and concentration of LTG. Calu-3 cells efficiently took up LTG in a time-dependent manner until 60 minutes after incubation, as reflected by an increased cell-associated fluorescence (Figure 4-3, A). Based on these experiments, a 30 minute incubation time was chosen for further experiments with LTG (Figure 4-3, A). LTG accumulation in Calu-3 cells indicated that a concentration of 100 nM was optimal for lysosomal sequestration studies (Figure 4-3, B) since above that concentration, the cell associated fluorescence appeared to be saturated.

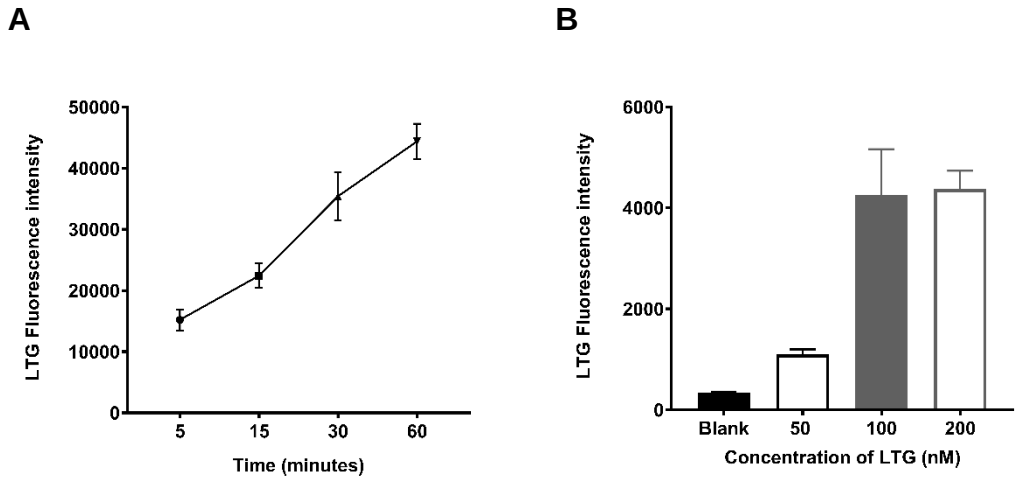


Figure 4-3. Time and concentration-dependent accumulation of LysoTracker™ Green (LTG) in Calu-3 cell.

Calu-3 cells (100 µL/well of 3.2× 10^5 cells/mL) were grown in collagen-coated 96-well microtiter plates and incubated in a humidified incubator at 37°C under 5% CO_2 for 48 hours. LysoTracker™ Green accumulation in Calu-3 cells was measured as a function of incubation time, (A) or LysoTracker™ Green concentration, (B) following incubation for 30 minutes. Data are presented as mean ± SD of four wells per each time point or concentrations from a single experiment.

4.3.2.2. Effect of cytosol-lysosomal pH gradient disruptors on LTG accumulation

LTG accumulation in Calu-3 cells was tested in the presence of various known cytosol-lysosomal pH gradient disruptors, bafilomycin A1, monensin and ammonium chloride (NH_4Cl), using concentrations reported in the literature (Drose and Altendorf 1997; Tapper and Sundler 1990). The effect of these inhibitors on LTG accumulation was tested following a variety of incubation conditions i.e. pre, co- and pre- and co-incubation. The presence of the inhibitors, in all conditions, significantly inhibited LTG accumulation in Calu-3 cells indicating the cytosol-lysosomal pH gradient is as driver for its sequestration (Figure 4-4).

The cell associated fluorescence of LTG was found to be 34.8 ± 13.0, 60.5 ± 7.9, and 25.6 ± 8.3% of control following pre-, co-, and pre-and co-incubations with bafilomycin A1, respectively (Figure 4-4, A). In the case of monensin, a 15.8 ± 3.9, 3.7 ± 0.3 and 5.8 ± 1.1% of control fluorescence was seen following pre-, co-, and pre-and co-incubations, respectively (Figure 4-4, B) while pre-, co-, and pre-and co-incubations with NH_4Cl resulted in a LTG fluorescence of 70.2 ± 11.0, 63.1 ± 13.5 and 15.1 ± 2.3% of control, respectively (Figure 4-4, C). Imipramine lowered the LTG fluorescence down to 33.0 ± 7.8, 10.8 ± 4.6 and 15.6 ± 1.7% of control following pre, co-incubation and pre-and co-incubation, respectively (Figure 4-4, D). Even though a combination of pre-and co-incubation conditions resulted in higher reductions in cell associated LTG fluorescence, co-incubation alone was chosen for further experiments. This was to shorten the experiment duration. Furthermore, the changes seen in LTG fluorescence following co-incubation experimental condition were found to be satisfactory for all the inhibitors tested.

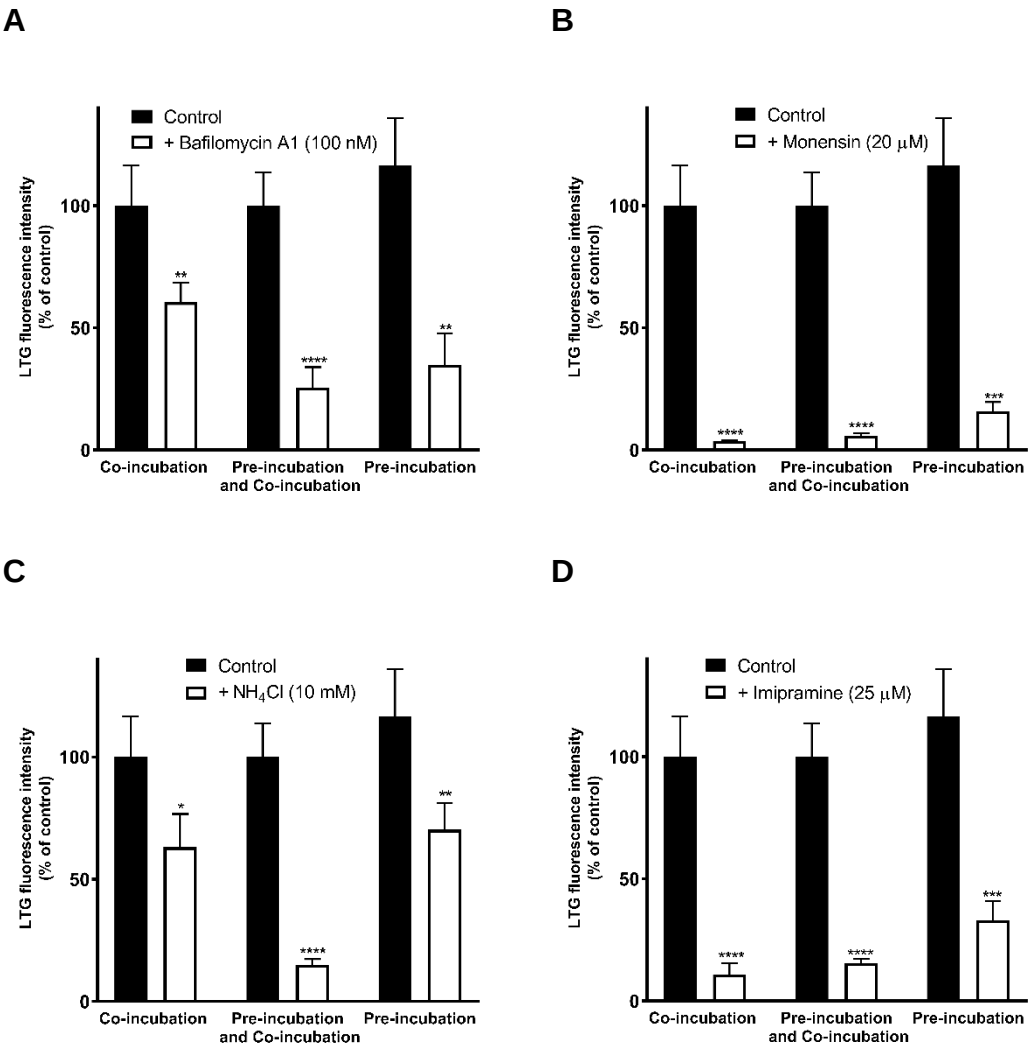


Figure 4-4. LysoTracker™ Green accumulation in Calu-3 cells under various incubation conditions.

Calu-3 cells were grown in collagen-coated 96-well microtiter plates (100 µL/well of 3.2× 10^5 cells/mL) and incubated in a humidified incubator at 37ºC under 5% CO_2 for 48 hours. LysoTracker™ Green accumulation was measured in Calu-3 cells under various incubation conditions with bafilomycin A1 (A), monensin (B), ammonium chloride (C) or (D) imipramine. For co-incubation only group, Calu-3 cells were incubated with solutions containing both, LTG and pH gradient disruptors for 30 minutes. While for pre- and co-incubation conditions, before incubating Calu-3 cells for 30 minutes with solutions containing both, LTG and pH gradient disruptors, Calu-3 cells were pre-incubated with pH gradient disruptors for 30 minutes. For pre-incubation only group, solution containing pH gradient disruptor was withdrawn from Calu-3 cells following 30 minutes of exposure, washed cells with HBSS and incubations were continued with only LTG solutions for additional 30 minutes. All the incubations were conducted at 37ºC in a humidified incubator under 5% CO_2 environment. Data are presented as the mean ± SD of four wells per condition from a single experiment.

4.3.2.3. Effect of various compounds on LTG accumulation

The ability of various compounds to get sequestered within the lysosomes of Calu-3 cells was assessed by testing their propensity to compete with the lysosomotropic LTG and reduce its fluorescence intensity following their co-incubation. For this purpose, compounds belonging to various chemical classes i.e. neutral (acetaminophen), acidic (ibuprofen), basic (imipramine) and zwitterion (L-carnitine) were tested. In addition, DS81, indacaterol, ipratropium and salbutamol were included as representatives of inhaled compounds. Each compound was co-incubated with LTG at five different concentrations to assess any concentration-dependent inhibitory effect on LTG accumulation.

Of all the compounds tested, no effect was seen on the LTG fluorescence in the presence of acetaminophen, ibuprofen and L-carnitine when tested up to 50 µM. These results indicate the presence of neutral, acidic and zwitterion compounds did not lead to any change in the cytosol-lysosomal pH gradient (Figure 4-5, B-D). However, the basic compound imipramine reduced the LTG fluorescence in a concentration dependent manner, with a ~70% reduction in LTG fluorescence at 50 µM (Figure 4-5, A).

In terms of inhaled compounds, confirming the confocal microscopy studies, co-incubation with DS81 caused significant reductions in LTG fluorescence in a concentration-dependent manner and resulted in LTG fluorescence of 37.4 ± 4.3 % of control at 50 µM (Figure 4-6, A). In contrast, no reductions in LTG fluorescence was seen with zwitterion indacaterol (Figure 4-6, B) and positively charged ipratropium (Figure 4-6, C). Although, salbutamol is a basic compound (pKa~9.4), it failed to alter the LTG fluorescence (Figure 4-6, D) when tested up to a concentration of 50 µM, maybe because of its lower lipophilicity (cLogP~0.44).

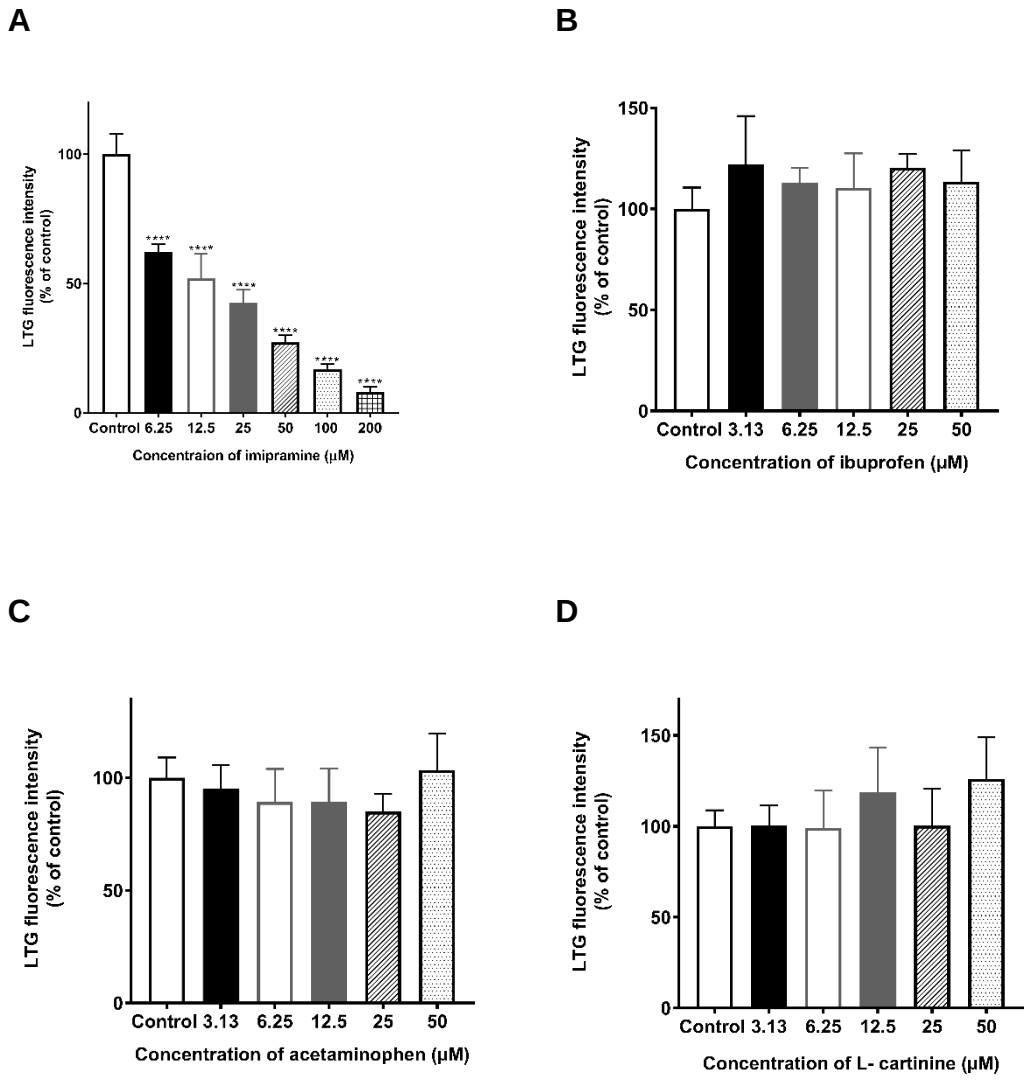


Figure 4-5. LysoTracker™ Green (LTG) accumulation in Calu-3 cells in the presence of compounds representing various chemical classes

Calu-3 cells were grown in collagen-coated 96-well microtiter plates (100 µL/well of 3.2× 10^5 cells/mL) and incubated in a humidified incubator at 37°C under 5% CO_2 for 48 hours. LysoTracker™ Green accumulation was measured in Calu-3 cells following co-incubation for 30 minutes in the presence of (A) imipramine - basic, (B) ibuprofen - acidic, (C) acetaminophen - neutral and (D) L-carnitine – zwitterion, as a function of their concentration. For imipramine data are presented as the mean ± SD of four wells per concentration from a single experiment. For ibuprofen, acetaminophen and L-carnitine data are presented as the mean ± SD of eight wells per concentration from two independent experiments. * indicates a statistically significant lower LTG uptake as compared to the control groups (**** $p<0.0001$).

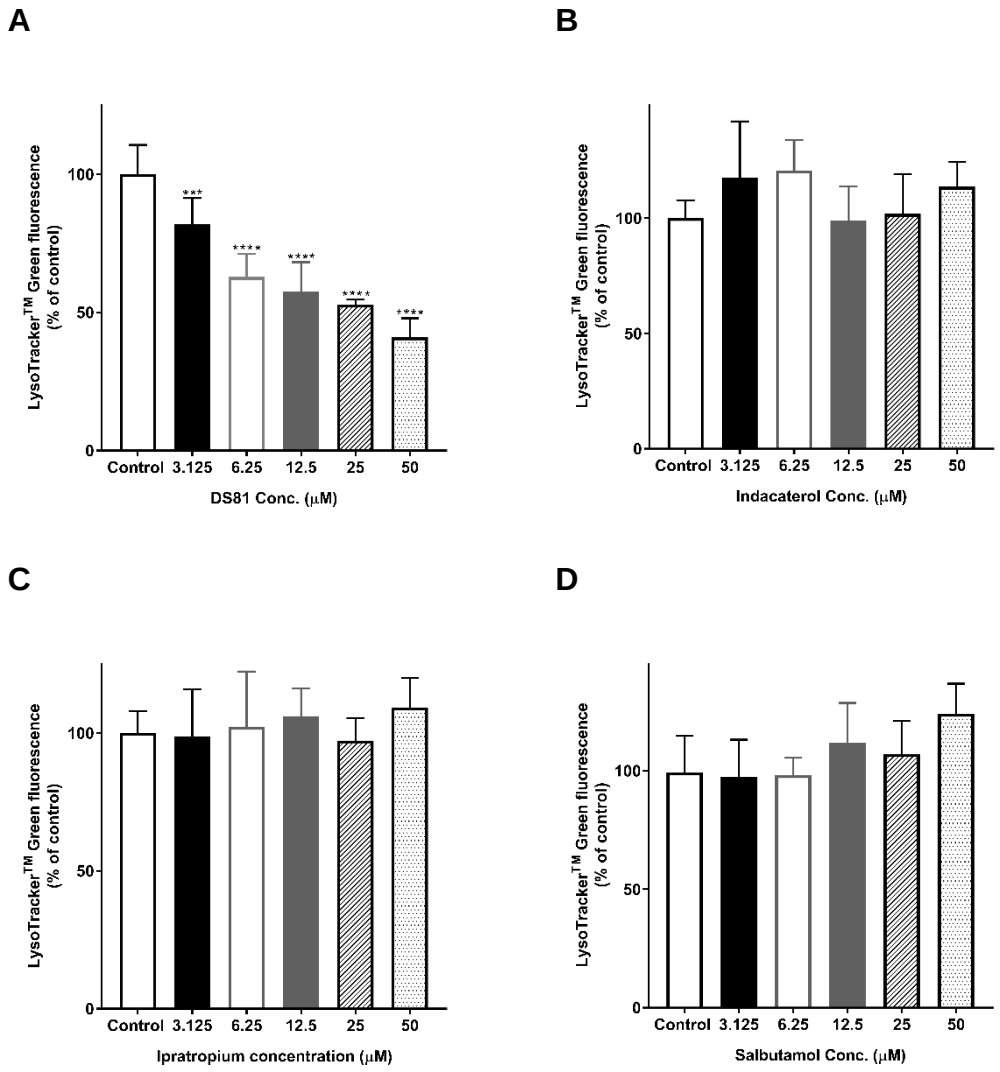


Figure 4-6. LysoTracker™ Green accumulation in Calu-3 cells in the presence of various inhaled compounds representing various chemical classes.

Calu-3 cells were grown in collagen-coated 96-well microtiter plates (100 µL/well of 3.2× 10^5 cells/mL) and incubated in a humidified incubator at 37°C under 5% CO_2 for 48 hours. LysoTracker™ Green accumulation in Calu-3 cells was studied following co-incubation for 30 minutes along with (A) DS81 - dibasic, (B) Indacaterol - zwitterion, (C) ipratropium - quaternary and (D) salbutamol – basic, as a function of their concentration. Data are presented as the mean ± SD of eight wells per concentration from two independent experiments. * indicates a statistically significant lower LTG uptake as compared to the control groups (*** $p<0.001$ and **** $p<0.0001$).

4.3.3. Isolation of lysosomes from Calu-3 cells

Following density gradient ultracentrifugation of Calu-3 cell lysates, various fractions (1 mL) of the supernatant were processed to collect the lysosomal pellet. The activity of the lysosomal specific acid phosphatase enzyme was measured in these fractions and represented as the % of enzyme activity detected in the total cell lysate, which indicate the recovery of lysosomes following the isolation procedures. The top three supernatant fractions showed the highest density of lysosomes as reflected by the acid phosphatase enzyme activity recovered (sum of enzyme activity in the top three fractions ~ 41.8 ± 19.5 % of total cell lysate enzyme activity (Figure 4-7). Consequently, compounds concentrations detected in these top three supernatant volumes whereas combined for the purpose of comparing compounds in terms of their ability to be associated with lysosomes.

The lysosomal associated compound concentration was represented as a percentage of total cell lysate concentration to account for permeability differences between compounds as reported earlier (Duvvuri, Feng, et al. 2004; Duvvuri, Gong, et al. 2004). Imipramine, which was included as a representative of lysosomotropic compound, showed 21.3 ± 0.4 % of total cell lysate levels within the lysosomal fraction (Figure 4-8, A). Following co-incubation with bafilomycin A1 and monensin, the lysosomal associated imipramine concentration was reduced significantly i.e. down to 45.8 ± 0.8 and 11.3 ± 1.2 % of the control group, respectively (Figure 4-8, B). These results shows the suitability of the current cell fractionation approach for isolating lysosomes from compound treated cells and determine compounds associated with these organelles.

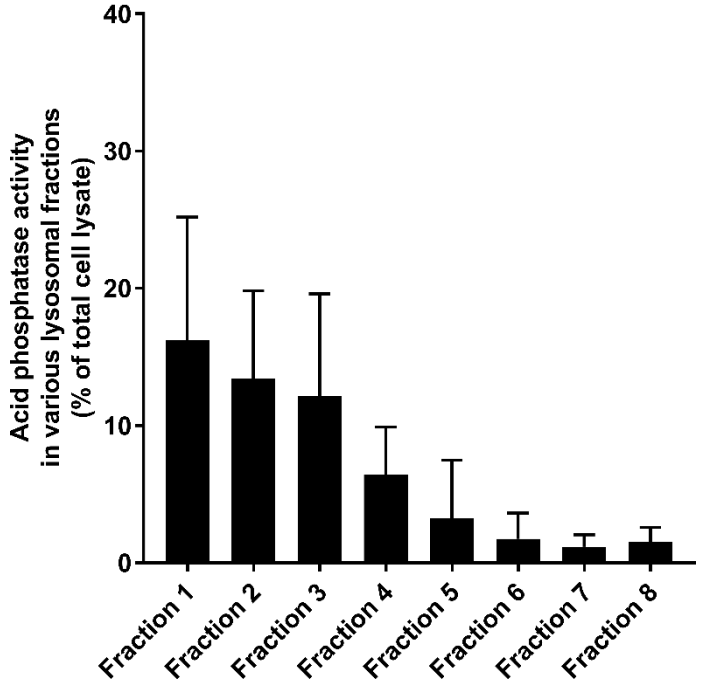
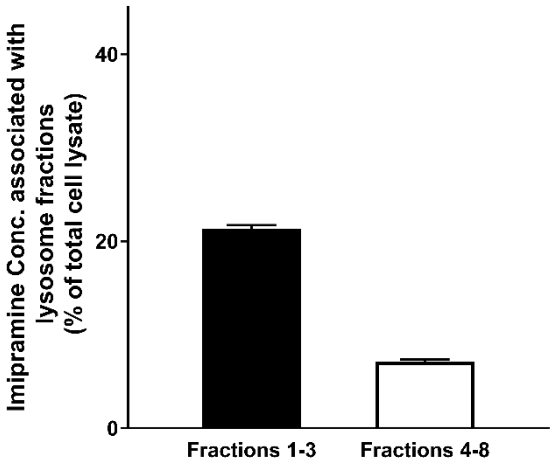


Figure 4-7. Recovery of acid phosphatase activity in various supernatant fractions following ultracentrifugation of cell lysate.

Calu-3 cell lysate was processed using Lysosomal Enrichment Kit (ThermoFisher Scientific, UK) to prepare post nuclear supernatant. This was placed on a discontinuous density gradient prepared using 60% OptiprepTM and this mixture was subjected for ultracentrifugation at 145,000g for 2 hours at 4oC. The resulting supernatant was collected into 8 individual tubes on ice as 1 mL fractions and subjected for centrifugation at 18000 g for 30 minutes at 4oC, after diluting with equal volume of cold PBS. The lysosomal pellet was collected after discarding the supernatant and reconstituted with 150 µL of PBS. These isolated lysosomal fractions were evaluated for acid phosphatase activity, a lysosomal specific enzyme using a commercially available kit (Sigma-Aldrich, UK). The acid phosphatase activity recovered in various fractions is represented as percentage of enzyme activity recovered in total cell lysate. Data are presented as the mean ± SD of sixty samples for each fraction from 5 independent experiments.

A



B

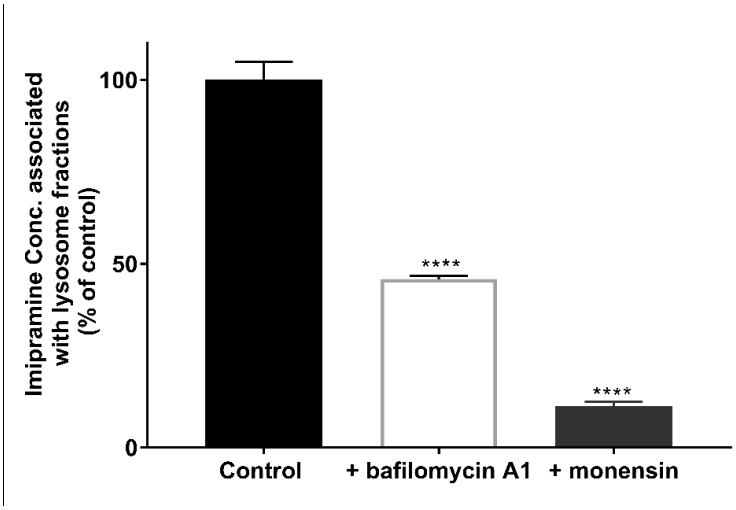


Figure 4-8. Imipramine concentrations associated with lysosomes

Lysosomes were isolated from Calu-3 cells treated with imipramine (10 µM) in the absence or presence of cytosol-lysosomal pH gradient disruptors, bafilomycin A1 (100 nM) or monensin (20 µM), using cell fractionation approach. (A) Imipramine concentrations associated with lysosomal fractions 1-3 and 4-8 were combined and represented as a % of imipramine concentrations with total cell lysate. Imipramine concentrations detected in the top 3 fractions (Fractions 1 - 3) were only considered for further analysis based on their association with lysosomal specific acid phosphatase enzyme activity. (B) Effect of pH gradient disruptors, bafilomycin A1 (100 nM) or monensin (20 µM) on imipramine concentrations associated with lysosomal fractions (sum of fractions 1 - 3) in comparison with control group. Data are presented as the mean ± SD (n= 3) from a single experiment.

4.4. Discussion

The studies presented herein established the presence of active lysosomes in Calu-3 cells and suitability of these bronchial epithelial cells for understanding the role of lysosomal sequestration in the cellular retention of inhaled compounds.

The sequestration of the lysosomotropic fluorescent amine LTG and the significant reduction in LTG accumulation following co-incubation with a variety of lysosomal alkalinising agents (i.e., bafilomycin A1, NH_4Cl and monensin) confirmed the presence of an efficient cytosolic-lysosomal pH gradient in Calu-3 cells. This was essential to establish in order to employ Calu-3 cells for investigating lysosomal sequestration of inhaled therapeutics as some of other cancer cell lines were reported to inherently lack a pH gradient between the cytosol and lysosomes (Altan et al. 1998; Assaraf 2015; Kokkonen et al. 2004)

Qualitative and semi-quantitative approaches employing LysoTracker® dyes have previously been well-established for studying the propensity of various molecules towards lysosomal accumulation. The fundamental principle of these methods involves evaluating the ability of the compounds to compete with LysoTracker® for their entry into the lysosomes and alkalinise the intralysosomal pH. For instance, the lysosomal accumulation of cationic amphiphilic drugs such as chlorpromazine and imipramine was systemically demonstrated by monitoring the reductions in LysoTracker® accumulation in HeLa cells (Lemieux, Percival, and Falgueyret 2004). Similar approaches were also employed for evaluating lysosomal sequestration using an immortalised human hepatic cell line (Kazmi et al. 2013), and rat and human alveolar macrophages (Ufuk et al. 2017; Ufuk et al. 2015).

In addition, in a high content screening assay, typical lysosomotropic compounds were characterised by a cLogP > 2 and a basic pKa > 6 (Nadanaciva et al. 2011). Lipophilic basic amines were implicated in an increased intra-lysosomal pH and thus, altered lysosomal accumulation of other basic compounds (Poole and Ohkuma 1981). This was reflected by the lowered accumulation of LTG in Calu-3 cells upon co-incubation with increasing concentrations of the lipophilic basic amine imipramine (pKa ~ 9.2;

clogP~4.5) (Figure 4-1, Figure 4-4). However, no inhibition of LTG accumulation was seen with acidic, neutral and zwitterion compounds when tested up to a concentration of 50 µM (Figure 4-4). The inhibitory concentration (IC50) of imipramine seen in the current study (97 µM) matched that reported in HeLa cells (100 µM), but was significantly different from that reported in immortalised human hepatic cells, Fa2N-4 (260 µM) and H9c2 cells (10.7 µM) (Kazmi et al. 2013; Lemieux, Percival, and Falgueyret 2004; Nadanaciva et al. 2011). This could be due to differences in the permeability of imipramine across cell membranes or a resistance shown by various cell lines against a change in intralysosomal pH in the presence of basic molecules. However, studies with LysoTracker® do not provide any quantitative information regarding compound accumulation in lysosomes. Furthermore, these assessments are only suitable for lipophilic basic compounds.

In order to identify or quantitate drug accumulation in the various organelles, the intracellular distribution of drugs is increasingly being measured, thus providing direct evidence for a cellular disposition of molecules (Zheng et al. 2011). In the current study, a discontinuous gradient method was applied for the isolation of lysosomes from Calu-3 cells for the purpose of quantifying the contribution of lysosomal sequestration to the total cell concentrations of inhaled compounds. Organ specific *in vitro* cell culture models were successfully utilised to increase understanding of cellular and intracellular drug disposition of molecules. For instance, sandwich-cultured hepatocytes (SCH) were applied to study hepatocellular drug accumulation mechanisms such as binding, active uptake and sequestration in organelles (Pfeifer et al. 2013). Direct quantification of compounds associated with lysosomes was also established where lysosomes were isolated from cultured cells or tissues, either prior to or after exposure to compounds (Krise 2016). For instance, Duvvuri et al, measured the lysosomal accumulation of LysoTracker® following isolation of lysosomes from leukemia cell line (HL-60) through magnetic chromatography (Duvvuri and Krise 2005). A cell fractionation approach was also applied for studying sub-cellular drug distribution including in lysosomes (Duvvuri, Feng, et al. 2004). The sensitivity of LysoTracker® accumulation in lysosomes was also demonstrated quantitatively following isolation of

lysosomes from cells treated with cytosol-lysosomal pH gradient disruptors. The recovery of lysosomes from cultured cells ranged from 15 to 29% based on the estimation of the activity of lysosomal specific enzymes and densitometric analysis of blots (Duvvuri, Feng, et al. 2004). The acid phosphatase enzyme recovery seen in the current study (Figure 4-7), matched earlier reports, where lysosomes were collected from the human leukemia cell lines U-937 or HL-60 using cell fractionation or magnetic chromatographic approaches, respectively (Duvvuri, Feng, et al. 2004; Duvvuri, Gong, et al. 2004).

Mechanisms of lysosomal sequestration of weakly basic amines was well-characterised, previously in purified lysosomes from rat liver using imipramine as a representative molecule (Ishizaki et al. 2000). These studies demonstrated that imipramine accumulation in lysosomes is predominantly driven by transmembrane pH difference, which was completely abolished by cytosol-lysosome pH gradient disruptors, bafilomycin A1 and ionophore agent, nigericin (Ishizaki et al. 2000). Also lysosomal uptake of this basic amine was shown to be independent of temperature, stimulated by the presence of ATP and inhibited by other lipophilic basic compounds (Ishizaki et al. 2000; Yokogawa et al. 2002). Current studies with imipramine demonstrates that combining cell fractionation approach with sensitive quantitative analytical procedures such as LC-MS/MS could be effectively used for measuring compounds associated with lysosomes (Figure 4-8, A and B). These procedures could help better-characterising intracellular distribution characteristics of inhaled molecules and study their cellular retention mechanisms.

4.5. Conclusion

In vitro airway epithelial models have traditionally been applied to study absorptive clearance of inhaled molecules such as permeability across the airway epithelium. However, their suitability for studying lung retention mechanisms such as lysosomal sequestration has not yet been demonstrated. Such investigations may facilitate high throughput screening of novel compounds for their lung retention potential. Also, the application of organ specific *in vitro* epithelia cell lines allows investigating drug disposition at the cellular level. Current studies are aimed in that direction and investigations with the lysosomotropic fluorescent marker LysoTracker® Green confirmed the presence of a cytosolic-lysosomal pH gradient in Calu-3 cells, a requirement for applying this cell line for lysosomal entrapment studies. The isolation of lysosomes from Calu-3 cells using cell fractionation approach followed by the quantification of compound concentrations associated with lysosomes using LC-MS/MS demonstrated the suitability of these procedures for characterising the lysosomal sequestration of inhaled molecules in bronchial epithelial cells. Thus, these investigations propose a novel application of Calu-3 cells for studying lysosomal sequestration of inhaled compounds.

Chapter Five

5. Understanding the role of lysosomal sequestration in the cellular disposition of inhaled compounds.

5.1. Introduction

For the effective management of respiratory diseases, achieving pharmacologically relevant concentrations of inhaled therapeutics at the target site for a sufficient period of time is essential (Backman et al. 2014). One of the major challenges in designing inhalational molecules is to counterbalance the high permeability of the lung tissue to achieve sustained therapeutic concentrations locally while minimising systemic exposure (Cooper, Ferguson, and Grime 2012).

Physicochemical properties of inhaled molecules control their permeability across the airway epithelium, binding to tissue components and sequestration in cellular compartments and thus influence residence time in the lungs (Backman et al. 2014). However, the effect of inhaled drug physicochemical properties on their lung absorption kinetics is not yet clearly understood. Such investigations developing relationships between molecular properties and lung absorption kinetics facilitate designing inhaled therapeutics with long lung retention (Yu and Rosania 2010).

There are a variety of experimental approaches for characterising lung disposition of inhaled molecules, ranging from *in vitro* cell permeability assays to *ex vivo* lung perfusion and *in vivo* pharmacokinetic investigations in pre-clinical species or human (Sakagami 2006). These models were typically employed for assessing the ability of inhaled molecules to be retained in the pulmonary tissue by monitoring their appearance in the systemic circulation or

disappearance from the lungs (Backman et al. 2017). For instance, earlier inhalation studies in rats characterised lung absorption of a variety of molecules based on the % of dose remaining in the lungs and indicated faster absorption for lipid-soluble molecules than lipid-insoluble compounds of similar molecular weight (Brown and Schanker 1983). Tronde and colleagues determined the absorption rate and pulmonary bioavailability for a set of low-molecular weight compounds in *ex vivo* lung perfusion and *in vivo* lung absorption studies, respectively and developed correlations with their permeability characteristics in Caco-2, an *in vitro* gastro-intestinal epithelial model (Tronde, Norden, Jeppsson, et al. 2003; Tronde, Norden, Marchner, et al. 2003). Recently, a quantitative structure activity relationship model was also proposed for inhalational compounds based on their absorption in an *ex vivo* rat lung perfusion model and physicochemical properties (Edwards et al. 2016). The above pre-clinical models are primordial for selecting inhaled drug candidates with sufficient lung affinity to progress further in the development process. However, their complexity prevents any mechanistic investigation of the parameters governing local drug accumulation. This has resulted in the current poor understanding of those parameters and in turn, difficulties in designing compounds with optimal efficacy (Backman et al. 2014; Perry et al. 2017).

Recently, precision-cut rat lung slices have been developed to investigate the lung retention properties of inhaled bronchodilators (Backstrom, Boger, et al. 2016; Backstrom, Lundqvist, et al. 2016). Although drug exposure in that model fails to capture the initial contact of inhaled molecules with the airway epithelium *in vivo*, the high lung tissue affinity of the long acting β2-agonists such as formoterol, salmeterol and indacaterol could successfully be estimated. Furthermore, lysosomal sequestration was indirectly shown to drive their prolonged residence time in the lungs (Backstrom, Boger, et al. 2016). However, these tissue based models are labour-intensive, technically challenging and do not allow high-throughput screening of compounds in early stages of drug discovery (Yu and Rosania 2010). Lung slice models fail to demonstrate the influence of lung tissue affinity factors such as lysosomal sequestration on vectorial transport of inhaled compounds across the airway

epithelium (Backstrom, Boger, et al. 2016). Also, lung slides do not provide information on the cell types promoting drug accumulation within the lung tissue or the actual contribution of lysosomal trapping in pulmonary drug disposition. Therefore, investigations in physiologically-relevant *in vitro* models are required to investigate drug trafficking at the cellular and subcellular level in the lungs. Calu-3 cells, which resemble native airway epithelium (Grainger et al. 2006) and demonstrates suitable properties for lysosomal sequestration studies (Chapter 4), could further be employed for investigating cellular retention mechanisms of inhaled molecules.

One of the cell-based approaches for characterising the cellular accumulation of compounds is to measure their cellular partition coefficient (K_p), the ratio of intracellular and extracellular concentrations (Chu et al. 2013). For example, a K_p of many fold-higher than unity for lipophilic compounds reflects their partitioning among cellular membranes and affinity to various cellular structures (Chu et al. 2013). Changes in K_p of compounds can be monitored to evaluate the role of organelles in the subcellular distribution of drugs. For instance, measuring K_p in presence or absence of cytosol-lysosomal pH-gradient disruptors is one of the well-established methods for investigating the role of lysosomal sequestration in the cellular accumulation of compounds (Zheng et al. 2011). Cell culture models also allow investigating cellular retention mechanisms at the organelle level following cell fractionation and these approaches have been utilised in rational synthesis of compounds for improving target site concentrations (Gong et al. 2007). Cell layers forming tight junctions can also be employed for studying lysosomal trapping as one of tissue retention mechanisms as demonstrated with the Caco-2 model (Hayeshi et al. 2008; Heikkinen, Monkkonen, and Korjamo 2009). However, no such investigations are reported for inhalational molecules using *in vitro* lung cell models. Such studies may facilitate better understanding of lung disposition across the airway epithelium at the cellular level.

5.2. Aims

The current chapter was aimed to explore the mechanisms controlling drug retention in the lung using the Calu-3 cell culture model. Five bronchodilators

and four investigational compounds were tested in the cell line and lung retention data were obtained in rats for the latter set of molecules in order to evaluate the predictive potential of *in vitro* data. Specific objectives include,

- Study cellular partition coefficient (K_p) of inhaled compounds belonging to various chemical classes in Calu-3 cells. Measure K_p for various compounds in the presence of cytosol - lysosomal pH gradient disruptors for assessing the contribution of lysosomal sequestration to their total intracellular concentrations.
- Measure the lysosomal associated concentrations of inhaled compounds following isolation of lysosomes from compound treated Calu-3 cells. Investigate the effect of structural modification on their lysosomal sequestration.
- Study the impact of lysosomal sequestration on the cellular retention and transepithelial transport of the compounds in ALI Calu-3 layers to better understand the role of cellular and subcellular distribution in pulmonary drug disposition.
- Understand the retention of compounds in rat lung tissue following intra-tracheal administration with the help of their permeability, cellular accumulation and lysosomal association in Calu-3 cell model.

5.3. Results

5.3.1. Cellular partition coefficient (K_p)

K_p was measured for various compounds in Calu-3 cells to understand the effect of physicochemical properties on their cellular accumulation. The role of lysosomal sequestration, as one possible cellular retention mechanisms of inhaled compounds was also assessed by co-incubating compounds with bafilomycin A1 or monensin.

For most of the compounds steady state K_p was achieved between 1 and 2h post incubation (Figure 5-1, A). A low cellular partition coefficient was seen for the permanently charged anti-cholinergic bronchodilators (K_p range: 0.3 ± 0.0 - 6.4 ± 0.8) (Figure 5-1, A). In contrast, higher cellular association was observed for dibase DS81 (K_p range: 6.6 ± 1.8 - 135.4 ± 14.3) and the lipophilic

β_2 agonists, formoterol, salmeterol and indacaterol (K_p range: 1.3 ± 0.3 - 734.9 ± 93.6) (Figure 5-1, A). The prototypical cationic amphiphilic drug imipramine also accumulated extensively in Calu-3 cells (K_p range: 70.5 ± 6.0 - 541.2 ± 60.4) (Figure 5-1, A).

Among basic compounds, as anticipated, lipophilicity determined their total cellular accumulation, with salmeterol (cLog P ~ 3.82) showing ~22 to 54 fold higher K_p than formoterol (cLog P ~ 1.91) (Figure 5-1, A). On the other hand, for the less lipophilic basic salbutamol (cLogP ~ 0.44), total cell concentrations were lower than the buffer concentrations throughout the experiment (K_p range: 0.1 ± 0.0 - 0.7 ± 0.1) (Figure 5-1, A). Zwitterion indacaterol (cLogP ~ 3.31) also showed extensive cell associated concentrations, with K_p ranging from 10.9 ± 0.6 to 261.8 ± 37.4 (Figure 5-1, A).

In the presence of bafilomycin A1, no change in K_p was seen for both ipratropium and salbutamol, (Figure 5-1, B and C), suggesting negligible lysosomal association for these molecules. On the other hand, both monensin and bafilomycin A1 lowered K_p of basic molecules, with the former being more efficient than latter in reducing cellular concentrations. For the majority of molecules, the effect of bafilomycin A1 was significant only towards the end of the incubation period, i.e. K_{p2h}. Following incubation with monensin, K_{p2h} of imipramine, DS81, formoterol and salmeterol was found to be 8, 7, 27 and 32% of the control group, respectively (Figure 5-2, A, B, C and D) whereas the presence of bafilomycin A1 resulted in a K_{p2h} which was 22, 58, 84 and 77% of control group for imipramine, DS81, formoterol and salmeterol, respectively (Figure 5-2, A, B, C and D). Only a moderate reduction in the K_{p2h} was observed for zwitterion indacaterol, where the presence of bafilomycin A1 and monensin resulted in a K_{p2h} of 66 and 76% of control group, respectively (Figure 5-2, E).

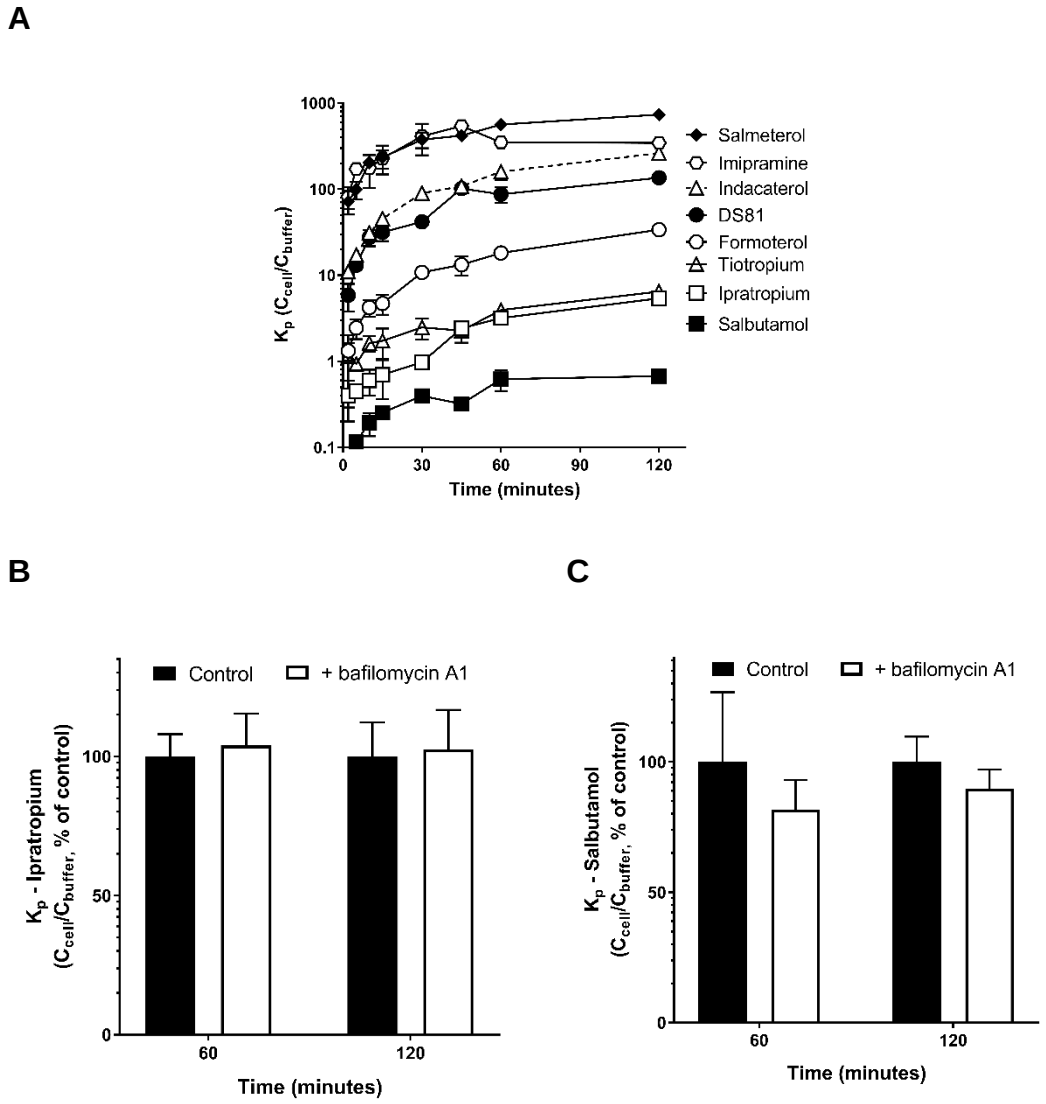


Figure 5-1 Cellular partition coefficient (K_p) of various compounds in Calu-3 cells.

Calu-3 cells were grown in collagen-coated 24-well plates (500 µL/well of 3.2× 10^5 cells/mL) by incubating at 37°C in a humidified incubator under 5% CO_2 for 3 days. (A) Cellular partition coefficient (K_p) in Calu-3 cells was measured at various time points (5 – 120 minutes) for a variety of compounds including inhaled molecules at 5 µM. K_p in the presence of bafilomycin A1 (100 nM) was measured following 60 and 120 minutes of co-incubations for ipratropium (B) and salbutamol (C) at 10 µM. For ipratropium (B), data are presented as the mean ± SD of n= 7 from two independent experiments. For salbutamol (C), data are presented as the mean ± SD of n= 4, from a single experiment.

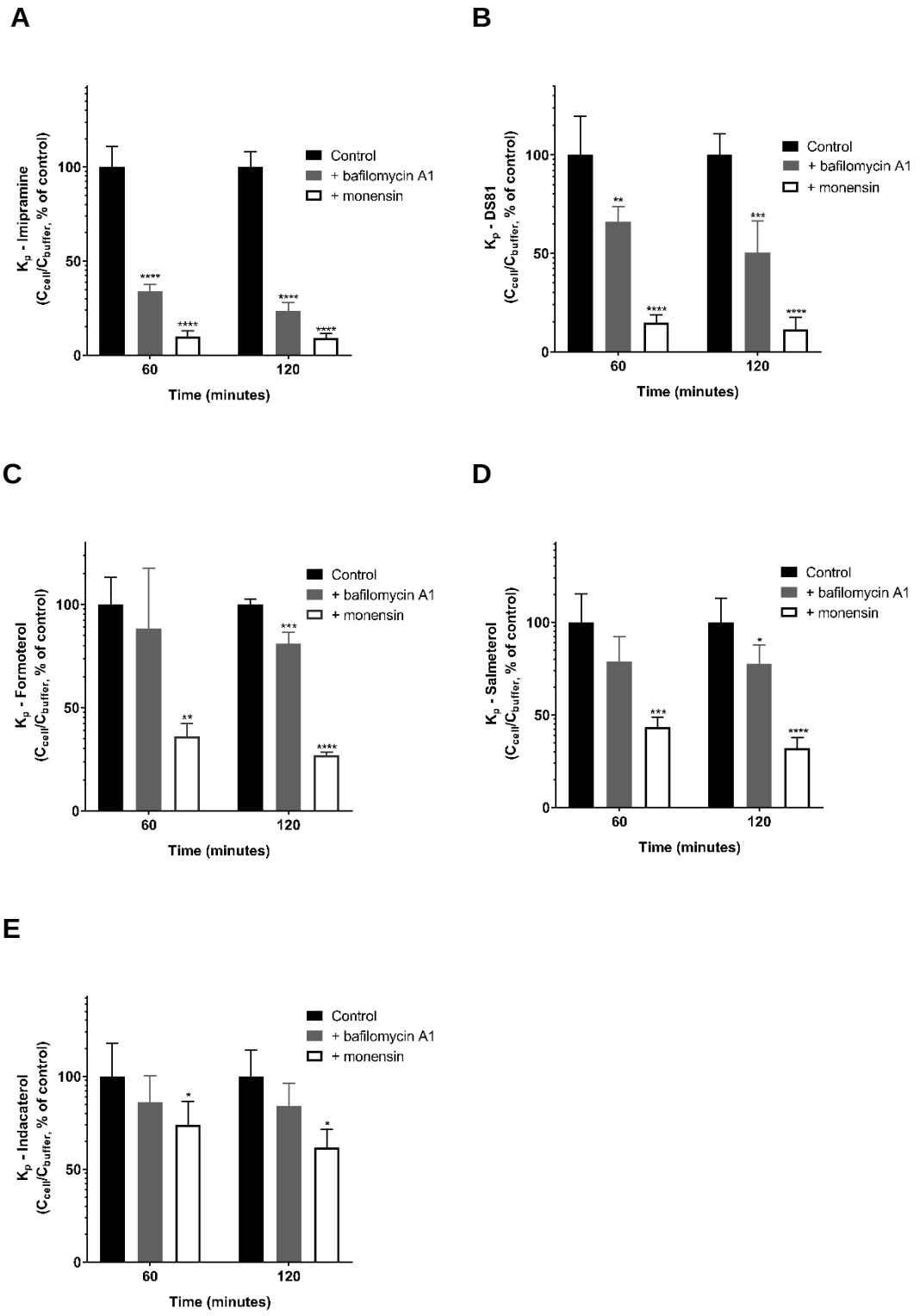


Figure 5-2. Cellular partition coefficient (K_p) for compounds in Calu-3 cells in the presence of cytosol-lysosomal pH gradient disruptors.

Calu-3 cells were grown in collagen-coated 24-well plates (500 µL/well of 3.2×10^5 cells/mL) by incubating at 37°C in a humidified incubator under 5% CO_2 for 3 days. Cellular partition coefficient (K_p) in Calu-3 cells was measured for various compounds at a concentration of 5 µM, in the presence or absence of

bafilomycin A1 (100 nM) or monensin (20 µM) following 60 and 120 minutes of co-incubation. For imipramine (A), DS81 (B), and indacaterol (E) data are presented as the mean ± SD of n= 7, from two independent experiments. For formoterol (C) and salmeterol (E) data are presented as the mean ± SD of n= 4, from a single experiment. * indicates a statistically significant lower cell accumulation as compared to the control group (* $p<0.05$, ** $p<0.01$, *** $p<0.001$ and **** $p<0.0001$).

5.3.2. Unbound fraction of compounds in Calu-3 cell lysate

The affinity of the different compounds towards cellular components was assessed by measuring unbound fraction following their incubation with Calu-3 cell lysate. For this, Calu-3 cell lysate spiked with the compounds was subjected to equilibrium dialysis. A higher unbound fraction (f_u) was seen with the permanently charged compounds, ipratropium (f_u ~ 0.71 ± 0.14) and tiotropium (f_u ~0.67 ± 0.03) (Figure 5-3). With respect to basic compounds, f_u decreased with an increase in their lipophilicity (Figure 5-3). The hydrophilic salbutamol did not show any affinity towards cellular components, as reflected by its f_u ~1 (Figure 5-3). The moderately lipophilic base formoterol displayed a higher unbound fraction (f_u ~0.73 ± 0.02) (Figure 5-3) than highly lipophilic salmeterol, which was characterised by the lowest unbound fraction in cell lysates (f_u ~0.08 ± 0.01) (Figure 5-3). While a ~4.7-fold higher f_u than salmeterol was seen for dibase DS81, zwitterionic indacaterol showed a f_u of 0.23 ± 0.03 (Figure 5-3).

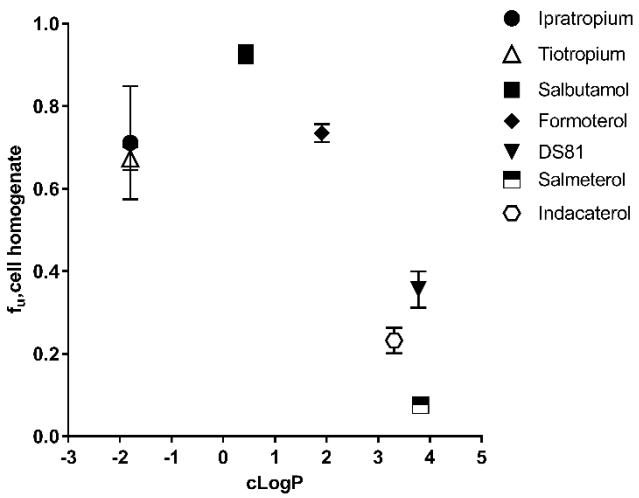


Figure 5-3. Relationship between cLogP and unbound fraction (f_u) of compounds in Calu-3 cell homogenate

Calu-3 cells (3.2× 10^5 cells/mL) homogenate containing compound (5 µM) was dialysed against HBSS using Rapid Equilibrium Dialysis devise at 60 rpm for 4 hours at 37^{o}C. At the end of the incubation, compound concentrations in buffer and cell lysate chambers were measured and used for calculating f_u in cell lysate. Data are presented as the mean ± SD, n=4 from a single experiment.

5.3.3. Quantification of lysosomal associated compound concentrations

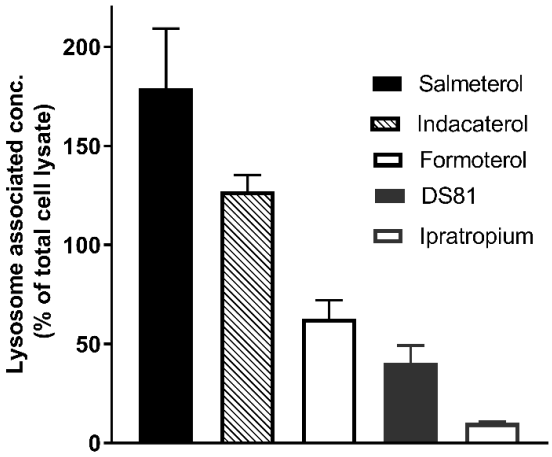
The association of the compounds with the lysosomes was quantified following isolation of lysosomal enriched fractions from Calu-3 cells treated with the compounds. Incubations were also performed in the presence and absence of bafilomycin A1 or monensin. Compound concentrations measured in the supernatant of the top three fractions were combined for data analysis purpose based on the highest acid phosphatase enzyme activity recovered in these fractions (Figure 4-7). The lysosomal associated compound was represented as percentage of total cell lysate concentration to account for permeability differences between compounds as reported earlier (Duvvuri, Gong, et al. 2004).

Of all the compounds tested, ipratropium showed a very low lysosomal accumulation (~7.8 ± 0.9 % of the total cell lysate, (Figure 5-4, A). Co-incubation of ipratropium with bafilomycin A1 or monensin did not alter its association with the lysosomal fractions (Figure 5-4, B). Salbutamol, formoterol

and salmeterol were included as representatives of basic molecules with similar pKa (~9) but differ with respect to their lipophilicity. For salmeterol, which is a long acting bronchodilator and a highly lipophilic molecule, all of the total cell lysate concentrations (126.8 ± 19.3 % of total cell lysate) were found to be associated with the lysosomal fraction (Figure 5-4, A). On the other hand, no lysosomal associated concentrations (< lower limit of quantification, 0.0039 µM) were detected for salbutamol. Formoterol showed 45.7 ± 8.8 % of the total cell lysate with the lysosomes (Figure 5-4, A). On similar lines, dibasic DS81 also highly accumulated within the lysosomes i.e. 38.5 ± 8.2 % of its total cell lysate concentration were measured in the lysosomal fraction (Figure 5-4, A). Interestingly, 78.7 ± 5.2 % of total cell lysate concentrations were found to be associated with the lysosomal fractions for indacaterol (Figure 5-4, A).

Incubations with pH gradient disruptors indicated that lysosomal accumulation of lipophilic basic molecules but not of zwitterions was driven by cytosolic-lysosomal pH gradient. When compared with the control group, cells co-incubated with monensin showed only 19.5 ± 4.9 and 13.8 ± 7.0 % of lysosomal associated salmeterol and formoterol, respectively (Figure 5-4, B) whereas the presence of bafilomycin A1 lowered their lysosomal concentrations by 37.4 ± 6.0 and 54.9 ± 6.8 % of control group, respectively (Figure 5-4, B). For dibasic DS81, the presence of monensin and bafilomycin A1 lead to lysosomal associated concentrations of 5.7 ± 2.0 and 31.8 ± 4.0 % of the control group, respectively (Figure 5-4, B). In contrast, both bafilomycin A1 and monensin failed to lower the lysosomal accumulation of indacaterol (164.9 ± 57.9 and 148.9 ± 11.3 % of control group in the presence of bafilomycin A1 and monensin, respectively) (Figure 5-4, B).

A



B

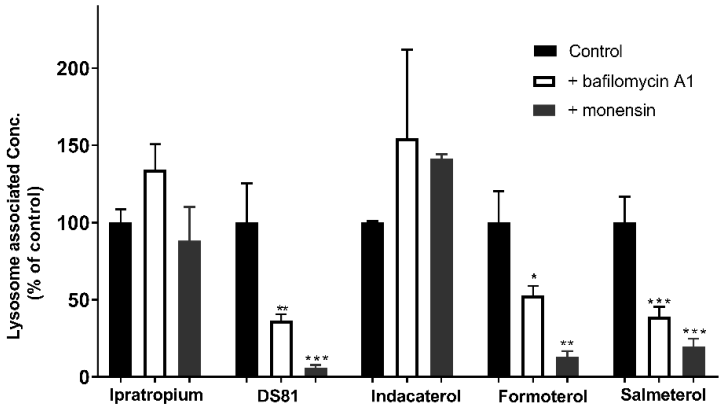


Figure 5-4. Lysosomal associated concentrations of various compounds.

Lysosomes were isolated from Calu-3 cells treated with various compounds (10 µM) in the absence or presence of cytosol-lysosomal pH gradient disruptors, bafilomycin A1 (100 nM) or monensin (20 µM), using cell fractionation approach. (A) Concentrations of various compounds associated with lysosomal fractions (fractions 1-3) were combined and represented as a % of compounds concentrations with total cell lysate. Compound concentrations detected in the top 3 fractions (Fractions 1 - 3) were only considered for further analysis based on their association with lysosomal specific acid phosphatase enzyme activity. (B) Effect of pH gradient disruptors, bafilomycin A1 or monensin on various compound concentrations associated with lysosomal fractions (sum of fractions 1 - 3) in comparison with control group. Data are presented as the mean ± SD (n= 3) from a single experiment. * indicates a statistically significant lower lysosomal association of compounds as compared to the control groups (* $p<0.05$, ** $p<0.01$, *** $p<0.001$ and **** $p<0.0001$).

5.3.4. Cellular retention and permeability of compounds in Calu-3 layers

Compound retention across Calu-3 layers was measured following exposure from their apical or basolateral side. In general, higher uptake (1.5 to 5.3-fold) was seen for most molecules following basolateral (BL) exposure than from the apical side (AP), except for salmeterol (BL/AP uptake ratio ~1) (Figure 5-6). Of all the molecules tested, zwitterion indacaterol showed the highest cell associated concentrations (ranged from 4.67 ± 0.75 to 8.85 ± 0.46 and 8.78 ± 1.85 to 13.91 ± 1.20 nmoles/mg of protein, from the apical or basolateral side, respectively (Figure 5-6, A). For the dibase DS81 and salmeterol, cell retention was ~ 1.3 to 3-fold lower than that of indacaterol throughout the experiment (Figure 5-6, B and C).

Comparatively, higher cellular concentrations were seen with salmeterol than with formoterol (i.e. ~ 6 to 10-fold and 1.2 to 1.7 - fold higher following apical and basolateral exposure, respectively) (Figure 5-6, D). On the other hand, permanently charged ipratropium showed lower levels of cell retention as compared to the other molecules (0.17 ± 0.03 and 0.38 ± 0.07 nmoles/mg of protein from apical and basolateral side, respectively at 2h (Figure 5-6, E).

In line with their higher uptake from the basolateral side, the P_{app} of molecules in the secretion direction (*b*-*a*) was found to be many fold higher than in the absorptive direction (*a*-*b*) resulting in efflux ratio > 2 for many molecules (range ~ 6-20), expect for salmeterol (efflux ratio~1) (Table 5-1).

5.3.5. Effect of bafilomycin A1 on cellular retention and permeability of compounds in Calu-3 layers

The effect of bafilomycin A1 on compound cellular retention and transepithelial transport was investigated both in the absorptive (apical to basolateral, *a*-*b*) and secret (basolateral to apical, *b*-*a*) directions. No effect on TEER values was seen due to the presence of bafilomycin A1 suggesting that it did not alter the tight junctions of Calu-3 layers (Figure 5-5). Changes in the cellular accumulation and P_{app} of inhaled molecules in the presence of bafilomycin A1 was assumed to be due to their altered lysosomal sequestration.

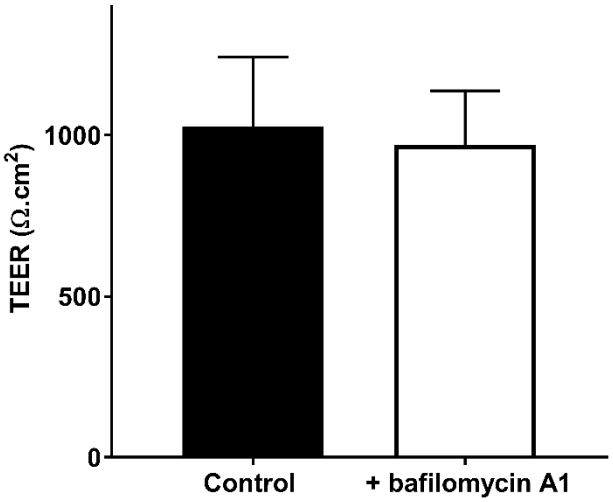


Figure 5-5. TEER values across Calu-3 layers following their incubations with HBSS alone (control) or HBSS containing bafilomycin A1.

Calu-3 cells were seeded at a density of 1 × 10^5 cells/cm^2 on 12-well Transwell® inserts and cultured under air-liquid interface culture conditions for 21 days at 37ºC in a humidified incubator under 5% CO_2. TEER values were measured across Calu-3 cell layers following their incubation with either HBSS alone (control) or HBSS containing bafilomycin A1 (100 nM) for 3 hours. Data is represented as the mean ± SD of twenty four layers per group from two independent experiments.

5.3.5.1. Effect of bafilomycin A1 in the absorptive direction

In the absorptive direction (*a-b*), the cellular concentrations of dibasic DS81 decreased by 81.9 ± 3.5 % of the control group upon co-incubation with bafilomycin A1 (Figure 5-6, B). The decrease in DS81 concentrations was characterised by a sharp decline within the first 60 minutes of incubation (Figure 5-6, B). These reductions in cellular accumulation resulted in an 18-fold (18.3 ± 1.4) increase in the absorptive P_{app} in the presence of bafilomycin A1 (Figure 5-7, B and Figure 5-8, A). In contrast, no change in cellular concentrations (91.8 ± 11.3 % of control at 2h) and P_{app} was seen for ipratropium in the presence of bafilomycin A1 following apical side exposure (Figure 5-6, E; Figure 5-7, D and Figure 5-8, A).

However, for salmeterol and formoterol, a gradual decrease in cell associated concentrations was observed as a function of time with bafilomycin A1 (Figure 5-6, C and D). At the end of incubation (120 minutes), the cellular concentration of salmeterol and formoterol was reduced by 41.9 ± 8.2 and 50.3 ± 7.8 % in

comparison with control groups, respectively (Figure 5-6, C and D). For indacaterol, only a moderate reduction in cell concentration (19.3 ± 9.3 % of control at 120 min) was observed when co-incubated with bafilomycin A1 (Figure 5-6, A). Consequently, the presence of bafilomycin A1 resulted in an increased P_{app} for formoterol, salmeterol and indacaterol by a 9.9 ± 0.4, 1.6 ± 0.3 and 3.5 ± 0.6 - fold respectively (Figure 5-7, A - C and Figure 5-8, A). In contrast, the P_{app} of salbutamol was unaltered by bafilomycin A1 (Figure 5-7, F and Figure 5-8, A). However, cellular retention was not measured for salbutamol.

5.3.5.2. Effect of bafilomycin A1 in the secretion direction

Following exposure from the basolateral side, bafilomycin A1 altered cellular concentrations for the lipophilic β2-agonists and dibase DS81 in a similar extent as seen following apical exposure (Figure 5-6). However, the extent of increase in the secretory P_{app} (*b-a*), as a consequence of lowered cellular accumulation was only moderate (2.7 ± 0.6-fold) for the dibase DS81 (Figure 5-7, B and Figure 5-8, B). While the P_{app} in *b-a* direction was unaltered for salmeterol (fold change: 1.3 ± 0.4), a 2-fold (2.0 ± 0.1) increase was seen for indacaterol (Figure 5-7, A and C; Figure 5-8, B).

Interestingly, the cellular concentrations of ipratropium were reduced by 44.9 ± 9.3 %, following basolateral exposure with bafilomycin A1 (Figure 5-6, E). It was unexpected as ipratropium was not associated with lysosomes given its permanently charged nature. This resulted in an 81% reduction in the drug P_{app} in the *b-a* direction (Figure 5-7, E and Figure 5-8, B). Along similar lines, bafilomycin A1 lowered the P_{app} of salbutamol and formoterol in the *b-a* direction by 93 and 75 % of control group, respectively (Figure 5-7, D and F; Figure 5-8, B).

5.3.5.3. Effect of bafilomycin A1 on the efflux ratio of various molecules

In the presence of bafilomycin A1, the apparent efflux ratio of the various molecules was lowered significantly depending on the pathway affected; i.e., cell retention vs. uptake mechanism. Bafilomycin A1 lowered the efflux ratio of DS81 and indacaterol, through increasing their absorptive P_{app} as a consequence of reduced lysosomal sequestration (Table 5-1, Figure 5-6, Figure 5-7 and Figure 5-8). On the other hand, for non-lysosomotropic compounds ipratropium and salbutamol, bafilomycin A1 abolished the efflux mechanism by reducing their uptake from the basolateral side (Table 5-1, Figure 5-6, Figure 5-7 and Figure 5-8). However, for formoterol, a combination of increased permeability in the absorptive direction and lowered uptake from the basolateral side could account for the reduction in its efflux ratio (Table 5-1, Figure 5-6, Figure 5-7 and Figure 5-8).

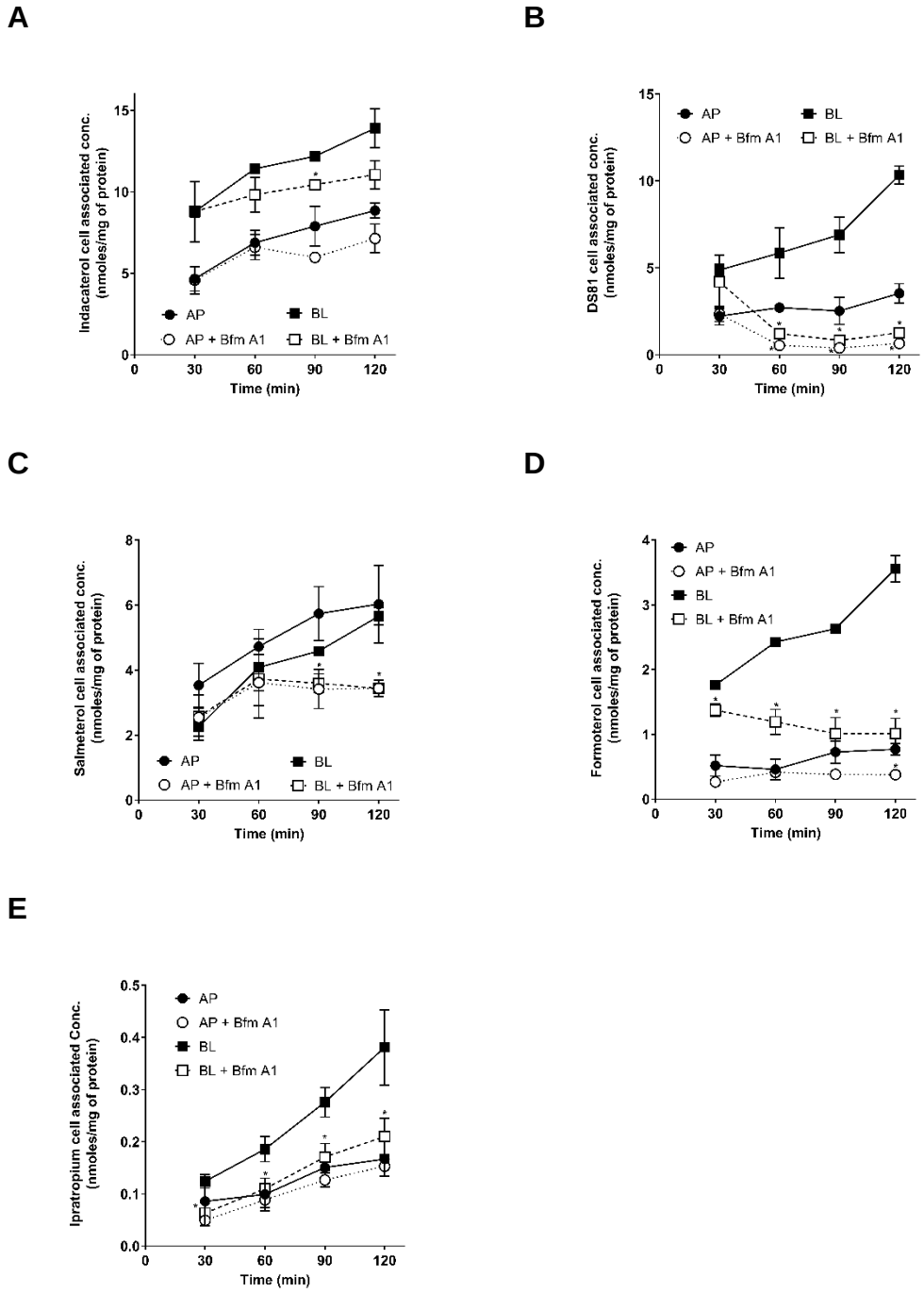


Figure 5-6. Cellular retention of various compounds in Calu-3 layers in the presence or absence of bafilomycin A1 (Bfm A1).

Calu-3 cells were seeded at a density of 1 × 10^5 cells/cm^2 on 12-well Transwell® inserts and cultured under air-liquid interface culture conditions for 21 days at 37°C in a humidified incubator under 5% CO_2. Calu-3 cell layers were incubated with various compounds (A) indacaterol, (B) DS81, (C) salmeterol, (D) formoterol and (E) ipratropium at 10 µM in the presence or absence of bafilomycin A1 (Bfm A1 - 100 nM). At various time points, compound solutions were withdrawn, cell layers were with washed with cold PBS and compound associated with the cell layers were measured. Each data point represents the mean ± SD of three layers from a single experiment. *

indicates a statistically significant reduction in cell associated concentration due to the presence of bafilomycin A1 when compared with their respective control group at each time point ($p<0.05$).

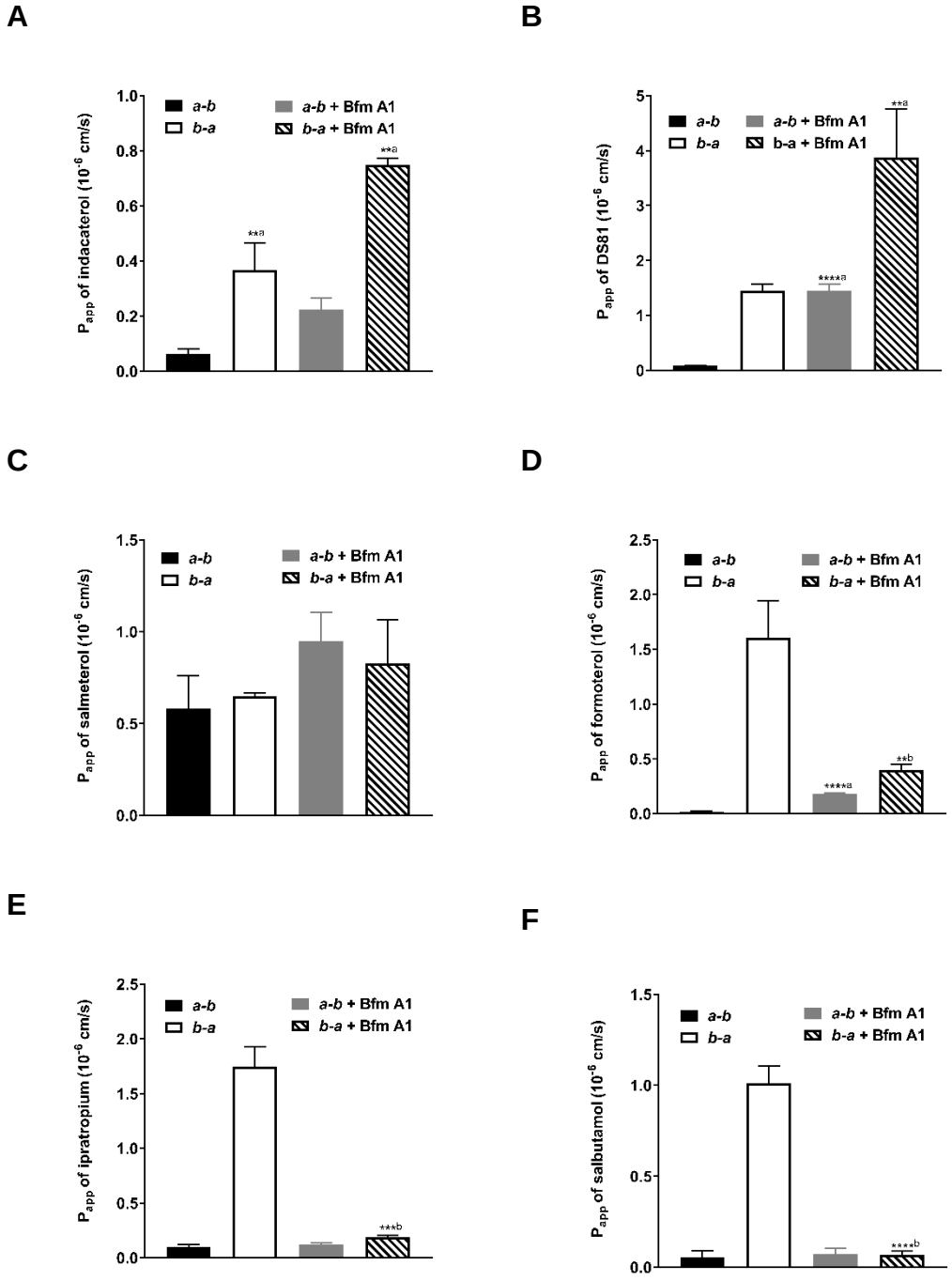
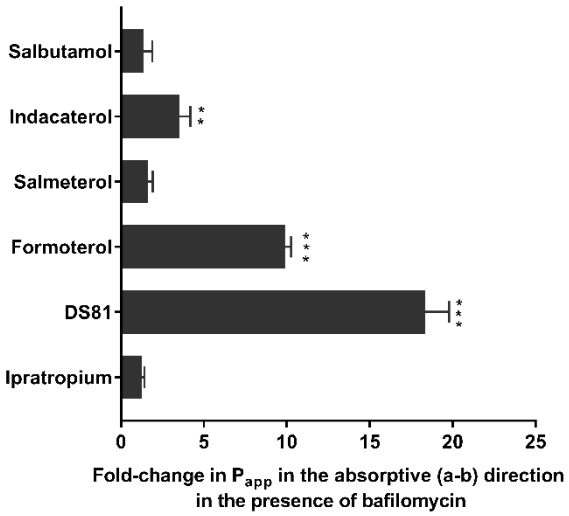


Figure 5-7. Permeability of various compounds in Calu-3 layers in the presence or absence of bafilomycin A1 (Bfm A1).

Calu-3 cells were seeded at a density of 1×10^5 cells/cm^2 on 12-well Transwell® inserts and cultured under air-liquid interface culture conditions for 21 days at 37°C in a humidified incubator under 5% CO_2. Coefficient of apparent permeability (P_{app}) was measured for various compounds at 10 µM in the apical to basolateral (*a-b*) and basolateral to apical (*b-a*) direction, in the

presence or absence of bafilomycin A1 (Bfm A1 – 100 nM). Data are presented as the mean ± SD of three layers from a single experiment. * indicates a statistically significant higher (*[a]) or lower (*[b]) permeability due to the presence of bafilomycin A1 when compared with control group (** p<0.01; *** p<0.001, ****p<0.0001).

A



B

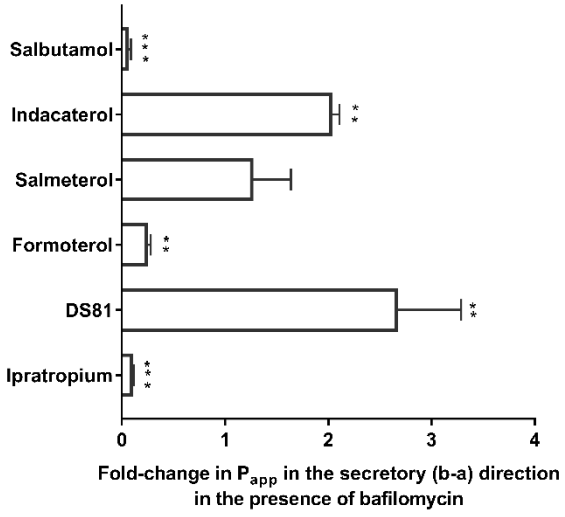


Figure 5-8. Fold-change in the permeability of inhaled compounds across Calu-3 cell layers in the presence of bafilomycin A1.

Calu-3 cells were seeded at a density of 1 × 10^5 cells/cm^2 on 12-well Transwell® inserts and cultured under air-liquid interface culture conditions for 21 days. Coefficient of apparent permeability (P_{app}) of various compounds were measured at 10 µM across Calu-3 layers in the presence or absence of bafilomycin A1 (100 nM). (A). Fold-change in the P_{app} of inhaled compounds in the absorptive direction (*a-b*) due to the presence of bafilomycin A1. (B).

Fold-change in the P_{app} of inhaled compounds in the secretion direction (*b-a*) due to the presence of bafilomycin A1. Data are presented as the mean ± SD of three layers from a single experiment. * indicates a statistically significant fold-change in the permeability due to the presence of bafilomycin A1 (** p<0.01, and ***p<0.001).

5.3.6. Influence of structural modification on intracellular accumulation, permeability and lung retention

Cellular disposition and lung retention in Calu-3 cells and rats, respectively was studied for a set of novel molecules comprising the mono base DS12 and the di base DS81 molecules along with their respective quaternary pairs DS13 and DS86. The structures and physico-chemical properties of these molecules are presented in the chapter 2 (Table 2-1).

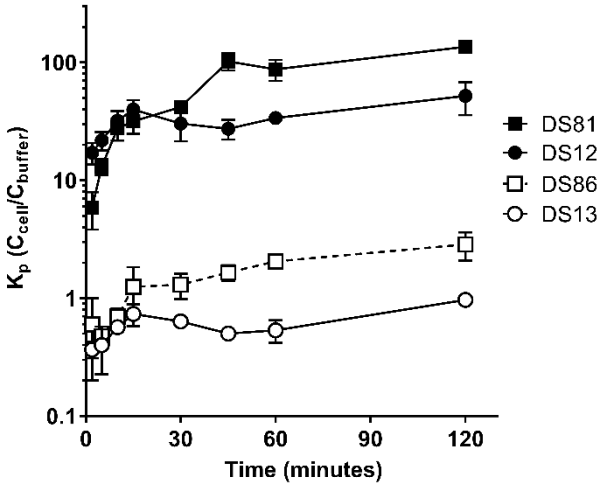
In comparison with the mono base DS12, a 2.6-fold higher intracellular accumulation (K_{p2h}) was seen for dibasic DS81 (Figure 5-9, A). Reflecting their total cell concentrations, much lower lysosomal associated concentrations were detected for DS12 than for DS81 (7.3 ± 3.0 vs. 38.5 ± 8.3 % of total cell lysate, respectively) (Table 5-2). Lysosomal association for DS12 and DS81 was also demonstrated by the changes in their K_{p2h} in the presence of the cytosol-lysosomal pH gradient disruptors, bafilomycin A1 or monensin (Figure 5-9, B). Introduction of a charge on the pyrrole ring of DS12 and DS81 significantly lowered their intracellular and lysosomal concentrations. This was evident by a ~ 48 and 58-fold lower K_{p2h} for DS13 and DS86 compared to their basic equivalent i.e. DS12 and DS81, respectively (Figure 5-9, A). In addition, no lysosomal concentrations could be detected for DS13 and DS86 (Table 5-2). The lack of lysosomal association for these quaternary compounds was also supported by their unchanged K_{p2h} in the presence of bafilomycin A1 (Figure 5-9, B). While monensin did not alter the K_{p2h} of DS13, there was a statistically significant reduction in the K_{p2h} of DS86. This could not be attributed to a change in its lysosomal sequestration as DS86 levels in the lysosomal enriched fractions were below the detection limit (Figure 5-9, B and Table 5-2).

When tested across Calu-3 layers, DS12 showed a many folds higher permeability (P_{app}) in the absorptive direction than dibasic DS81 (5.18 ± 0.45

vs. 0.08 ± 0.01, $\times 10^{-6}$ cm/s) (Table 5-2). The presence of a permanent charge resulted in a very low P_{app} (0.04 ± 0.01, $\times 10^{-6}$ cm/s) for DS13, in comparison with DS12. On the other hand, similar P_{app} was seen for the quaternary base DS86 (P_{app} ~ 0.10 ± 0.02, $\times 10^{-6}$ cm/s) in comparison with dibasic DS81 (0.08 ± 0.01, $\times 10^{-6}$ cm/s) (Table 5-2). Except for the highly permeable DS12, all other molecules showed a significant secretion across the Calu-3 layers, resulting in efflux ratios > 2 (Table 5-2).

Permeability and intracellular accumulation in Calu-3 cells reflected the extent of lung retention following IT administration in rats for the basic and quaternary compounds. A very low lung retention for DS12 was reflected by its short absorption half-life ($t_{1/2}$ ~ 0.6 ± 0.1h) (Figure 5-10, Table 5-2). In contrast, a long lung retention was observed for DS13, DS81 and DS86, indicated by their absorption half-lives of 10.0 ± 2.1, 20.5 ± 7.2, and 22.6 ± 5.6h, respectively (Figure 5-10, Table 5-2).

A



B

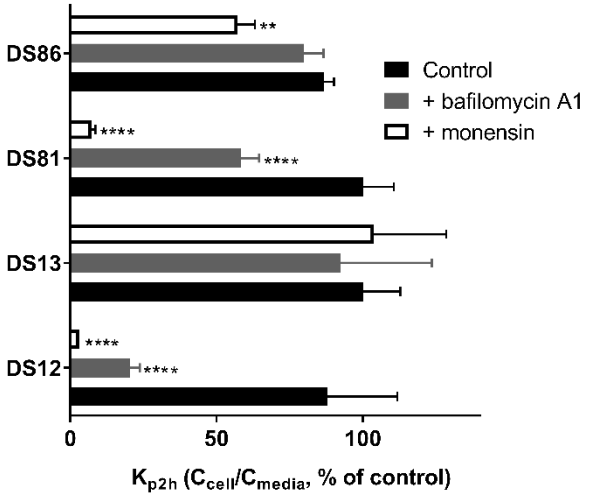


Figure 5-9. Comparative cellular partition coefficient (K_p) of basic (DS12 & DS81) and their quaternary pairs (DS13 & DS86) in Calu-3 cells.

Calu-3 cells were grown in collagen-coated 24-well plates (500 µL/well of 3.2× 10^5 cells/mL) by incubating at 37°C in a humidified incubator under 5% CO_2 for 3 days. (A). Cellular partition coefficient (K_p) in Calu-3 cells was measured for various compounds at 5 µM, as function of incubation time. (B) K_p in the presence of bafilomycin A1 (100 nM) or monensin (20 µM) for DS12, DS13, DS81 and DS86 following incubation for 2h (K_{p2h}). Each bar or data point represents the mean ± SD of four wells from a single experiment. * indicates a statistically significant reduction in the compound accumulation as compared with the control (** $p<0.01$ and **** $p<0.0001$).

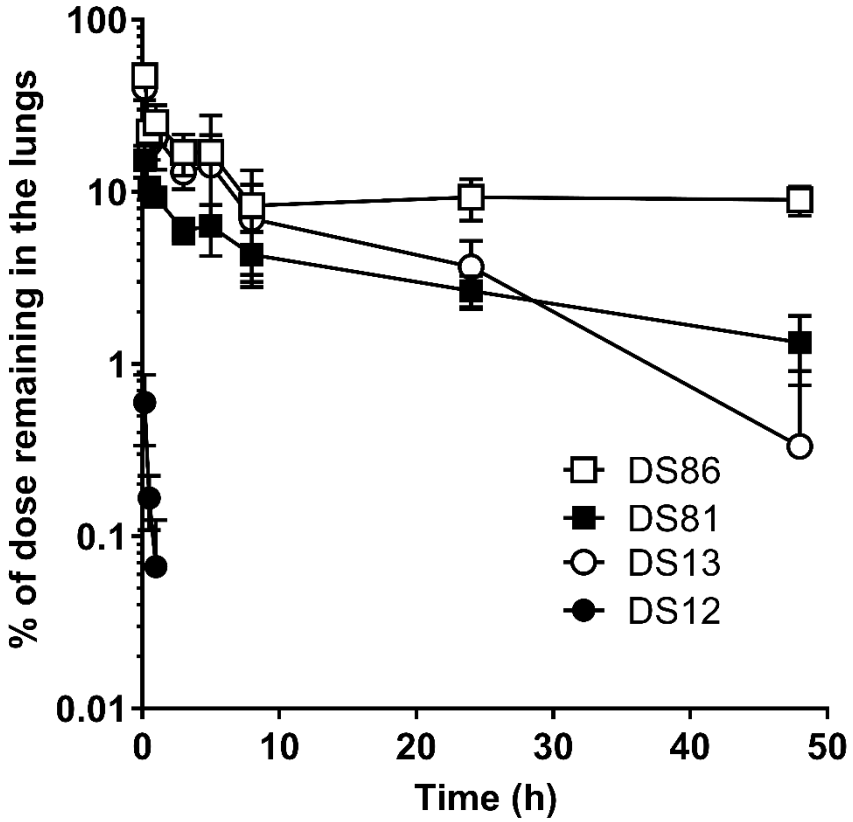


Figure 5-10. Percentage of administered dose remaining in the lungs at various time points for various novel compounds in male SD rats following intratracheal administration.

Compounds DS12 (monobasic), DS81 (dibase) and their quaternary counter parts, DS13 and DS86, respectively were dissolved in PBS and administered through intratracheal instillation in male SD rats; Dose administered – 0.1 mg/kg for DS12 and 0.2 mg/kg for remaining compounds. At various time points animals were sacrificed and lungs were collected from the rats. Compound concentrations in the lungs were measured and represented as % of dose remaining in the lungs. Each data point represents the mean ± SD, N=3 from a single experiment.

Compound	Efflux ratio (P_{app}, *b-a* / P_{app}, *a-b*)	
	Control	+ bafilomycin A1
Ipratropium	17.7 ± 1.9	1.5 ± 0.2
DS81	18.3 ± 1.5	2.7 ± 0.6
Salbutamol	18.5 ± 1.8	0.9 ± 0.3
Formoterol	nc [a]	2.2 ± 0.3
Indacaterol	5.8 ± 1.6	3.3 ± 0.1
Salmeterol	1.1 ± 0.0	0.9 ± 0.2

Table 5-1. Effect of bafilomycin A1 on the efflux ratio of inhaled compounds in Calu-3 layers

Coefficient of apparent permeability (P_{app}) was measured in Calu-3 layers for various compounds at 10 µM in absorption (*a-b*) and secretion direction (*b-a*) in the presence or absence of bafilomycin A1 (100 nM). P_{app} in *b-a* direction was divided with that in *a-b* direction to calculate efflux ratio. Data is presented as mean ± SD (n=3) from a single experiment. [a] not calculated as *a-b* direction samples showed poor and variable response in control group.

Compound		**DS12**	**DS13**	**DS81**	**DS86**
Chemical class		Mono base	Quaternary	Di base	Base quaternary
P_{app} (10^{-6} cm/s)	***a-b***	5.18 ± 0.45	0.04 ± 0.01	0.08 ± 0.01	0.10 ± 0.03
	b-a	6.62 ± 0.76	0.70 ± 0.10	1.45 ± 0.12	1.71 ± 0.32
Efflux ratio		1.3	17.5	18.1	17.1
Lysosomal accumulation	**Control (% of total cell lysate)**	7.3 ± 3.0	NR	38.5 ± 8.2	NR
	+ bafilomycin A1 (% of control)	NR	NR	67.5 ± 5.0	NR
Lung absorption half –life in rats ($t_{1/2}$, h)		0.6 ± 0.1	10.0 ± 2.1	20.5 ± 7.2	22.6 ± 5.6

Table 5-2. Coefficient of apparent permeability (P_{app}) across Calu-3 layers, lysosomal accumulation and lung absorption half-lives in rats for DS12, DS13, DS81 and DS86.

Coefficient of apparent permeability (P_{app}) was measured in Calu-3 layers for various compounds at 10 µM in absorption (*a*-*b*) and secretion direction (*b*-*a*). P_{app} in *b*-*a* direction was divided with that in *a*-*b* direction to calculate efflux ratio. For determining lysosomal accumulation of compounds, lysosomes were isolated from Calu-3 cells treated with various compounds (10 µM) in the absence or presence of cytosol-lysosomal pH gradient disruptors, bafilomycin A1 (100 nM) or monensin (20 µM), using cell fractionation approach. Concentrations of various compounds associated with lysosomal fractions (fractions 1-3) were combined and represented as a % of compound concentrations with total cell lysate. Lung absorption half-life was determined for the compounds based on % of administered dose remaining at various time points in rat lungs following their intra-tracheal administration. Data are presented as mean ± SD (n=3/4) from a single experiment; NR – not reportable; concentrations were found to be lower than the limit of quantitation (LLOQ) in lysosomal fractions.

5.4. Discussion

The main aim of these investigations was to understand the cellular retention mechanisms of inhaled compounds in the lungs applying the *in vitro* airway epithelial model Calu-3. Our findings demonstrate lysosomal sequestration, along with binding to intracellular components attribute a high lung affinity to the long acting β2-agonist bronchodilators while for dibase compounds lysosomal sequestration alone appears to determine their lung retention. The current study also re-established the low cellular association and epithelial permeability of the permanently charged compounds including anti-cholinergic bronchodilator, ipratropium.

Inhaled bronchodilators face epithelial membrane and cellular sequestration organelles such as lysosomes, on their transit towards their target site (airway smooth muscle) (Backman et al. 2014). Physicochemical properties i.e. pKa and lipophilicity of compounds determine their permeability across the airway epithelium as well as their cellular distribution, including retention in lysosomes (Cooper, Ferguson, and Grime 2012). For compounds with basic pKa and high lipophilicity, both intracellular binding and lysosomal sequestration could determine their cellular retention. On the other hand, compounds with low pKa and lipophilicity tend to show lower intracellular concentrations due to the absence of any cellular depot driving their accumulation (Siebert et al. 2004).

This was evident in the present study with high accumulation (K_p) in Calu-3 cells for dibase DS81 and long acting β_2 agonists (salmeterol, formoterol and indacaterol) (Figure 5-1, A). Significant reductions in K_p following disruption of vesicular pH gradient confirmed their association with lysosomes (Figure 5-2). However, for the more hydrophilic base salbutamol, a very low K_p (< 1) suggests a poor affinity for intracellular components, including for lysosomes, especially as its K_p was unaltered with disruption of pH gradient (Figure 5-1, A and C). In comparison with basic and lipophilic molecules, a lower K_p for the anticholinergic bronchodilators (ipratropium and tiotropium) indicated a limited cell distribution (Figure 5-1, A). Also, no role of cytosolic-lysosomal pH gradient in their intracellular distribution was evident, as expected from their permanent positive charge (Figure 5-1, B).

The accumulation characteristics (K_p) of the different classes of molecules in Calu-3 cells were in agreement with their distribution volumes ($V_{u,lung}$) reported in a rat lung slice model (Backstrom, Lundqvist, et al. 2016). For instance salbutamol, ipratropium and tiotropium were characterised by a small $V_{u,lung}$ (2.2, 12.9 and 3.9 mL/kg, respectively). In contrast, a larger $V_{u,lung}$ was reported for a dibasic molecule (2972 mL/kg), and a 391, 49 and 17-fold higher $V_{u,lung}$ for salmeterol, indacaterol and formoterol than salbutamol, respectively (Backstrom, Lundqvist, et al. 2016). Furthermore, the presence of monensin in lung slices resulted in a reduction of $V_{u,lung}$, by 30% for indacaterol and ~70% for both salmeterol and formoterol (Backstrom, Boger, et al. 2016). Similar reductions were seen in the accumulation of these compounds in Calu-3 cells, in the presence of pH gradient disruptors (Figure 5-2). Previously, pronounced (21 to 40%) reductions in K_p were also reported for β_2 agonists in a rat macrophage cell line in presence of pH disruptors (Ufuk et al. 2015). These results suggested that cellular retention mechanisms driven by the lipophilicity and basicity of molecules are easily translatable between tissue and cell based models. This was also demonstrated by Pfeifer et al., where comparable subcellular distribution of compounds was seen between rat sandwich-cultured hepatocytes and isolated perfused rat liver (Pfeifer et al. 2013). Similarly, current results are supportive of Calu-3 as an alternate model for enquiring lung tissue retention mechanisms.

Studies with imipramine, a prototypical cationic amphiphilic drug and a lysosomotropic marker, established the utility of the Calu-3 model for investigating lysosomal sequestration of inhaled compounds. For instance, the extensive accumulation seen for imipramine in Calu-3 cells (Figure 5-1, A) was in agreement with previous reports in a macrophage cell line (K_p – 347 ± 60, lung slices (tissue/media ratio: 61 to 99) and in rabbit lungs (tissue/media ratio ~17.0 ± 1.8 at 0.5 µM) (Drew et al. 1981; Junod 1972; Ufuk et al. 2015). Also, the reduction in imipramine K_p with abolition of the pH gradient (Figure 5-2, A) was similar to earlier reports, where the presence of NH_4Cl or monensin lowered K_p by 70, 59 - 64 and 46 % of control in alveolar macrophages, lung slices and in immortalised hepatocytes, respectively (Daniel and Wojcikowski 1997; Kazmi et al. 2013; Ufuk et al. 2015).

In addition to pH dependent sequestration mechanisms, binding to lysosomal membranes and phospholipids is assumed to potentiate basic compound accumulation in lysosomes (MacIntyre and Cutler 1988; Yokogawa et al. 2002). Measuring compound concentrations at the lysosomal level facilitated understanding of the relative contribution of pH gradient and/or binding in the lysosomal accumulation of compounds. For instance, reductions in lysosomal concentrations of basic compounds following cytosol-lysosomal pH gradient disruption reflected changes in their total cellular levels (Figure 5-4). However, no reductions with lysosomal concentrations were seen for indacaterol following pH disruption (Figure 5-4). These results indicate, cellular accumulation of indacaterol could be predominantly driven by binding to cellular components such as phospholipids, facilitated by its lipophilic and zwitterion properties as suggested by the 'plasmalemma diffusion microkinetic' theory (Anderson, Linden, and Rabe 1994; Lombardi, Cuenoud, and Kramer 2009). The higher binding of lipophilic β_2 agonists than that of polar drugs such as ipratropium was in agreement with a role of non-specific binding in their cellular distribution (Figure 5-3).

Permeability measurements across Calu-3 in the presence or absence of cytosol-lysosomal pH gradient disruption helped to appreciate the relative contribution of lysosomal sequestration and non-specific binding as a tissue affinity factor for inhaled compounds. For instance, the predominant role of lysosomal sequestration as a 'lung affinity' mechanism was evident for dibase compound DS81 since this significantly impeded its permeability (Figure 5-6, Figure 5-7 and Figure 5-8). However, for β_2 agonists increases in permeability of molecules due to 'freed drug' from lysosomes following pH disruption, appears to be depend on cellular binding. This is demonstrated by a lower fold-increase in the P_{app} of salmeterol than formoterol in the absorption direction (*a-b*), even though both showed similar extent of reductions (~50 % of control) in cellular concentrations (Figure 5-6, Figure 5-7 and Figure 5-8). On the other hand, a moderate reductions (~19% of control) in the cellular concentrations of indacaterol lead to a 3.5 - fold increase in its permeability (Figure 5-6, Figure 5-7 and Figure 5-8).These differences could be attributed to their ionisation state at physiological pH, where indacaterol and salmeterol are assumed to be

predominantly in zwitterion and cation forms, respectively (Lombardi, Cuenoud, and Kramer 2009). It was hypothesised that zwitterions permeate membranes more effectively than cations or anions, thus explaining the faster onset of action for indacaterol than for salmeterol (Lombardi, Cuenoud, and Kramer 2009). On the other hand, the higher unbound fraction in Calu-3 cell lysates for DS81 than for salmeterol and indacaterol explains the relatively low contribution of intracellular binding in the cellular disposition of these molecules (Figure 5-3).

Even though this may not be relevant for inhalation therapy, the effects of bafilomycin A1 following basolateral exposure thrown some insights onto drug secretion mechanisms across the airway epithelium. Earlier studies with ipratropium and formoterol established an active secretion across the Calu-3 apical membrane coupled with uptake mechanisms across the basolateral side (Mukherjee, Pritchard, and Bosquillon 2012; Chapter 3). The current study, while re-confirming these observations, showed a similar mechanism could be involved in the basolateral uptake of salbutamol. Interestingly, bafilomycin A1 lowered the secretion of ipratropium, formoterol and salbutamol, as a consequence of reduced uptake from basolateral side (Figure 5-6, Figure 5-7 and Figure 5-8, Table 5-1). Considering no effect of bafilomycin A1 on the apical uptake and absorptive P_{app} of ipratropium (Figure 5-6, Figure 5-7 and Figure 5-8), a known substrate of OCT transporters (Hendrickx et al. 2013), its basolateral inhibitory actions could be attributed to non-OCT mechanisms.

In order to design molecules with long lung retention, it is essential to understand the structural properties required for a high lung tissue affinity. Cellular disposition studies in Calu-3 with novel chemical analogues illustrated the effect of structural modification on lung retention mechanisms. For instance, increased lung tissue retention as a consequence of higher lysosomal association was evident with a dibasic compound (Figure 5-9 and Figure 5-10) which is characterised by a long absorption half-life. However, for mono bases, poor lung retention was in line with its higher permeability, probably as a consequence of lower cellular retention and lysosomal association than the dibasic molecule (Figure 5-9 and Figure 5-10, Table 5-2). On the other hand, low cellular accumulation with no association with lysosomes for quaternary

compounds was in agreement with their permanent charge (Figure 5-9, Table 5-2). These reinforce the low intrinsic permeability of quaternary compounds facilitating their lung retention (Figure 5-10, Table 5-2).

While cell fractionation approach employed in this study claimed to provide pure lysosomal fractions, non-specific binding to membranes could potentially interfere with lysosomal concentrations. These approaches are well-recognised to be associated with various technical difficulties such as cross contamination with other organelles and release of accumulated drug during isolation procedures (Pfeifer et al. 2013). Hence investigations with isolated lysosomes using radiolabelled compounds may be required in order to fully appreciate the role of lysosomal sequestration as a lung affinity factor for inhaled compounds.

Monitoring the local drug distribution of inhaled bronchodilators is essential as they determine the dosing frequency and therapeutic outcome of inhaled bronchodilators (Backman et al. 2017). Current studies may aid in understanding cellular level availability of drugs and help to optimise compound properties for a better lung retention. While incorporating lysosomal sequestration improved *in vitro* - *in vivo* correlations for basic drug distribution in the lungs, including cellular uptake mechanisms was considered to further improve these correlations (Assmus, Houston, and Galetin 2017). Thus, well-established airway epithelial models like Calu-3 with relevant drug transport and metabolic properties (Florea et al. 2003) may be invaluable to assess inhaled drug distribution at the cellular level.

5.5. Conclusion

Previous investigations for characterising the lysosomal sequestration as lung retention mechanism for inhaled molecules were limited to rodent lung tissue models. However, the use of rodent tissue models could lead to species differences and may not represent drug distribution in the human lung. Also, evidence for the impact of lysosomal sequestration on absorptive clearance of inhaled molecules across the airway epithelial barrier is not yet demonstrated. The current chapter presented the application of the human based *in vitro* airway epithelial model Calu-3 for the purpose of studying inhaled drug

retention mechanisms for an improved cellular level understanding of drug distribution in the lungs.

The investigations presented here, through mechanistic studies in the bronchial epithelial model Calu-3, delineated various mechanisms likely to contribute to inhaled drug retention such as lysosomal sequestration, non-specific binding and permeability across the airway epithelium. Studies in Calu-3 cells successfully demonstrated lysosomal association as one of the cell retention mechanisms for lipophilic basic inhaled compounds such as the long acting β_2 – agonist bronchodilators. For permanently charged compounds, their lung retention was attributed to a low intrinsic permeability as these molecules showed negligible lysosomal association. Both permeability and cellular retention measurements in Calu-3 model could partly explain the lung retention of various novel molecules with differing structural features following their intra-tracheal instillation in rats. Thus, current investigations demonstrated the application of the Calu-3 model for investigating inhaled drug disposition and indicate the potential of Calu-3 cells for reducing the number of animal experiments in the area of inhalational drug delivery.

However, most of the studies presented in this chapter were performed using only a single passage of Calu-3 cells and hence, a caution is required for extending the observations reported in the present study for other molecules. Further studies employing multiple Calu-3 cell passages would increase the confidence in the results presented here.

Chapter Six

6. General Discussion

The majority of the existing lung tissue or cell based experimental approaches for characterising drug disposition in the lungs measure either their absorptive clearance across the epithelial barrier (e.g., *in vivo* lung absorption, *ex vivo* lung perfusion and *in vitro* permeability) or total lung tissue concentrations (e.g., whole lung homogenate or lung slice model) (Backman et al. 2017; Cooper, Ferguson, and Grime 2012; Darquenne et al. 2016). As a consequence, inhaled drug interaction with the various physiological barriers in the lungs and how the lung environment influences the fate of drug molecules is not yet fully understood (Backman et al. 2017; Cooper, Ferguson, and Grime 2012). Current investigations focussed on improving mechanistic understanding of inhaled drug interaction with the lung tissue and their distribution at the cellular level using the human bronchial epithelial cell line Calu-3. The Calu-3 cell line is well-characterised in terms of cell size, volume, tight junction formation and as a permeability model under physiologically relevant air-liquid interface culture conditions (Florea et al. 2003; Forbes et al. 2015; Foster et al. 2000; Grainger et al. 2006; Min et al. 2016).

In the current study, upon culturing using well-established protocols (Hutter et al. 2014; Min et al. 2016; Mukherjee, Pritchard, and Bosquillon 2012), Calu-3 layers formed tight junctions as indicated by TEER values and the coefficient of apparent permeability (P_{app}) of paracellular markers which were comparable with earlier reports (Figure 3-2) (Forbes and Ehrhardt 2005). Permeability characteristics of various compounds across Calu-3 layers were in accordance with their physicochemical properties and explained their lung retention in rats (Figure 5-10). For instance, a permanently charged compound and its monobasic analogue were characterised by a low and high P_{app}, respectively in the absorptive direction (*a*-*b*) in Calu-3 layers (Table 5-2). These P_{app} values

were in inverse relationship with their lung absorption half-lives (Table 5-2), reinforcing a low permeability as one of the lung retention mechanisms of inhaled compounds. A dibasic compound was also characterised by a significantly lower permeability than a monobasic compound, explaining its long lung absorption half-life (Table 5-2) (Figure 5-7). The current results are in agreement with previous studies where long absorption half-lives were reported for quaternary ammonium and basic compounds, which were attributed to their intrinsic low permeability and high tissue affinity, respectively (Cooper, Ferguson, and Grime 2012). Thus, the current results with Calu-3 layers demonstrate their utility as a screening model for inhalational compounds for testing their lung absorption potential. Even though previous investigation suggests a good correlation between lung absorption in rats and permeability in Calu-3 layers, the compounds included were not relevant for inhalation therapy (Mathia et al. 2002). Further, the present investigations tested structural analogues of same chemical series (DS12 vs. DS13 and DS81 vs. DS86, Table 5-2) allowing testing the effect of structural features on permeability characteristics of molecules under similar experimental conditions.

This is the first report where lung drug transporters were implicated for both uptake and release of inhaled molecules across airway epithelium, thus suggesting their influence on local concentrations in the lungs. Most of the inhaled molecules were characterised by their polarised transport across Calu-3 layers as a consequence of their significantly higher P_{app} in the *b-a* direction than in the *a-b* (Figure 3-3, Table 5-1, Table 5-2). These results are in contradiction to highly anticipated OCT/OCTN uptake transporter mediated absorption processes (Hendrickx et al. 2013; Nakanishi et al. 2011; Nakanishi et al. 2013) and indicates the presence of more efficient secretion mechanisms across the luminal side. Also, permeability along with drug uptake and release measurements for ipratropium in Calu-3 layers, in the presence or absence of various chemical inhibitors of transporters, lead to hypothesise the existence of an efficient transporter-mediated uptake and secretion across the airway epithelium (Figure 3-6, Figure 3-7). These support Calu-3 cell layers as a suitable model for understanding inhaled drug interaction with transporters

proteins and their influence on local drug concentrations in the lungs. Previous studies demonstrated the applicability of the Calu-3 model for investing the role of transporter proteins relevant for inhaled therapeutics including OCT1, OCT3, OCTN1, OCTN2, MDR1 and MRPs (Hutter et al. 2014; Mukherjee, Pritchard, and Bosquillon 2012). Also, recently the expression of MATE transporters was confirmed, which mediate efflux of their substrates from cells, on the apical membranes of the human airway epithelium (Berg et al. 2018). However, further investigations are required to confirm the presence of MATE transporters in Calu-3 layers to implicate their role in the secretion of organic cations as seen for ipratropium (Chapter 3).

Cellular retention of inhaled molecules as a consequence of their affinity towards various cellular components could facilitate their retention in the lungs through lowering their absorptive clearance across the airway epithelium (Backman et al. 2017; Cooper, Ferguson, and Grime 2012). However, systemic investigations demonstrating the role of retention mechanisms for increased lung tissue affinity are lacking at cellular level. The results presented in the Chapter 5 of the current study filled that gap, demonstrating the presence of efficient retention mechanisms for lipophilic basic amines and zwitterions (Figure 5-1) which showed extensive intracellular association and binding in Calu-3 cells. On the other hand, low binding to cellular components and intracellular association for permanently charged compounds indicate a lack of such mechanisms in their cellular disposition (Figure 5-1). Also for basic amines with similar basicity (pKa), their lipophilicity (cLogP) appears to have driven their intracellular accumulation and lysosomal association (Figure 5-1,Figure 5-4). This was evident for inhaled molecules in the current study, where for molecules such as salmeterol (high pKa and lipophilicity), both lysosomal association and extensive cell binding was seen (Figure 5-3, Figure 5-4). However, salbutamol (similar pKa but lower lipophilicity than salmeterol) showed negligible cellular and lysosomal association with a high unbound fraction in the presence of Calu-3 cell lysate (Figure 5-3, Figure 5-4). These cellular accumulation characteristics of inhaled compounds were in excellent agreement with their recently reported lung distribution volumes ($V_{u,\ lung}$) in a lung slice model (Backstrom, Lundqvist, et al. 2016). A large $V_{u,\ lung}$ seen for

basic compounds was attributed to their sequestration in acidic lysosomes, while this was attributed to non-specific binding to various tissue components for a zwitterion (Backstrom, Lundqvist, et al. 2016). In an extension to the above report with a rat lung slice model, current investigations in Calu-3 cells provided direct evidence for the lysosomal association of basic and zwitterion molecules as a proportion of their intracellular concentrations. In addition, cellular disposition studies across the Calu-3 layers demonstrated, for the first time, the relative role of lysosomal sequestration and non-specific binding as impeding factors for lowering the absorptive clearance of various inhaled compounds (Figure 5-8). Thus, studies presented in the chapter 5 supports the suitability of Calu-3 cell layers for understanding the contribution of tissue affinity factors such as lysosomal sequestration and non-specific binding in the overall cellular disposition of inhaled molecules across the airway epithelium.

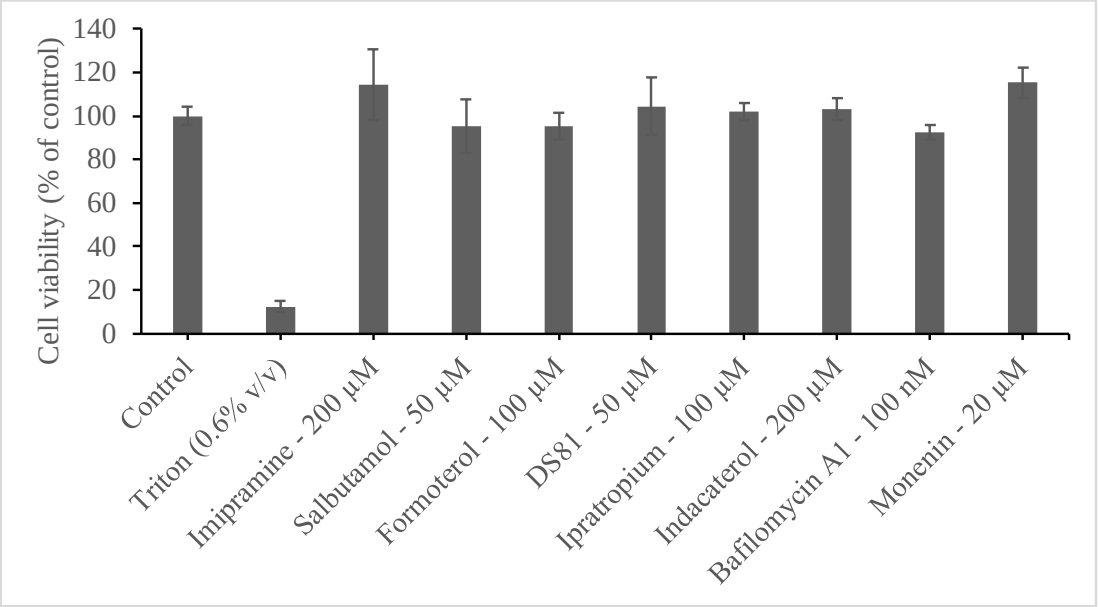
6.1. Conclusions

The cellular disposition of a variety of inhaled compounds was characterised using Calu-3 cells as a representative model of the airway epithelium. It was demonstrated that transporter-mediated uptake and release mechanisms influence the local concentrations of permanently charged compounds such as ipratropium. Also, the relative role of lysosomal sequestration and nonspecific binding as tissue affinity factors for lipophilic basic amines and zwitterions was elucidated. These investigations in Calu-3 cell systems explained lung retention mechanisms in the rat lungs for molecules with differing physicochemical properties. Thus, contributions of this work include cellular level understanding of various factors affecting both absorptive clearance and tissue retention of inhaled compounds across the airway epithelium. It is hoped that these investigations support using Calu-3 model for mechanistic understanding of inhaled drug disposition in the lungs at cellular level and reduce the usage of animal-based experiments for this purpose.

Appendix A. Chromatographic conditions, calibration curve range and lower limit of quantitation (LLOQ) for various compounds

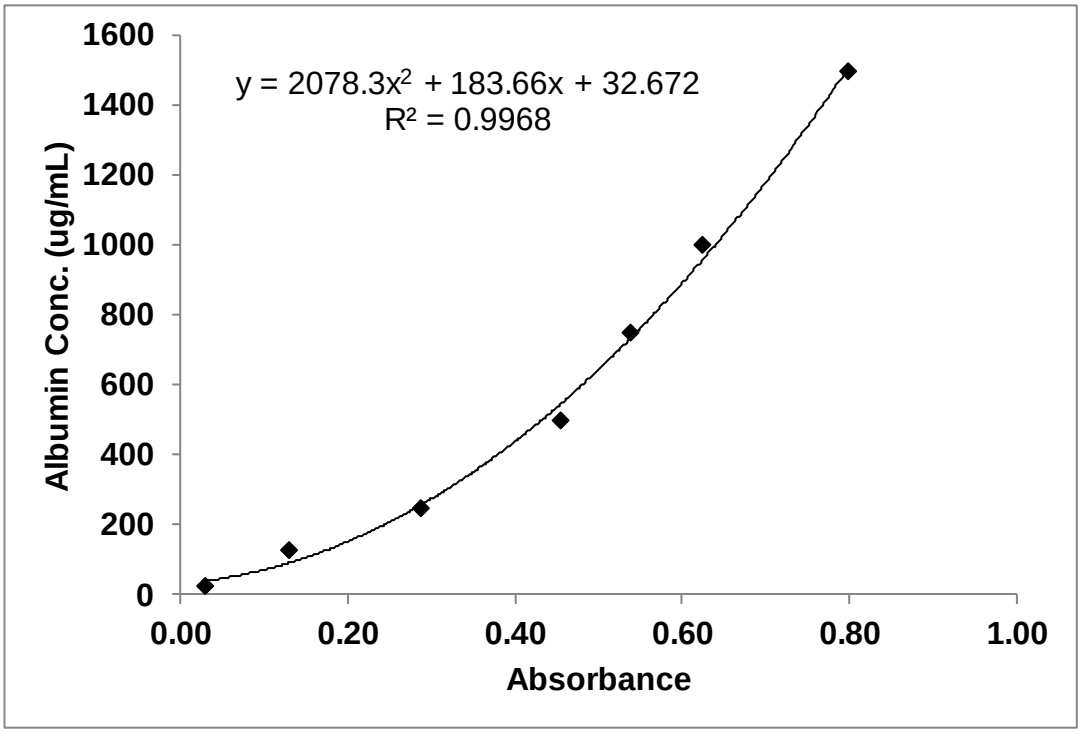
<table>
<tr><th>Compound</th><th>CC range (µM)</th><th>LLOQ (µM)</th><th>Retention time (min)</th><th>Liquid chromatography method</th><th>Column</th></tr>
<tr><td>DS12</td><td>0.0039 - 0.5</td><td>0.0039</td><td>2.41</td><td rowspan="10">Gradient conditions
<table><tr><td>Time (min)</td><td>% of methanol with 0.1% formic acid</td></tr><tr><td>0</td><td>45</td></tr><tr><td>2</td><td>90</td></tr><tr><td>3</td><td>90</td></tr><tr><td>6.5</td><td>45</td></tr></table></td><td rowspan="10">ACE Excel 2 C18-AR
(50 x 2.1 mm)</td></tr>
<tr><td>DS13</td><td>0.0039 - 0.5</td><td>0.0039</td><td>2.02</td></tr>
<tr><td>DS81</td><td>0.001 - 0.25</td><td>0.001</td><td>1.42</td></tr>
<tr><td>DS86</td><td>0.0078 - 0.5</td><td>0.0078</td><td>1.32</td></tr>
<tr><td>Ipratropium</td><td>0.001 - 0.25</td><td>0.001</td><td>1.41</td></tr>
<tr><td>Tiotropium</td><td>0.002 - 0.125</td><td>0.002</td><td>1.52</td></tr>
<tr><td>Glycopyrronium</td><td>0.002 - 0.25</td><td>0.002</td><td>3.21</td></tr>
<tr><td>Formoterol</td><td>0.0078 - 0.5</td><td>0.0078</td><td>1.38</td></tr>
<tr><td>Salmeterol</td><td>0.0078 - 0.5</td><td>0.0078</td><td>3.98</td></tr>
<tr><td>Indacaterol</td><td>0.0078 - 1</td><td>0.0078</td><td>4.18</td></tr>
<tr><td>Metaprolol</td><td>0.002 - 0.5</td><td>0.002</td><td>1.42</td></tr>
<tr><td>Salbutamol</td><td>0.0039 - 0.25</td><td>0.0039</td><td>3.74</td><td>Isocratic method - Methonol with 0.1% formic acid and water with 0.1% formic acid (50:50 v/v)</td><td rowspan="2">Synergi 4 µm Hydro-RP 80A
150 x 2 mm</td></tr>
<tr><td>Imipramine</td><td>0.001 - 0.5</td><td>0.001</td><td>2.19</td><td>Isocratic method - Methonol with 0.1% formic acid and water with 0.1% formic acid (60:40 v/v)</td></tr>
</table>

Appendix B. Effect of various compounds on Calu-3 cell viability.



Calu-3 cells were seeded in 96-well microtiter plates (3.2× 10^5 cells/mL) and incubated at 37ºC in a humidified incubator under 5% CO_2 for 48 hours. Cells were incubated with various test compounds for 30 minutes and incubations were continued for additional 3 hours following the addition of a 20 µL of the MTS containing reagent. Cells treated with a solution of 0.6% v/v Triton X-100 was included as a positive control, while control cells were only incubated with blank HBSS (pH 7.4). At the end of the incubation the formation of a soluble formazan product, indicator of metabolically active cells, was measured at 490 nm using multimode microplate reader Spark® 10M (Tecan). Cell viability was represented as % of control group cells. Data are presented as the mean ± SD (n=4) from a single experiment.

Appendix C. Calibration curve generated using known concentrations of bovine serum albumin for determining the total protein concentrations of cell lysates collected from inserts of a 12-well Transwells® plate and 24-well tissue culture plate.



Calu-3 cells were seeded at a density of 1×10^5 cells/cm^2 or 3.2×10^5 cells/mL on 12-well Transwell® inserts or in collagen-coated 24-well plates, respectively. Cells in Transwell® inserts were cultured under air-liquid interface culture conditions for 21 days, whereas 24-well plates were managed for 3-days at 37ºC in a humidified incubator under 5% CO_2. Cell lysates (5 µL) were collected from Transwell® inserts (n=4) or 24-well plate (n=6) and protein concentration measurements were determined using Coomassie (Bradford) Protein Assay reagent (Thermo Scientific™).

Protein concentrations (µg/mL) are represented below as mean ± SD, from a single experiment:

Transwell® inserts (n=4)	24-well plate (n=6)
884.4 ± 270.6	860.7 ± 209.3

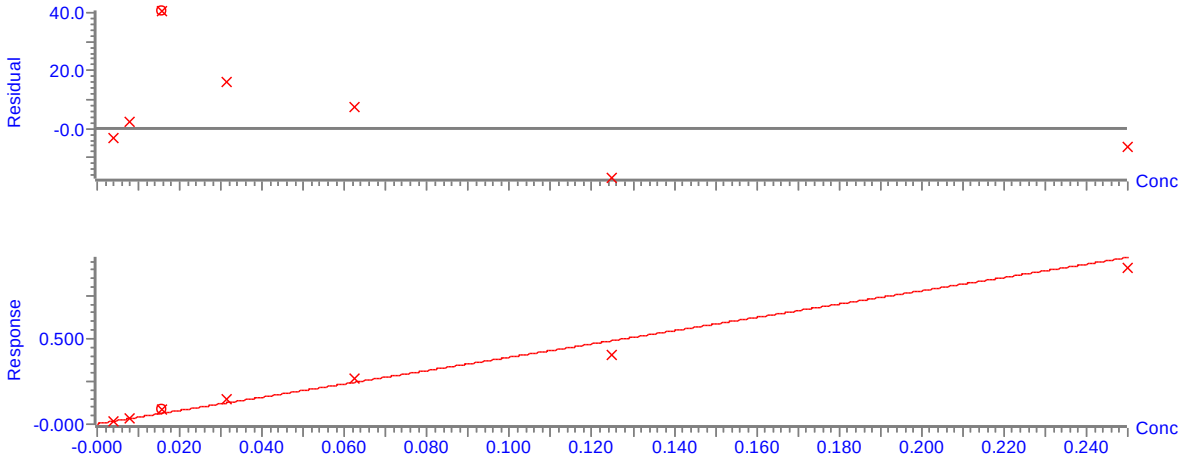
Appendix D. Multiple reaction monitoring (MRM) transitions, cone voltage and collision energy for all the compounds

Compound	MRM transition	Cone Voltage (CV)	Collision energy (CE)
DS12	312.5>167.2	28	16
DS13	326.5>116.2	40	22
DS81	411.2>166.5	22	34
DS86	425.2>99.5	50	34
Ipratropium	332.2>165.9	40	28
Tiotropium	392.1>151.9	40	28
Glycopyrronium	318.1>116.1	34	28
Formoterol	345>148.9	45	18
Salmeterol	416.2>398	35	15
Indacaterol	393>173	35	16
Imipramine	281.2>86	15	35
Tolbutamide	271.03>172	25	28
Salbutamol	240.1>148.1	35	20
Metaprolol	268.5>115.9	35	20

.

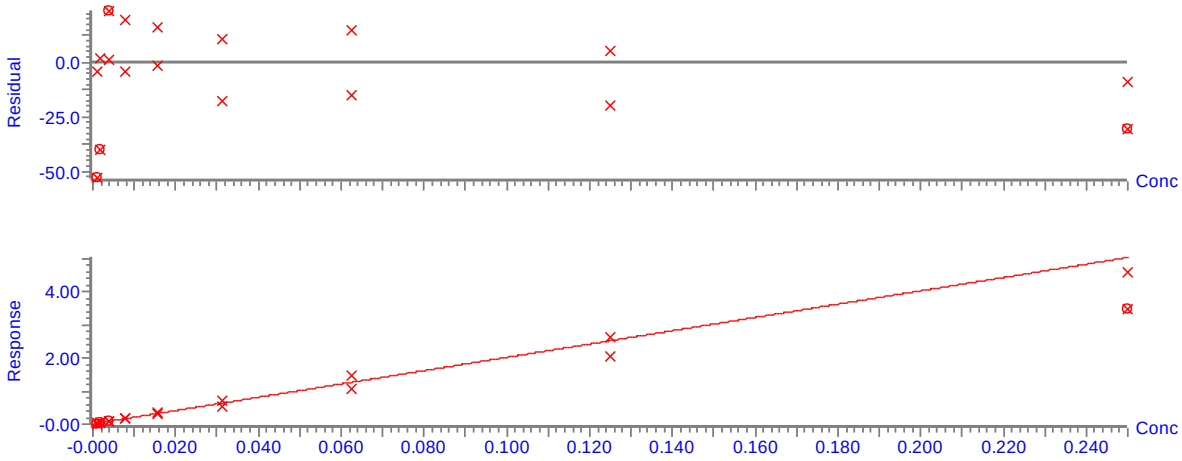
Appendix E. Representative calibration curve of formoterol

Compound name: FORM
Correlation coefficient: r = 0.990956, r^2 = 0.981994
Calibration curve: 3.87915 * x + 0.00280563
Response type: Internal Std (Ref 2), Area * (IS Conc. / IS Area)
Curve type: Linear, Origin: Exclude, Weighting: 1/x^2, Axis trans: None



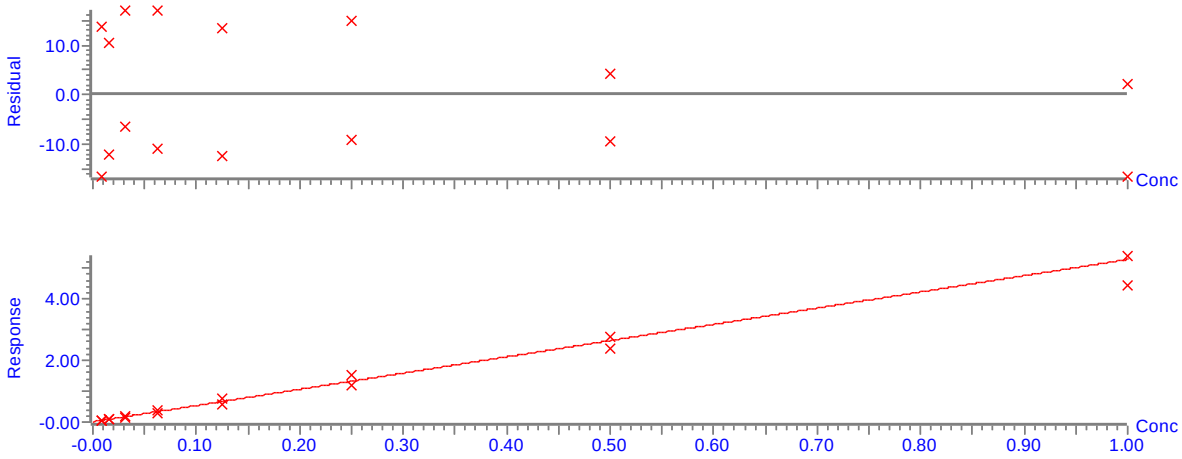
Appendix F. Representative calibration curve of DS81

Compound name: DS081
Correlation coefficient: r = 0.990284, r^2 = 0.980662
Calibration curve: 20.1115 * x + 0.0111441
Response type: Internal Std (Ref 2), Area * (IS Conc. / IS Area)
Curve type: Linear, Origin: Exclude, Weighting: 1/x^2, Axis trans: None



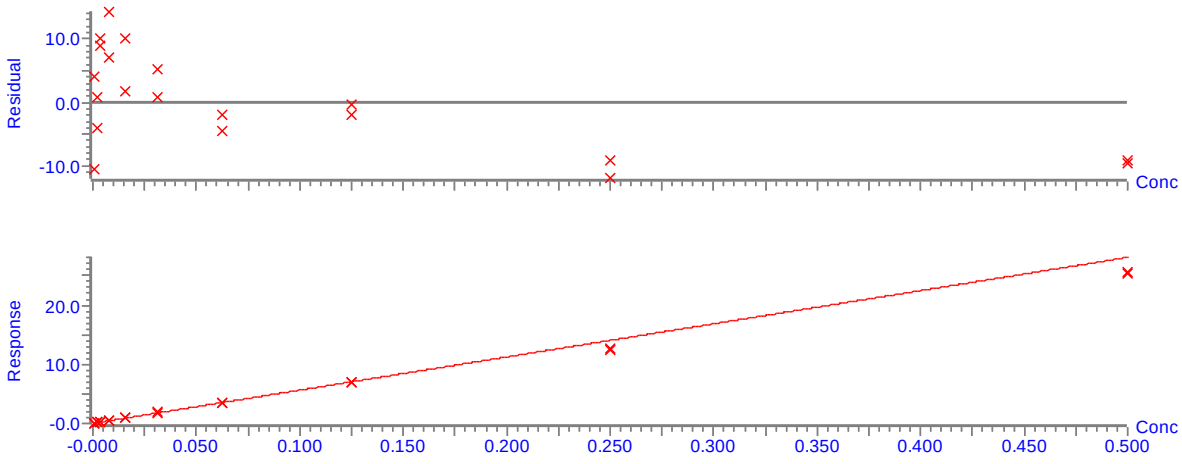
Appendix G. Representative calibration curve of indacaterol

Compound name: Indacaterol
Correlation coefficient: r = 0.987956, r^2 = 0.976057
Calibration curve: 5.26789 * x + 0.0100775
Response type: Internal Std (Ref 2), Area * (IS Conc. / IS Area)
Curve type: Linear, Origin: Exclude, Weighting: 1/x^2, Axis trans: None



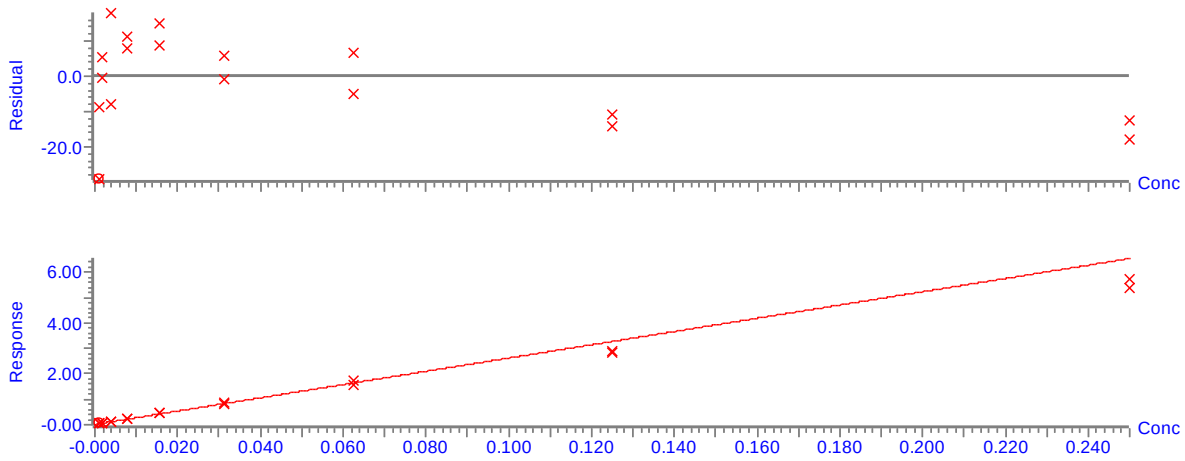
Appendix H. Representative calibration curve of imipramine

Compound name: imipramine
Correlation coefficient: r = 0.995966, r^2 = 0.991949
Calibration curve: 56.1264 * x + 0.02341
Response type: Internal Std (Ref 2), Area * (IS Conc. / IS Area)
Curve type: Linear, Origin: Exclude, Weighting: 1/x^2, Axis trans: None



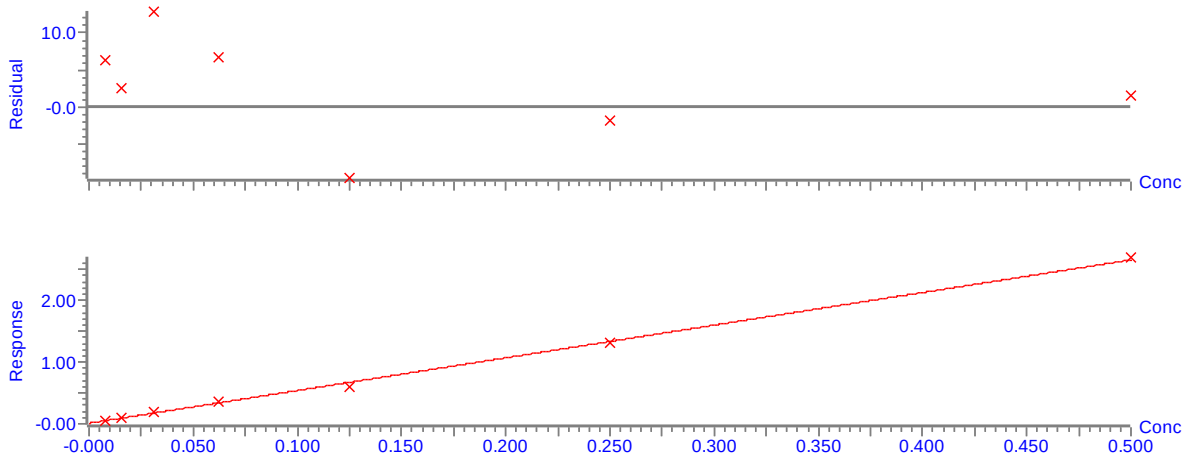
Appendix I. Representative calibration curve of ipratropium

Compound name: Ipratropium
Correlation coefficient: r = 0.991967, r^2 = 0.983998
Calibration curve: 26.1284 * x + 0.0112981
Response type: Internal Std (Ref 2), Area * (IS Conc. / IS Area)
Curve type: Linear, Origin: Exclude, Weighting: 1/x^2, Axis trans: None



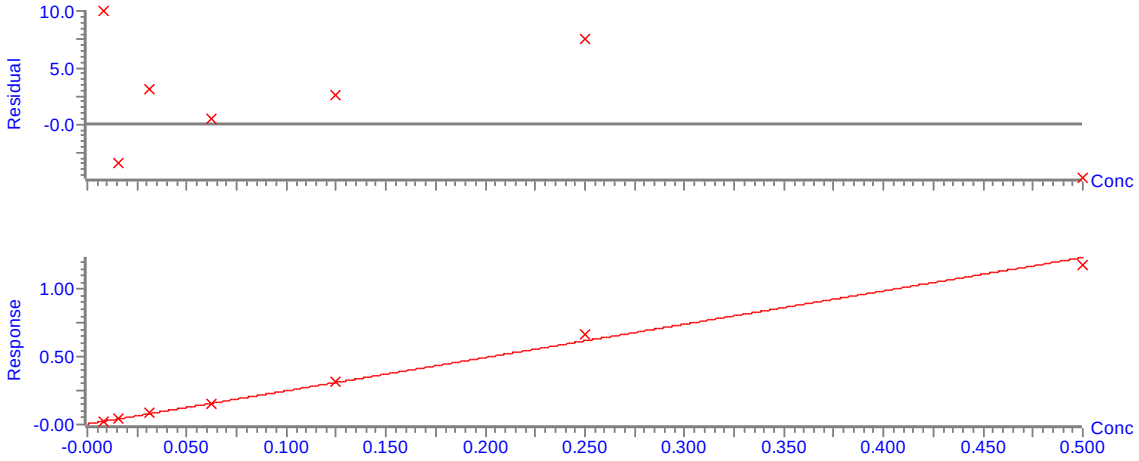
Appendix J. Representative calibration curve of salmeterol

Compound name: SALM
Correlation coefficient: r = 0.998594, r^2 = 0.997189
Calibration curve: 5.30309 * x + 0.00766848
Response type: Internal Std (Ref 2), Area * (IS Conc. / IS Area)
Curve type: Linear, Origin: Include, Weighting: 1/x, Axis trans: None



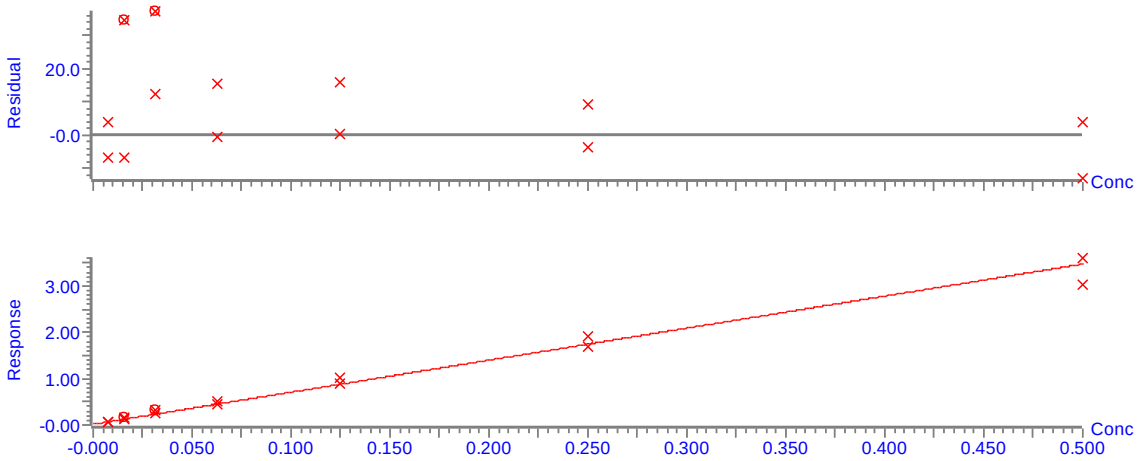
Appendix K. Representative calibration curve of DS12

Compound name: DS12
Correlation coefficient: r = 0.998286, r^2 = 0.996574
Calibration curve: 2.45855 * x + 0.00299731
Response type: Internal Std (Ref 2), Area * (IS Conc. / IS Area)
Curve type: Linear, Origin: Include, Weighting: 1/x, Axis trans: None



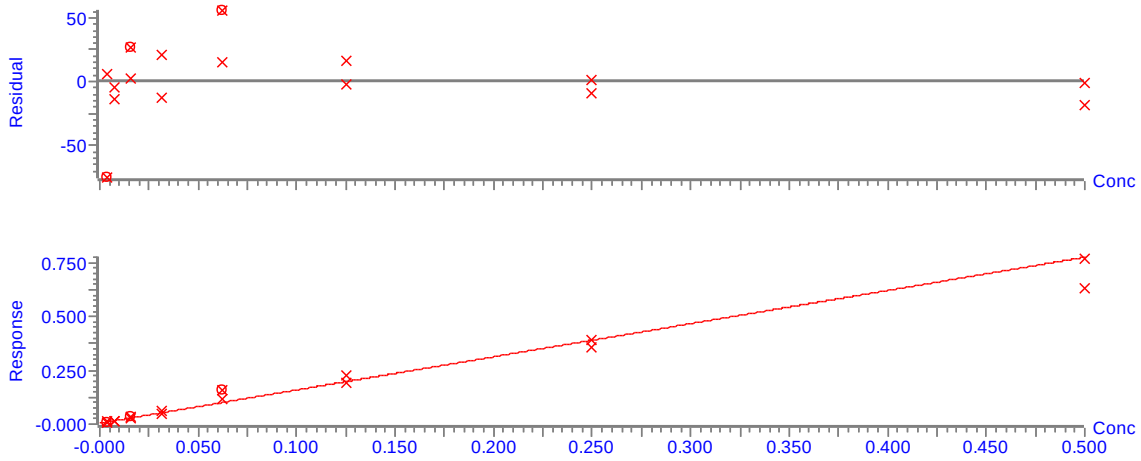
Appendix L. Representative calibration curve of DS13

Compound name: DS13
Correlation coefficient: r = 0.994725, r^2 = 0.989479
Calibration curve: 6.91542 * x + 0.01643
Response type: Internal Std (Ref 2), Area * (IS Conc. / IS Area)
Curve type: Linear, Origin: Include, Weighting: 1/x, Axis trans: None



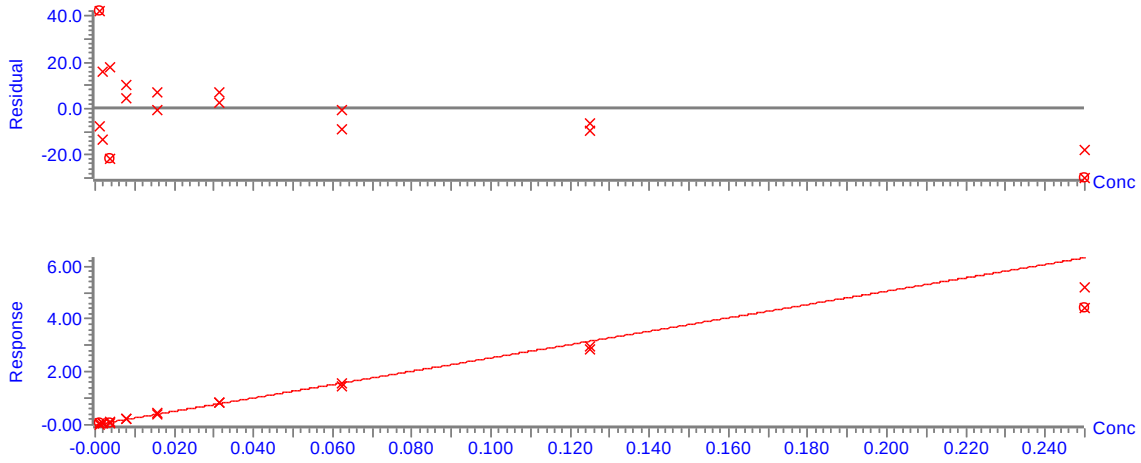
Appendix M. Representative calibration curve of DS86

Compound name: DS086
Correlation coefficient: r = 0.989636, r^2 = 0.979380
Calibration curve: 1.54285 * x + 0.00468252
Response type: Internal Std (Ref 2), Area * (IS Conc. / IS Area)
Curve type: Linear, Origin: Exclude, Weighting: 1/x^2, Axis trans: None



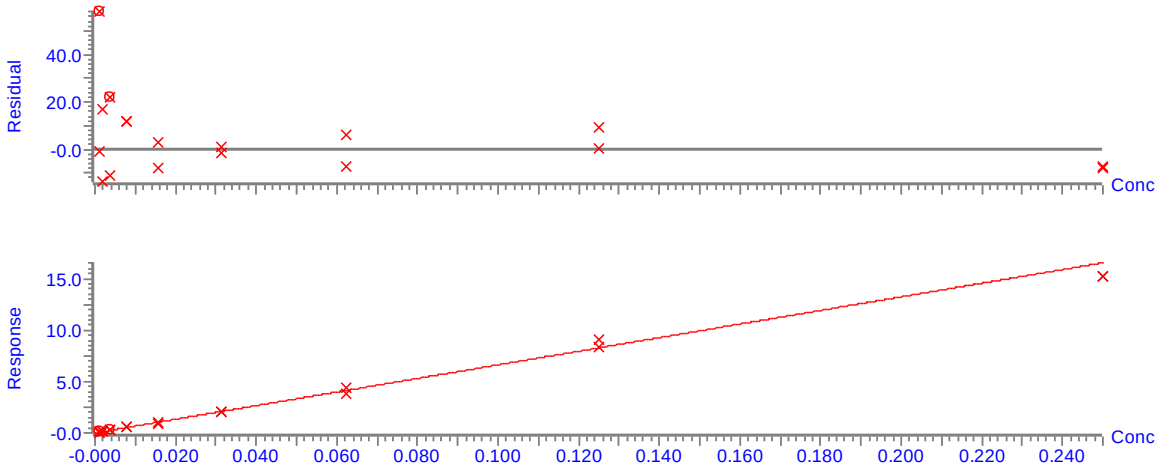
Appendix N. Representative calibration curve of tiotropium

Compound name: tiotropium
Correlation coefficient: r = 0.992460, r^2 = 0.984977
Calibration curve: 25.2579 * x + 0.00226949
Response type: Internal Std (Ref 2), Area * (IS Conc. / IS Area)
Curve type: Linear, Origin: Exclude, Weighting: 1/x^2, Axis trans: None



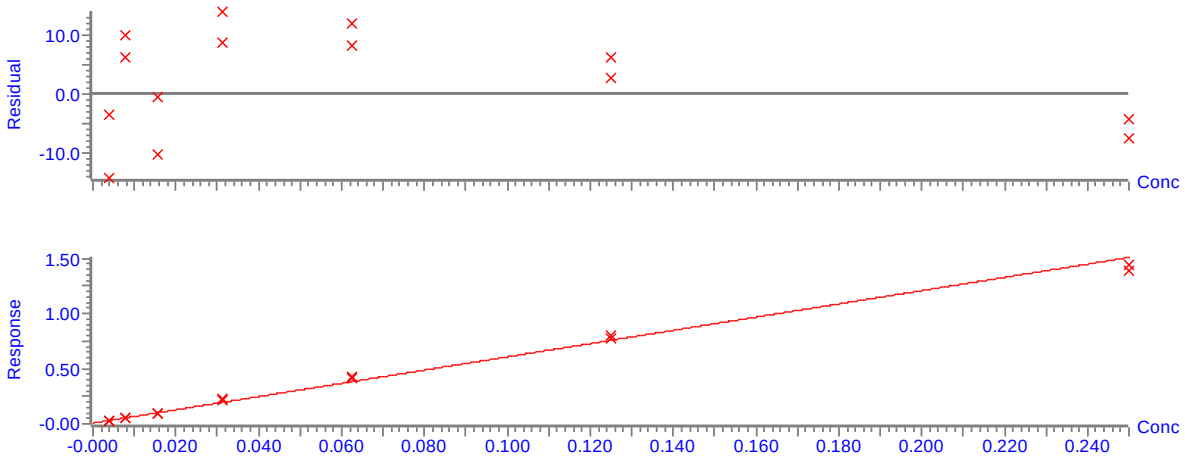
Appendix O. Representative calibration curve of glycopyrronium

Compound name: Glycopyrronium
Correlation coefficient: r = 0.994612, r^2 = 0.989252
Calibration curve: 66.3105 * x + -0.0108381
Response type: Internal Std (Ref 2), Area * (IS Conc. / IS Area)
Curve type: Linear, Origin: Exclude, Weighting: 1/x^2, Axis trans: None



Appendix P. Representative calibration curve of salbutamol

Compound name: Salbutamol
Correlation coefficient: r = 0.996864, r^2 = 0.993737
Calibration curve: 6.01359 * x + 0.00632307
Response type: Internal Std (Ref 2), Area * (IS Conc. / IS Area)
Curve type: Linear, Origin: Include, Weighting: 1/x, Axis trans: None

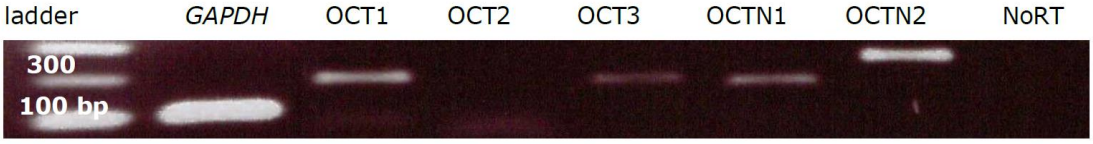


Appendix Q. Stability of compounds in Hank's balanced salt solution (pH 7.4) following storage in a freezer (- 20ºC) for 7 days [a].

Compound	% of the concentrations on day 7 in comparison to the average concentration on day 0.
DS12	87.4 ± 10.4
DS13	100.7 ± 6.0
DS81	128.0 ± 6.6
DS86	82.4 ± 2.4
Ipratropium	108.3 ± 8.8
Tiotropium	96.4 ± 3.4
Glycopyrronium	124.2 ± 9.9
Salbutamol	108.2 ± 6.2
Formoterol	105.6 ± 4.3
Salmeterol	131.3 ± 8.3
Imipramine	94.3 ± 2.5

[a] Data are mean ± SD (n=3). Stability data was not generated for indacaterol.

Appendix R. Expression of OCT\OCTN transporter genes in Calu-3 cells assessed using semi-quantitative PCR.



Calu-3 cells were seeded at a density of 1 × 10^5 cells/cm^2 and cultured for 21 days on 12-well Transwell® inserts under air-liquid interface culture conditions in a humidified incubator at 37ºC under 5% CO_2. Expression of OCT1, OCT3, OCTN1 and OCTN2 transporter genes in the current batch of Calu-3 layers was confirmed Dr Ligia Shemiss using semi-quantitative PCR studies as reported earlier from our lab (Mukherjee, Pritchard, and Bosquillon 2012). The transporter gene expression was performed in three different cell passages. Data was reproduced from Dr Ligia Shemiss PhD thesis with the permission (Shemiss 2016).

Aichler, M., and A. Walch. 2015. 'MALDI Imaging mass spectrometry: current frontiers and perspectives in pathology research and practice', *Lab Invest*, 95: 422-31.

Al-Jayyoussi, G., D. F. Price, K. Kreitmeyr, J. P. Keogh, M. W. Smith, M. Gumbleton, and C. J. Morris. 2015. 'Absorption of ipratropium and l-carnitine into the pulmonary circulation of the ex-vivo rat lung is driven by passive processes rather than active uptake by OCT/OCTN transporters', *Int J Pharm*, 496: 834-41.

Al-Jayyoussi, Ghaith, Daniel F. Price, Danielle Francombe, Glyn Taylor, Mathew W. Smith, Chris Morris, Chris D. Edwards, Peter Eddershaw, and Mark Gumbleton. 2013. 'Selectivity in the impact of P-glycoprotein upon pulmonary absorption of airway-dosed substrates: A study in ex vivo lung models using chemical inhibition and genetic knockout', *J Pharm Sci*, 102: 3382-94.

Altan, N., Y. Chen, M. Schindler, and S. M. Simon. 1998. 'Defective acidification in human breast tumor cells and implications for chemotherapy', *J Exp Med*, 187: 1583-98.

Anderson, G. P., A. Linden, and K. F. Rabe. 1994. 'Why are long-acting beta-adrenoceptor agonists long-acting?', *Eur Respir J*, 7: 569-78.

Assaraf, Benny Zhitomirsky and Yehuda G. 2015. 'The role of cytoplasmic-to-lysosomal pH gradient in hydrophobic weak base drug sequestration in lysosomes', *Cancer Cell & Microenvironment*, 2: 1-7.

Assmus, F., J. B. Houston, and A. Galetin. 2017. 'Incorporation of lysosomal sequestration in the mechanistic model for prediction of tissue distribution of basic drugs', *Eur J Pharm Sci*, 109: 419-30.

Backman, P., H. Adelmann, G. Petersson, and C. B. Jones. 2014. 'Advances in inhaled technologies: understanding the therapeutic challenge, predicting clinical performance, and designing the optimal inhaled product', *Clin Pharmacol Ther*, 95: 509-20.

Backman, P., S. Arora, W. Couet, B. Forbes, W. de Kruijf, and A. Paudel. 2017. 'Advances in experimental and mechanistic computational models to understand pulmonary exposure to inhaled drugs', *Eur J Pharm Sci*.

Backstrom, E., E. Boger, A. Lundqvist, M. Hammarlund-Udenaes, and M. Friden. 2016. 'Lung Retention by Lysosomal Trapping of Inhaled Drugs Can Be Predicted In Vitro With Lung Slices', *J Pharm Sci*, 105: 3432-39.

Backstrom, E., G. Hamm, A. Nilsson, B. M. Fihn, N. Strittmatter, P. Andren, R. J. A. Goodwin, and M. Friden. 2018. 'Uncovering the regional localization of inhaled salmeterol retention in the lung', *Drug Deliv*, 25: 838-45.

Backstrom, E., A. Lundqvist, E. Boger, P. Svanberg, P. Ewing, M. Hammarlund-Udenaes, and M. Friden. 2016. 'Development of a Novel Lung Slice Methodology for Profiling of Inhaled Compounds', *J Pharm Sci*, 105: 838-45.

Barnes, P. J., S. Bonini, W. Seeger, M. G. Belvisi, B. Ward, and A. Holmes. 2015. 'Barriers to new drug development in respiratory disease', *Eur Respir J*, 45: 1197-207.

Behrens, I., and T. Kissel. 2003. 'Do cell culture conditions influence the carrier-mediated transport of peptides in Caco-2 cell monolayers?', *Eur J Pharm Sci*, 19: 433-42.

Berg, T., T. Hegelund-Myrback, J. Ockinger, X. H. Zhou, M. Brannstrom, M. Hagemann-Jensen, V. Werkstrom, J. Seidegard, J. Grunewald, M. Nord, and L. Gustavsson. 2018. 'Expression of MATE1, P-gp, OCTN1 and OCTN2, in epithelial and immune cells in the lung of COPD and healthy individuals', *Respir Res*, 19: 68.

Bleasby, K., J. C. Castle, C. J. Roberts, C. Cheng, W. J. Bailey, J. F. Sina, A. V. Kulkarni, M. J. Hafey, R. Evers, J. M. Johnson, R. G. Ulrich, and J. G. Slatter. 2006. 'Expression profiles of 50 xenobiotic transporter genes in humans and pre-clinical species: a resource for investigations into drug disposition', *Xenobiotica*, 36: 963-88.

Bleasby, K., S. Chauhan, and C. D. Brown. 2000. 'Characterization of MPP+ secretion across human intestinal Caco-2 cell monolayers: role of P-glycoprotein and a novel Na(+)-dependent organic cation transport mechanism', *Br J Pharmacol*, 129: 619-25.

Bo Olsson, Eva Bondesson, Lars Borgström, Staffan Edsbäcker, Stefan Eirefelt, Katarina Ekelund, Lena Gustavsson, and Tove Hegelund-Myrbäck 2011. *Pulmonary Drug Metabolism, Clearance, and Absorption* (Controlled Release Society).

Boer, F. 2003. 'Drug handling by the lungs', *Br J Anaesth*, 91: 50-60.

Bosquillon, C. 2010. 'Drug transporters in the lung--do they play a role in the biopharmaceutics of inhaled drugs?', *J Pharm Sci*, 99: 2240-55.

Bosquillon, C., M. Madlova, N. Patel, N. Clear, and B. Forbes. 2017. 'A Comparison of Drug Transport in Pulmonary Absorption Models: Isolated Perfused rat Lungs, Respiratory Epithelial Cell Lines and Primary Cell Culture', *Pharm Res*, 34: 2532-40.

Bourdet, D. L., G. M. Pollack, and D. R. Thakker. 2006. 'Intestinal absorptive transport of the hydrophilic cation ranitidine: a kinetic modeling approach to elucidate the role of uptake and efflux transporters and paracellular vs. transcellular transport in Caco-2 cells', *Pharm Res*, 23: 1178-87.

Bourdet, D. L., and D. R. Thakker. 2006. 'Saturable absorptive transport of the hydrophilic organic cation ranitidine in Caco-2 cells: role of pH-dependent organic cation uptake system and P-glycoprotein', *Pharm Res*, 23: 1165-77.

Briske-Anderson, M. J., J. W. Finley, and S. M. Newman. 1997. 'The influence of culture time and passage number on the morphological and physiological development of Caco-2 cells', *Proc Soc Exp Biol Med*, 214: 248-57.

Brown, R. A., Jr., and L. S. Schanker. 1983. 'Absorption of aerosolized drugs from the rat lung', *Drug Metab Dispos*, 11: 355-60.

Byron, Peter R. 1993. 'Physicochemical Effects on Lung Disposition of Pharmaceutical Aerosols', *Aerosol Science and Technology*, 18: 223-29.

Cazzola, M., C. P. Page, L. Calzetta, and M. G. Matera. 2012. 'Pharmacology and therapeutics of bronchodilators', *Pharmacol Rev*, 64: 450-504.

Cesar-Razquin, A., B. Snijder, T. Frappier-Brinton, R. Isserlin, G. Gyimesi, X. Bai, R. A. Reithmeier, D. Hepworth, M. A. Hediger, A. M. Edwards, and G. Superti-Furga. 2015. 'A Call for Systematic Research on Solute Carriers', *Cell*, 162: 478-87.

Chai, A. B., A. J. Ammit, and I. C. Gelissen. 2017. 'Examining the role of ABC lipid transporters in pulmonary lipid homeostasis and inflammation', *Respir Res*, 18: 41.

Chen, J., J. Brockmoller, T. Seitz, J. Konig, M. V. Tzvetkov, and X. Chen. 2017. 'Tropane alkaloids as substrates and inhibitors of human organic cation transporters of the SLC22 (OCT) and the SLC47 (MATE) families', *Biol Chem*, 398: 237-49.

Choo, E. F., and L. Salphati. 2018. 'Leveraging Humanized Animal Models to Understand Human Drug Disposition: Opportunities, Challenges, and Future Directions', *Clin Pharmacol Ther*, 103: 188-92.

Chu, X., K. Korzekwa, R. Elsby, K. Fenner, A. Galetin, Y. Lai, P. Matsson, A. Moss, S. Nagar, G. R. Rosania, J. P. Bai, J. W. Polli, Y. Sugiyama, and K. L. Brouwer. 2013. 'Intracellular drug concentrations and transporters: measurement, modeling, and implications for the liver', *Clin Pharmacol Ther*, 94: 126-41.

Codrons, V., F. Vanderbist, B. Ucakar, V. Preat, and R. Vanbever. 2004. 'Impact of formulation and methods of pulmonary delivery on absorption of parathyroid hormone (1-34) from rat lungs', *J Pharm Sci*, 93: 1241-52.

Cook, D., D. Brown, R. Alexander, R. March, P. Morgan, G. Satterthwaite, and M. N. Pangalos. 2014. 'Lessons learned from the fate of AstraZeneca's drug pipeline: a five-dimensional framework', *Nat Rev Drug Discov*, 13: 419-31.

Cooper, A. E., D. Ferguson, and K. Grime. 2012. 'Optimisation of DMPK by the inhaled route: challenges and approaches', *Curr Drug Metab*, 13: 457-73.

Cui, Y., J. Konig, and D. Keppler. 2001. 'Vectorial transport by double-transfected cells expressing the human uptake transporter SLC21A8 and the apical export pump ABCC2', *Mol Pharmacol*, 60: 934-43.

Daniel, W. A., and J. Wojcikowski. 1997. 'Interactions between promazine and antidepressants at the level of cellular distribution', *Pharmacol Toxicol*, 81: 259-64.

Daniel, W. A., and J. Wojcikowski. 1999. 'Lysosomal trapping as an important mechanism involved in the cellular distribution of perazine and in pharmacokinetic interaction with antidepressants', *Eur Neuropsychopharmacol*, 9: 483-91.

Daniel, W. A., J. Wojcikowski, and A. Palucha. 2001. 'Intracellular distribution of psychotropic drugs in the grey and white matter of the brain: the role of lysosomal trapping', *Br J Pharmacol*, 134: 807-14.

Darquenne, C., J. S. Fleming, I. Katz, A. R. Martin, J. Schroeter, O. S. Usmani, J. Venegas, and O. Schmid. 2016. 'Bridging the Gap Between Science and Clinical Efficacy: Physiology, Imaging, and Modeling of Aerosols in the Lung', *J Aerosol Med Pulm Drug Deliv*, 29: 107-26.

de Duve, C., T. de Barsy, B. Poole, A. Trouet, P. Tulkens, and F. Van Hoof. 1974. 'Commentary. Lysosomotropic agents', *Biochem Pharmacol*, 23: 2495-531.

de Kanter, R., M. Monshouwer, D. K. Meijer, and G. M. Groothuis. 2002. 'Precision-cut organ slices as a tool to study toxicity and metabolism of xenobiotics with special reference to non-hepatic tissues', *Curr Drug Metab*, 3: 39-59.

De Kanter, R., P. Olinga, M. H. De Jager, M. T. Merema, D. K. Meijer, and G. M. Groothius. 1999. 'Organ slices as an in vitro test system for drug metabolism in human liver, lung and kidney', *Toxicol In Vitro*, 13: 737-44.

de Kruijf, W., and C. Ehrhardt. 2017. 'Inhalation delivery of complex drugs-the next steps', *Curr Opin Pharmacol*, 36: 52-57.

de Souza Carvalho, C., N. Daum, and C. M. Lehr. 2014. 'Carrier interactions with the biological barriers of the lung: advanced in vitro models and challenges for pulmonary drug delivery', *Adv Drug Deliv Rev*, 75: 129-40.

Ding, X., and L. S. Kaminsky. 2003. 'Human extrahepatic cytochromes P450: function in xenobiotic metabolism and tissue-selective chemical toxicity in the respiratory and gastrointestinal tracts', *Annu Rev Pharmacol Toxicol*, 43: 149-73.

Dolovich, M., and R. Labiris. 2004. 'Imaging drug delivery and drug responses in the lung', *Proc Am Thorac Soc*, 1: 329-37.

Drew, R., Z. H. Siddik, E. G. Mimnaugh, and T. E. Gram. 1981. 'Species and dose differences in the accumulation of imipramine by mammalian lungs', *Drug Metab Dispos*, 9: 322-6.

Drose, S., and K. Altendorf. 1997. 'Bafilomycins and concanamycins as inhibitors of V-ATPases and P-ATPases', *J Exp Biol*, 200: 1-8.

Duvvuri, M., W. Feng, A. Mathis, and J. P. Krise. 2004. 'A cell fractionation approach for the quantitative analysis of subcellular drug disposition', *Pharm Res*, 21: 26-32.

Duvvuri, M., Y. Gong, D. Chatterji, and J. P. Krise. 2004. 'Weak base permeability characteristics influence the intracellular sequestration site in the multidrug-resistant human leukemic cell line HL-60', *J Biol Chem*, 279: 32367-72.

Duvvuri, M., and J. P. Krise. 2005. 'A novel assay reveals that weakly basic model compounds concentrate in lysosomes to an extent greater than pH-partitioning theory would predict', *Mol Pharm*, 2: 440-8.

Edwards, C. D., C. Luscombe, P. Eddershaw, and E. M. Hessel. 2016. 'Development of a Novel Quantitative Structure-Activity Relationship Model to Accurately Predict Pulmonary Absorption and Replace Routine Use of the Isolated Perfused Respiring Rat Lung Model', *Pharm Res*, 33: 2604-16.

Ehrhardt, C. 2017. 'Inhalation Biopharmaceutics: Progress Towards Comprehending the Fate of Inhaled Medicines', *Pharm Res*, 34: 2451-53.

Ehrhardt, C., C. Kneuer, M. Laue, U. F. Schaefer, K. J. Kim, and C. M. Lehr. 2003. '16HBE14o- human bronchial epithelial cell layers express P-

glycoprotein, lung resistance-related protein, and caveolin-1', *Pharm Res*, 20: 545-51.

Ensing, K., R. A. de Zeeuw, G. D. Nossent, G. H. Koeter, and P. J. Cornelissen. 1989. 'Pharmacokinetics of ipratropium bromide after single dose inhalation and oral and intravenous administration', *Eur J Clin Pharmacol*, 36: 189-94.

Fahrmayr, C., J. Konig, D. Auge, M. Mieth, and M. F. Fromm. 2012. 'Identification of drugs and drug metabolites as substrates of multidrug resistance protein 2 (MRP2) using triple-transfected MDCK-OATP1B1-UGT1A1-MRP2 cells', *Br J Pharmacol*, 165: 1836-47.

Fernandes, C. A., and R. Vanbever. 2009. 'Preclinical models for pulmonary drug delivery', *Expert Opin Drug Deliv*, 6: 1231-45.

Fisher, R. L., M. S. Smith, S. J. Hasal, K. S. Hasal, A. J. Gandolfi, and K. Brendel. 1994. 'The use of human lung slices in toxicology', *Hum Exp Toxicol*, 13: 466-71.

Florea, B. I., M. L. Cassara, H. E. Junginger, and G. Borchard. 2003. 'Drug transport and metabolism characteristics of the human airway epithelial cell line Calu-3', *J Control Release*, 87: 131-8.

Forbes, B., P. Backman, D. Christopher, M. Dolovich, B. V. Li, and B. Morgan. 2015. 'In Vitro Testing for Orally Inhaled Products: Developments in Science-Based Regulatory Approaches', *AAPS J*, 17: 837-52.

Forbes, B., and C. Ehrhardt. 2005. 'Human respiratory epithelial cell culture for drug delivery applications', *Eur J Pharm Biopharm*, 60: 193-205.

Forbes, B., and A. B. Lansley. 1998. 'Differences in drug transport across bronchial and gastrointestinal drug absorption models', *Journal of Pharmacy and Pharmacology*, 50: 96-96.

Forbes, I. I. 2000. 'Human airway epithelial cell lines for in vitro drug transport and metabolism studies', *Pharm Sci Technolo Today*, 3: 18-27.

Foster, K. A., M. L. Avery, M. Yazdanian, and K. L. Audus. 2000. 'Characterization of the Calu-3 cell line as a tool to screen pulmonary drug delivery', *Int J Pharm*, 208: 1-11.

Giacomini, K. M., S. M. Huang, D. J. Tweedie, L. Z. Benet, K. L. Brouwer, X. Chu, A. Dahlin, R. Evers, V. Fischer, K. M. Hillgren, K. A. Hoffmaster, T. Ishikawa, D. Keppler, R. B. Kim, C. A. Lee, M. Niemi, J. W. Polli, Y. Sugiyama, P. W. Swaan, J. A. Ware, S. H. Wright, S. W. Yee, M. J. Zamek-Gliszczynski, and L. Zhang. 2010. 'Membrane transporters in drug development', *Nat Rev Drug Discov*, 9: 215-36.

Goh, L. B., K. J. Spears, D. Yao, A. Ayrton, P. Morgan, C. Roland Wolf, and T. Friedberg. 2002. 'Endogenous drug transporters in in vitro and in vivo models for the prediction of drug disposition in man', *Biochem Pharmacol*, 64: 1569-78.

GOLD. 2018. "Global Strategy for the Diagnosis, Management, and Prevention of Chronic Obstructive Lung Disease 2018 Report; available from: http://goldcopd.org.

Gong, Y., Z. Zhao, D. J. McConn, B. Beaudet, M. Tallman, J. D. Speake, D. M. Ignar, and J. P. Krise. 2007. 'Lysosomes contribute to anomalous pharmacokinetic behavior of melanocortin-4 receptor agonists', *Pharm Res*, 24: 1138-44.

Gorboulev, V., J. C. Ulzheimer, A. Akhoundova, I. Ulzheimer-Teuber, U. Karbach, S. Quester, C. Baumann, F. Lang, A. E. Busch, and H. Koepsell. 1997. 'Cloning and characterization of two human polyspecific organic cation transporters', *DNA Cell Biol*, 16: 871-81.

Gordon, S., M. Daneshian, J. Bouwstra, F. Caloni, S. Constant, D. E. Davies, G. Dandekar, C. A. Guzman, E. Fabian, E. Haltner, T. Hartung, N. Hasiwa, P. Hayden, H. Kandarova, S. Khare, H. F. Krug, C. Kneuer, M. Leist, G. Lian, U. Marx, M. Metzger, K. Ott, P. Prieto, M. S. Roberts, E. L. Roggen, T. Tralau, C. van den Braak, H. Walles, and C. M. Lehr. 2015. 'Non-animal models of epithelial barriers (skin, intestine and lung) in research, industrial applications and regulatory toxicology', *Altex*, 32: 327-78.

Graaf, I. A., G. M. Groothuis, and P. Olinga. 2007. 'Precision-cut tissue slices as a tool to predict metabolism of novel drugs', *Expert Opin Drug Metab Toxicol*, 3: 879-98.

Grainger, C. I., L. L. Greenwell, D. J. Lockley, G. P. Martin, and B. Forbes. 2006. 'Culture of Calu-3 cells at the air interface provides a representative model of the airway epithelial barrier', *Pharm Res*, 23: 1482-90.

Grundemann, D., V. Gorboulev, S. Gambaryan, M. Veyhl, and H. Koepsell. 1994. 'Drug excretion mediated by a new prototype of polyspecific transporter', *Nature*, 372: 549-52.

Grundemann, D., B. Schechinger, G. A. Rappold, and E. Schomig. 1998. 'Molecular identification of the corticosterone-sensitive extraneuronal catecholamine transporter', *Nat Neurosci*, 1: 349-51.

Gumbleton, M., G. Al-Jayyoussi, A. Crandon-Lewis, D. Francombe, K. Kreitmeyr, C. J. Morris, and M. W. Smith. 2011. 'Spatial expression and functionality of drug transporters in the intact lung: objectives for further research', *Adv Drug Deliv Rev*, 63: 110-8.

Haghi, M., H. X. Ong, D. Traini, and P. Young. 2014. 'Across the pulmonary epithelial barrier: Integration of physicochemical properties and human cell models to study pulmonary drug formulations', *Pharmacol Ther*, 144: 235-52.

Haghi, M., P. M. Young, D. Traini, R. Jaiswal, J. Gong, and M. Bebawy. 2010. 'Time- and passage-dependent characteristics of a Calu-3 respiratory epithelial cell model', *Drug Dev Ind Pharm*, 36: 1207-14.

Han, T. K., W. R. Proctor, C. L. Costales, H. Cai, R. S. Everett, and D. R. Thakker. 2015. 'Four cation-selective transporters contribute to apical uptake and accumulation of metformin in Caco-2 cell monolayers', *J Pharmacol Exp Ther*, 352: 519-28.

Hann, M. M., and G. L. Simpson. 2014. 'Intracellular drug concentration and disposition--the missing link?', *Methods*, 68: 283-5.

Harada, R. N., and J. E. Repine. 1985. 'Pulmonary host defense mechanisms', *Chest*, 87: 247-52.

Hastedt, Jayne E., Per Bäckman, Andrew R. Clark, William Doub, Anthony Hickey, Guenther Hochhaus, Phil J. Kuehl, Claus-Michael Lehr, Peter Mauser, Jason McConville, Ralph Niven, Masahiro Sakagimi, and Jeffry G. Weers. 2016. 'Scope and relevance of a pulmonary biopharmaceutical classification system AAPS/FDA/USP Workshop March 16-17th, 2015 in Baltimore, MD', *AAPS Open*, 2: 1.

Hayeshi, R., C. Masimirembwa, S. Mukanganyama, and A. L. Ungell. 2008. 'Lysosomal trapping of amodiaquine: impact on transport across intestinal epithelia models', *Biopharm Drug Dispos*, 29: 324-34.

Hediger, M. A., B. Clemencon, R. E. Burrier, and E. A. Bruford. 2013. 'The ABCs of membrane transporters in health and disease (SLC series): introduction', *Mol Aspects Med*, 34: 95-107.

Heikkinen, A. T., J. Monkkonen, and T. Korjamo. 2009. 'Kinetics of cellular retention during Caco-2 permeation experiments: role of lysosomal sequestration and impact on permeability estimates', *J Pharmacol Exp Ther*, 328: 882-92.

Hendrickx, R., J. G. Johansson, C. Lohmann, R. M. Jenvert, A. Blomgren, L. Borjesson, and L. Gustavsson. 2013. 'Identification of novel substrates and structure-activity relationship of cellular uptake mediated by human organic cation transporters 1 and 2', *J Med Chem*, 56: 7232-42.

Hendrickx, R., E. Lamm Bergstrom, D. L. I. Janzen, M. Friden, U. Eriksson, K. Grime, and D. Ferguson. 2017. 'Translational model to predict pulmonary pharmacokinetics and efficacy in man for inhaled bronchodilators', *CPT Pharmacometrics Syst Pharmacol*.

Hickey, A. J. 2013. 'Back to the future: inhaled drug products', *J Pharm Sci*, 102: 1165-72.

Higgins, C. F. 1992. 'ABC transporters: from microorganisms to man', *Annu Rev Cell Biol*, 8: 67-113.

Higgins, J. W., D. W. Bedwell, and M. J. Zamek-Gliszczynski. 2012. 'Ablation of both organic cation transporter (OCT)1 and OCT2 alters metformin pharmacokinetics but has no effect on tissue drug exposure and pharmacodynamics', *Drug Metab Dispos*, 40: 1170-7.

Hohlfeld, J. M., A. Sharma, J. A. van Noord, P. J. Cornelissen, E. Derom, L. Towse, V. Peterkin, and B. Disse. 2014. 'Pharmacokinetics and pharmacodynamics of tiotropium solution and tiotropium powder in chronic obstructive pulmonary disease', *J Clin Pharmacol*, 54: 405-14.

Horvath, G., N. Schmid, M. A. Fragoso, A. Schmid, G. E. Conner, M. Salathe, and A. Wanner. 2007. 'Epithelial organic cation transporters ensure pH-dependent drug absorption in the airway', *Am J Respir Cell Mol Biol*, 36: 53-60.

Hukkanen, J., O. Pelkonen, J. Hakkola, and H. Raunio. 2002. 'Expression and regulation of xenobiotic-metabolizing cytochrome P450 (CYP) enzymes in human lung', *Crit Rev Toxicol*, 32: 391-411.

Hutter, V., D. Y. Chau, C. Hilgendorf, A. Brown, A. Cooper, V. Zann, D. I. Pritchard, and C. Bosquillon. 2014. 'Digoxin net secretory transport in bronchial

epithelial cell layers is not exclusively mediated by P-glycoprotein/MDR1', *Eur J Pharm Biopharm*, 86: 74-82.

Ijuin, R., T. Takashima, Y. Watanabe, Y. Sugiyama, and M. Suzuki. 2012. 'Synthesis of [(11)C]dehydropravastatin, a PET probe potentially useful for studying OATP1B1 and MRP2 transporters in the liver', *Bioorg Med Chem*, 20: 3703-9.

Ingoglia, F., R. Visigalli, B. M. Rotoli, A. Barilli, B. Riccardi, P. Puccini, and V. Dall'Asta. 2015. 'Functional characterization of the organic cation transporters (OCTs) in human airway pulmonary epithelial cells', *Biochim Biophys Acta*, 1848: 1563-72.

Ingoglia, F., R. Visigalli, B. M. Rotoli, A. Barilli, B. Riccardi, P. Puccini, and V. Dall'Asta. 2016. 'Functional activity of L-carnitine transporters in human airway epithelial cells', *Biochim Biophys Acta*, 1858: 210-9.

Ishizaki, J., K. Yokogawa, F. Ichimura, and S. Ohkuma. 2000. 'Uptake of imipramine in rat liver lysosomes in vitro and its inhibition by basic drugs', *J Pharmacol Exp Ther*, 294: 1088-98.

Junod, A. F. 1972. 'Accumulation of 14 C-imipramine in isolated perfused rat lungs', *J Pharmacol Exp Ther*, 183: 182-7.

Kaneko, K., M. Tanaka, A. Ishii, Y. Katayama, T. Nakaoka, S. Irie, H. Kawahata, T. Yamanaga, Y. Wada, T. Miyake, K. Toshimoto, K. Maeda, Y. Cui, M. Enomoto, E. Kawamura, N. Kawada, J. Kawabe, S. Shiomi, H. Kusuhara, Y. Sugiyama, and Y. Watanabe. 2018. 'A Clinical Quantitative Evaluation of Hepatobiliary Transport of [(11)C]Dehydropravastatin in Humans Using Positron Emission Tomography', *Drug Metab Dispos*, 46: 719-28.

Karlgren, M., I. Simoff, M. Backlund, C. Wegler, M. Keiser, N. Handin, J. Muller, P. Lundquist, A. C. Jareborg, S. Oswald, and P. Artursson. 2017. 'A CRISPR-Cas9 Generated MDCK Cell Line Expressing Human MDR1 Without Endogenous Canine MDR1 (cABCB1): An Improved Tool for Drug Efflux Studies', *J Pharm Sci*, 106: 2909-13.

Kaufmann, A. M., and J. P. Krise. 2007. 'Lysosomal sequestration of amine-containing drugs: analysis and therapeutic implications', *J Pharm Sci*, 96: 729-46.

Kazmi, F., T. Hensley, C. Pope, R. S. Funk, G. J. Loewen, D. B. Buckley, and A. Parkinson. 2013. 'Lysosomal sequestration (trapping) of lipophilic amine (cationic amphiphilic) drugs in immortalized human hepatocytes (Fa2N-4 cells)', *Drug Metab Dispos*, 41: 897-905.

Kekuda, R., P. D. Prasad, X. Wu, H. Wang, Y. J. Fei, F. H. Leibach, and V. Ganapathy. 1998. 'Cloning and functional characterization of a potential-sensitive, polyspecific organic cation transporter (OCT3) most abundantly expressed in placenta', *J Biol Chem*, 273: 15971-9.

Keogh, J. P., and J. R. Kunta. 2006. 'Development, validation and utility of an in vitro technique for assessment of potential clinical drug-drug interactions involving P-glycoprotein', *Eur J Pharm Sci*, 27: 543-54.

Khanvilkar, K., M. D. Donovan, and D. R. Flanagan. 2001. 'Drug transfer through mucus', *Adv Drug Deliv Rev*, 48: 173-93.

Klein, S. G., J. Hennen, T. Serchi, B. Blomeke, and A. C. Gutleb. 2011. 'Potential of coculture in vitro models to study inflammatory and sensitizing effects of particles on the lung', *Toxicol In Vitro*, 25: 1516-34.

Knight, D. A., and S. T. Holgate. 2003. 'The airway epithelium: structural and functional properties in health and disease', *Respirology*, 8: 432-46.

Koepsell, H. 2011. 'Substrate recognition and translocation by polyspecific organic cation transporters', *Biol Chem*, 392: 95-101.

Koepsell, H. 2013. 'The SLC22 family with transporters of organic cations, anions and zwitterions', *Mol Aspects Med*, 34: 413-35.

Koepsell, H., K. Lips, and C. Volk. 2007. 'Polyspecific organic cation transporters: structure, function, physiological roles, and biopharmaceutical implications', *Pharm Res*, 24: 1227-51.

Kokkonen, N., A. Rivinoja, A. Kauppila, M. Suokas, I. Kellokumpu, and S. Kellokumpu. 2004. 'Defective acidification of intracellular organelles results in aberrant secretion of cathepsin D in cancer cells', *J Biol Chem*, 279: 39982-8.

Konig, J., O. Zolk, K. Singer, C. Hoffmann, and M. F. Fromm. 2011. 'Double-transfected MDCK cells expressing human OCT1/MATE1 or OCT2/MATE1: determinants of uptake and transcellular translocation of organic cations', *Br J Pharmacol*, 163: 546-55.

Kopplow, K., K. Letschert, J. Konig, B. Walter, and D. Keppler. 2005. 'Human hepatobiliary transport of organic anions analyzed by quadruple-transfected cells', *Mol Pharmacol*, 68: 1031-8.

Kornhuber, J., A. W. Henkel, T. W. Groemer, S. Stadtler, O. Welzel, P. Tripal, A. Rotter, S. Bleich, and S. Trapp. 2010. 'Lipophilic cationic drugs increase the permeability of lysosomal membranes in a cell culture system', *J Cell Physiol*, 224: 152-64.

Kreft, M. E., U. D. Jerman, E. Lasic, N. Hevir-Kene, T. L. Rizner, L. Peternel, and K. Kristan. 2015. 'The characterization of the human cell line Calu-3 under different culture conditions and its use as an optimized in vitro model to investigate bronchial epithelial function', *Eur J Pharm Sci*, 69: 1-9.

Krise, Nadia Hamid and Jeffrey P. 2016. 'The Mechanisms and Therapeutic Consequences of Amine-Containing Drug Sequestration in Lysosomes.' in, *Lysosomes: Biology, Diseases, and Therapeutics*.

Kummer, W., S. Wiegand, S. Akinci, I. Wessler, A. H. Schinkel, J. Wess, H. Koepsell, R. V. Haberberger, and K. S. Lips. 2006. 'Role of acetylcholine and polyspecific cation transporters in serotonin-induced bronchoconstriction in the mouse', *Respir Res*, 7: 65.

Kusuhara, H. 2013. 'Imaging in the study of membrane transporters', *Clin Pharmacol Ther*, 94: 33-6.

Kuteykin-Teplyakov, K., C. Luna-Tortos, K. Ambroziak, and W. Loscher. 2010. 'Differences in the expression of endogenous efflux transporters in MDR1-transfected versus wildtype cell lines affect P-glycoprotein mediated drug transport', *Br J Pharmacol*, 160: 1453-63.

Langer, O. 2016. 'Use of PET Imaging to Evaluate Transporter-Mediated Drug-Drug Interactions', *J Clin Pharmacol*, 56 Suppl 7: S143-56.

Langmann, T., R. Mauerer, A. Zahn, C. Moehle, M. Probst, W. Stremmel, and G. Schmitz. 2003. 'Real-time reverse transcription-PCR expression profiling of the complete human ATP-binding cassette transporter superfamily in various tissues', *Clin Chem*, 49: 230-8.

Le Prieur, E., E. Vaz, A. Bion, F. Dionnet, and J. P. Morin. 2000. 'Toxicity of diesel engine exhausts in an in vitro model of lung slices in biphasic organotypic culture: induction of a proinflammatory and apoptotic response', *Arch Toxicol*, 74: 460-6.

Lee, K., and D. R. Thakker. 1999. 'Saturable transport of H2-antagonists ranitidine and famotidine across Caco-2 cell monolayers', *J Pharm Sci*, 88: 680-7.

Lemieux, B., M. D. Percival, and J. P. Falgueyret. 2004. 'Quantitation of the lysosomotropic character of cationic amphiphilic drugs using the fluorescent basic amine Red DND-99', *Anal Biochem*, 327: 247-51.

Lena Gustavsson, Cynthia Bosquillon, Mark Gumbleton, Tove Hegelund-Myrbäck, Takeo Nakanishi, Dan Price, Ikumi Tamai and Xiao-Hong Zhou. 2016. *Drug Transporters in the Lung: Expression and Potential Impact on Pulmonary Drug Disposition*.

Leslie, E. M., R. G. Deeley, and S. P. Cole. 2005. 'Multidrug resistance proteins: role of P-glycoprotein, MRP1, MRP2, and BCRP (ABCG2) in tissue defense', *Toxicol Appl Pharmacol*, 204: 216-37.

Leusch, A., B. Eichhorn, G. Muller, and K. L. Rominger. 2001. 'Pharmacokinetics and tissue distribution of the anticholinergics tiotropium and ipratropium in the rat and dog', *Biopharm Drug Dispos*, 22: 199-212.

Li, J., D. A. Volpe, Y. Wang, W. Zhang, C. Bode, A. Owen, and I. J. Hidalgo. 2011. 'Use of transporter knockdown Caco-2 cells to investigate the in vitro efflux of statin drugs', *Drug Metab Dispos*, 39: 1196-202.

Linton, K. J. 2007. 'Structure and function of ABC transporters', *Physiology (Bethesda)*, 22: 122-30.

Lips, K. S., A. Luhrmann, T. Tschernig, T. Stoeger, F. Alessandrini, V. Grau, R. V. Haberberger, H. Koepsell, R. Pabst, and W. Kummer. 2007. 'Down-regulation of the non-neuronal acetylcholine synthesis and release machinery in acute allergic airway inflammation of rat and mouse', *Life Sci*, 80: 2263-9.

Lips, K. S., C. Volk, B. M. Schmitt, U. Pfeil, P. Arndt, D. Miska, L. Ermert, W. Kummer, and H. Koepsell. 2005. 'Polyspecific cation transporters mediate luminal release of acetylcholine from bronchial epithelium', *Am J Respir Cell Mol Biol*, 33: 79-88.

Liu, X., L. Jin, J. W. Upham, and M. S. Roberts. 2013. 'The development of models for the evaluation of pulmonary drug disposition', *Expert Opin Drug Metab Toxicol*, 9: 487-505.

Lombardi, D., B. Cuenoud, and S. D. Kramer. 2009. 'Lipid membrane interactions of indacaterol and salmeterol: do they influence their pharmacological properties?', *Eur J Pharm Sci*, 38: 533-47.

MacIntyre, A. C., and D. J. Cutler. 1988. 'The potential role of lysosomes in tissue distribution of weak bases', *Biopharm Drug Dispos*, 9: 513-26.

Manford, F., Y. Riffo-Vasquez, D. Spina, C. P. Page, A. J. Hutt, V. Moore, F. Johansson, and B. Forbes. 2008. 'Lack of difference in pulmonary absorption of digoxin, a P-glycoprotein substrate, in mdr1a-deficient and mdr1a-competent mice', *J Pharm Pharmacol*, 60: 1305-10.

Mann, A., H. Han, and S. Eyal. 2016. 'Imaging transporters: Transforming diagnostic and therapeutic development', *Clin Pharmacol Ther*, 100: 479-88.

Marceau, F., C. Roy, and J. Bouthillier. 2014. 'Assessment of cation trapping by cellular acidic compartments', *Methods Enzymol*, 534: 119-31.

Marko-Varga, G., T. E. Fehniger, M. Rezeli, B. Dome, T. Laurell, and A. Vegvari. 2011. 'Drug localization in different lung cancer phenotypes by MALDI mass spectrometry imaging', *J Proteomics*, 74: 982-92.

Marshall, L. J., W. Oguejiofor, R. S. Willetts, H. R. Griffiths, and A. Devitt. 2015. 'Developing accurate models of the human airways', *J Pharm Pharmacol*, 67: 464-72.

Mathia, N. R., J. Timoszyk, P. I. Stetsko, J. R. Megill, R. L. Smith, and D. A. Wall. 2002. 'Permeability characteristics of calu-3 human bronchial epithelial cells: in vitro-in vivo correlation to predict lung absorption in rats', *J Drug Target*, 10: 31-40.

Matsumoto, T., H. Kushida, S. Matsushita, Y. Oyama, T. Suda, J. Watanabe, Y. Kase, and M. Setou. 2017. 'Distribution Analysis via Mass Spectrometry Imaging of Ephedrine in the Lungs of Rats Orally Administered the Japanese Kampo Medicine Maoto', *Sci Rep*, 7: 44098.

Min, K. A., G. R. Rosania, C. K. Kim, and M. C. Shin. 2016. 'Functional and cytometric examination of different human lung epithelial cell types as drug transport barriers', *Arch Pharm Res*, 39: 359-69.

Mohan, H. K., T. Routledge, P. Cane, L. Livieratos, J. R. Ballinger, and A. M. Peters. 2016. 'Does the Clearance of Inhaled (99m)Tc-Sestamibi Correlate with Multidrug Resistance Protein 1 Expression in the Human Lung?', *Radiology*, 280: 924-30.

Monteil, C., E. Le Prieur, S. Buisson, J. P. Morin, M. Guerbet, and J. M. Jouany. 1999. 'Acrolein toxicity: comparative in vitro study with lung slices and pneumocytes type II cell line from rats', *Toxicology*, 133: 129-38.

Morgan, P., D. G. Brown, S. Lennard, M. J. Anderton, J. C. Barrett, U. Eriksson, M. Fidock, B. Hamren, A. Johnson, R. E. March, J. Matcham, J. Mettetal, D. J. Nicholls, S. Platz, S. Rees, M. A. Snowden, and M. N. Pangalos. 2018. 'Impact of a five-dimensional framework on R&D productivity at AstraZeneca', *Nat Rev Drug Discov*, 17: 167-81.

Morgan, P., P. H. Van Der Graaf, J. Arrowsmith, D. E. Feltner, K. S. Drummond, C. D. Wegner, and S. D. Street. 2012. 'Can the flow of medicines be improved? Fundamental pharmacokinetic and pharmacological principles toward improving Phase II survival', *Drug Discov Today*, 17: 419-24.

Mukherjee, M., D. I. Pritchard, and C. Bosquillon. 2012. 'Evaluation of air-interfaced Calu-3 cell layers for investigation of inhaled drug interactions with organic cation transporters in vitro', *Int J Pharm*, 426: 7-14.

Mukker, J. K., R. S. P. Singh, and H. Derendorf. 2016. 'Ciclesonide: A Pro-Soft Drug Approach for Mitigation of Side Effects of Inhaled Corticosteroids', *J Pharm Sci*, 105: 2509-14.

Muller, F., J. Konig, E. Hoier, K. Mandery, and M. F. Fromm. 2013. 'Role of organic cation transporter OCT2 and multidrug and toxin extrusion proteins MATE1 and MATE2-K for transport and drug interactions of the antiviral lamivudine', *Biochem Pharmacol*, 86: 808-15.

Murgia, X., B. Loretz, O. Hartwig, M. Hittinger, and C. M. Lehr. 2018. 'The role of mucus on drug transport and its potential to affect therapeutic outcomes', *Adv Drug Deliv Rev*, 124: 82-97.

Nadanaciva, S., S. Lu, D. F. Gebhard, B. A. Jessen, W. D. Pennie, and Y. Will. 2011. 'A high content screening assay for identifying lysosomotropic compounds', *Toxicol In Vitro*, 25: 715-23.

Nahar, K., N. Gupta, R. Gauvin, S. Absar, B. Patel, V. Gupta, A. Khademhosseini, and F. Ahsan. 2013. 'In vitro, in vivo and ex vivo models for studying particle deposition and drug absorption of inhaled pharmaceuticals', *Eur J Pharm Sci*, 49: 805-18.

Nakamura, T., T. Nakanishi, T. Haruta, Y. Shirasaka, J. P. Keogh, and I. Tamai. 2010. 'Transport of ipratropium, an anti-chronic obstructive pulmonary disease drug, is mediated by organic cation/carnitine transporters in human bronchial epithelial cells: implications for carrier-mediated pulmonary absorption', *Mol Pharm*, 7: 187-95.

Nakanishi, T., T. Haruta, Y. Shirasaka, and I. Tamai. 2011. 'Organic cation transporter-mediated renal secretion of ipratropium and tiotropium in rats and humans', *Drug Metab Dispos*, 39: 117-22.

Nakanishi, T., Y. Hasegawa, T. Haruta, T. Wakayama, and I. Tamai. 2013. 'In vivo evidence of organic cation transporter-mediated tracheal accumulation of the anticholinergic agent ipratropium in mice', *J Pharm Sci*, 102: 3373-81.

Nichols, J. E., J. A. Niles, S. P. Vega, L. B. Argueta, A. Eastaway, and J. Cortiella. 2014. 'Modeling the lung: Design and development of tissue engineered macro- and micro-physiologic lung models for research use', *Exp Biol Med (Maywood)*, 239: 1135-69.

Nickel, S., C. G. Clerkin, M. A. Selo, and C. Ehrhardt. 2016. 'Transport mechanisms at the pulmonary mucosa: implications for drug delivery', *Expert Opin Drug Deliv*, 13: 667-90.

Nigam, S. K. 2018. 'The SLC22 Transporter Family: A Paradigm for the Impact of Drug Transporters on Metabolic Pathways, Signaling, and Disease', *Annu Rev Pharmacol Toxicol*, 58: 663-87.

Okamura, T., T. Kikuchi, M. Okada, H. Wakizaka, and M. R. Zhang. 2013. 'Imaging of activity of multidrug resistance-associated protein 1 in the lungs', *Am J Respir Cell Mol Biol*, 49: 335-40.

Okuda, M., H. Saito, Y. Urakami, M. Takano, and K. Inui. 1996. 'cDNA cloning and functional expression of a novel rat kidney organic cation transporter, OCT2', *Biochem Biophys Res Commun*, 224: 500-7.

Oltra-Noguera, D., V. Mangas-Sanjuan, A. Centelles-Sanguesa, I. Gonzalez-Garcia, G. Sanchez-Castano, M. Gonzalez-Alvarez, V. G. Casabo, V. Merino, I. Gonzalez-Alvarez, and M. Bermejo. 2015. 'Variability of permeability estimation from different protocols of subculture and transport experiments in cell monolayers', *J Pharmacol Toxicol Methods*, 71: 21-32.

Ong, H. X., D. Traini, and P. M. Young. 2013. 'Pharmaceutical applications of the Calu-3 lung epithelia cell line', *Expert Opin Drug Deliv*, 10: 1287-302.

Otsuka, M., T. Matsumoto, R. Morimoto, S. Arioka, H. Omote, and Y. Moriyama. 2005. 'A human transporter protein that mediates the final excretion step for toxic organic cations', *Proc Natl Acad Sci U S A*, 102: 17923-8.

Patton, J. S., and P. R. Byron. 2007. 'Inhaling medicines: delivering drugs to the body through the lungs', *Nat Rev Drug Discov*, 6: 67-74.

Patton, J. S., C. S. Fishburn, and J. G. Weers. 2004. 'The lungs as a portal of entry for systemic drug delivery', *Proc Am Thorac Soc*, 1: 338-44.

Patton, John S. 1996. 'Mechanisms of macromolecule absorption by the lungs', *Adv Drug Deliv Rev*, 19: 3-36.

Perry, M. W. D., K. Bjorhall, B. Bonn, J. Carlsson, Y. Chen, A. Eriksson, L. Fredlund, H. Hao, N. S. Holden, K. Karabelas, H. Lindmark, F. Liu, N. Pemberton, J. Petersen, S. Rodrigo Blomqvist, R. W. Smith, T. Svensson, I. Terstiege, C. Tyrchan, W. Yang, S. Zhao, and L. Oster. 2017. 'Design and Synthesis of Soluble and Cell-Permeable PI3Kdelta Inhibitors for Long-Acting Inhaled Administration', *J Med Chem*, 60: 5057-71.

Pfeifer, N. D., K. B. Harris, G. Z. Yan, and K. L. Brouwer. 2013. 'Determination of intracellular unbound concentrations and subcellular localization of drugs in rat sandwich-cultured hepatocytes compared with liver tissue', *Drug Metab Dispos*, 41: 1949-56.

Polli, J. W., K. L. Olson, J. P. Chism, L. S. John-Williams, R. L. Yeager, S. M. Woodard, V. Otto, S. Castellino, and V. E. Demby. 2009. 'An unexpected synergist role of P-glycoprotein and breast cancer resistance protein on the central nervous system penetration of the tyrosine kinase inhibitor lapatinib (N-{3-chloro-4-[(3-fluorobenzyl)oxy]phenyl}-6-[5-({[2-(methylsulfonyl)ethyl]amino }methyl)-2-furyl]-4-quinazolinamine; GW572016)', *Drug Metab Dispos*, 37: 439-42.

Poole, B., and S. Ohkuma. 1981. 'Effect of weak bases on the intralysosomal pH in mouse peritoneal macrophages', *J Cell Biol*, 90: 665-9.

Price, D. F., C. N. Luscombe, P. J. Eddershaw, C. D. Edwards, and M. Gumbleton. 2017. 'The Differential Absorption of a Series of P-Glycoprotein Substrates in Isolated Perfused Lungs from Mdr1a/1b Genetic Knockout Mice can be Attributed to Distinct Physico-Chemical Properties: an Insight into Predicting Transporter-Mediated, Pulmonary Specific Disposition', *Pharm Res*, 34: 2498-516.

Prideaux, B., V. Dartois, D. Staab, D. M. Weiner, A. Goh, L. E. Via, C. E. Barry, 3rd, and M. Stoeckli. 2011. 'High-sensitivity MALDI-MRM-MS imaging of moxifloxacin distribution in tuberculosis-infected rabbit lungs and granulomatous lesions', *Anal Chem*, 83: 2112-8.

Proctor, W. R., X. Ming, D. Bourdet, T. K. Han, R. S. Everett, and D. R. Thakker. 2016. 'Why Does the Intestine Lack Basolateral Efflux Transporters for Cationic Compounds? A Provocative Hypothesis', *J Pharm Sci*, 105: 484-96.

Quistgaard, E. M., C. Low, F. Guettou, and P. Nordlund. 2016. 'Understanding transport by the major facilitator superfamily (MFS): structures pave the way', *Nat Rev Mol Cell Biol*, 17: 123-32.

Ritchie, T. J., C. N. Luscombe, and S. J. Macdonald. 2009. 'Analysis of the calculated physicochemical properties of respiratory drugs: can we design for inhaled drugs yet?', *J Chem Inf Model*, 49: 1025-32.

Rives, M. L., J. A. Javitch, and A. D. Wickenden. 2017. 'Potentiating SLC transporter activity: Emerging drug discovery opportunities', *Biochem Pharmacol*, 135: 1-11.

Rubakhin, S. S., J. C. Jurchen, E. B. Monroe, and J. V. Sweedler. 2005. 'Imaging mass spectrometry: fundamentals and applications to drug discovery', *Drug Discov Today*, 10: 823-37.

Ruge, C. A., J. Kirch, and C. M. Lehr. 2013. 'Pulmonary drug delivery: from generating aerosols to overcoming biological barriers-therapeutic possibilities and technological challenges', *Lancet Respir Med*, 1: 402-13.

Ruparelia, P., H. K. Cheow, J. W. Evans, L. Banney, S. Shankar, K. R. Szczepura, A. E. Swift, J. R. Ballinger, N. G. Hartman, E. R. Chilvers, and A. M. Peters. 2008. 'Pulmonary elimination rate of inhaled 99mTc-sestamibi radioaerosol is delayed in healthy cigarette smokers', *Br J Clin Pharmacol*, 65: 611-4.

Sakagami, M. 2006. 'In vivo, in vitro and ex vivo models to assess pulmonary absorption and disposition of inhaled therapeutics for systemic delivery', *Adv Drug Deliv Rev*, 58: 1030-60.

Sakamoto, A., T. Matsumaru, N. Yamamura, Y. Uchida, M. Tachikawa, S. Ohtsuki, and T. Terasaki. 2013. 'Quantitative expression of human drug transporter proteins in lung tissues: analysis of regional, gender, and interindividual differences by liquid chromatography-tandem mass spectrometry', *J Pharm Sci*, 102: 3395-406.

Sakolish, C. M., M. B. Esch, J. J. Hickman, M. L. Shuler, and G. J. Mahler. 2016. 'Modeling Barrier Tissues In Vitro: Methods, Achievements, and Challenges', *EBioMedicine*, 5: 30-9.

Salomon, J. J., and C. Ehrhardt. 2012. 'Organic cation transporters in the blood-air barrier: expression and implications for pulmonary drug delivery', *Ther Deliv*, 3: 735-47.

Salomon, J. J., Y. Hagos, S. Petzke, A. Kuhne, J. C. Gausterer, K. Hosoya, and C. Ehrhardt. 2015. 'Beta-2 Adrenergic Agonists Are Substrates and Inhibitors of Human Organic Cation Transporter 1', *Mol Pharm*, 12: 2633-41.

Schanker, L. S. 1978. 'Drug absorption from the lung', *Biochem Pharmacol*, 27: 381-5.

Scheer, N., P. Balimane, M. D. Hayward, S. Buechel, G. Kauselmann, and C. R. Wolf. 2012. 'Generation and characterization of a novel multidrug resistance protein 2 humanized mouse line', *Drug Metab Dispos*, 40: 2212-8.

Scheer, N., M. Snaith, C. R. Wolf, and J. Seibler. 2013. 'Generation and utility of genetically humanized mouse models', *Drug Discov Today*, 18: 1200-11.

Scheffer, G. L., A. C. Pijnenborg, E. F. Smit, M. Muller, D. S. Postma, W. Timens, P. van der Valk, E. G. de Vries, and R. J. Scheper. 2002. 'Multidrug resistance related molecules in human and murine lung', *J Clin Pathol*, 55: 332-9.

Schinkel, A. H., and J. W. Jonker. 2003. 'Mammalian drug efflux transporters of the ATP binding cassette (ABC) family: an overview', *Adv Drug Deliv Rev*, 55: 3-29.

Schinkel, A. H., J. J. Smit, O. van Tellingen, J. H. Beijnen, E. Wagenaar, L. van Deemter, C. A. Mol, M. A. van der Valk, E. C. Robanus-Maandag, H. P. te Riele, and et al. 1994. 'Disruption of the mouse mdr1a P-glycoprotein gene leads to a deficiency in the blood-brain barrier and to increased sensitivity to drugs', *Cell*, 77: 491-502.

Schneider, M., M. Windbergs, N. Daum, B. Loretz, E. M. Collnot, S. Hansen, U. F. Schaefer, and C. M. Lehr. 2013. 'Crossing biological barriers for advanced drug delivery', *Eur J Pharm Biopharm*, 84: 239-41.

Shemiss, Ligia. 2016. 'Probing the Role of Organic Cation Transporters in Respiratory Epithelial Cell Proliferation in vitro', PhD Thesis, University of Nottingham. http://eprints.nottingham.ac.uk/38527/1/Ligia-Final%20PhD%20thesis.pdf.

Shitara, Y., H. Sato, and Y. Sugiyama. 2005. 'Evaluation of drug-drug interaction in the hepatobiliary and renal transport of drugs', *Annu Rev Pharmacol Toxicol*, 45: 689-723.

Siebert, G. A., D. Y. Hung, P. Chang, and M. S. Roberts. 2004. 'Ion-trapping, microsomal binding, and unbound drug distribution in the hepatic retention of basic drugs', *J Pharmacol Exp Ther*, 308: 228-35.

Simoff, I., M. Karlgren, M. Backlund, A. C. Lindstrom, F. Z. Gaugaz, P. Matsson, and P. Artursson. 2016. 'Complete Knockout of Endogenous Mdr1 (Abcb1) in MDCK Cells by CRISPR-Cas9', *J Pharm Sci*, 105: 1017-21.

Somers, G. I., N. Lindsay, B. M. Lowdon, A. E. Jones, C. Freathy, S. Ho, A. J. Woodrooffe, M. K. Bayliss, and G. R. Manchee. 2007. 'A comparison of the expression and metabolizing activities of phase I and II enzymes in freshly isolated human lung parenchymal cells and cryopreserved human hepatocytes', *Drug Metab Dispos*, 35: 1797-805.

Stein, S. W. , and C. G. Thiel. 2017. 'The History of Therapeutic Aerosols: A Chronological Review', *J Aerosol Med Pulm Drug Deliv*, 30: 20-41.

Strong, P., K. Ito, J. Murray, and G. Rapeport. 2018. 'Current approaches to the discovery of novel inhaled medicines', *Drug Discov Today*.

Taghikhani, E., M. F. Fromm, and J. Konig. 2017. 'Assays for Analyzing the Role of Transport Proteins in the Uptake and the Vectorial Transport of Substances Affecting Cell Viability', *Methods Mol Biol*, 1601: 123-35.

Takano, H., S. Ito, X. Zhang, H. Ito, M. R. Zhang, H. Suzuki, K. Maeda, H. Kusuhara, T. Suhara, and Y. Sugiyama. 2017. 'Possible Role of Organic Cation Transporters in the Distribution of [(11)C]Sulpiride, a Dopamine D2 Receptor Antagonist', *J Pharm Sci*, 106: 2558-65.

Tamai, I., R. Ohashi, J. Nezu, H. Yabuuchi, A. Oku, M. Shimane, Y. Sai, and A. Tsuji. 1998. 'Molecular and functional identification of sodium ion-dependent, high affinity human carnitine transporter OCTN2', *J Biol Chem*, 273: 20378-82.

Tamai, I., H. Yabuuchi, J. Nezu, Y. Sai, A. Oku, M. Shimane, and A. Tsuji. 1997. 'Cloning and characterization of a novel human pH-dependent organic cation transporter, OCTN1', *FEBS Lett*, 419: 107-11.

Tapper, H., and R. Sundler. 1990. 'Role of lysosomal and cytosolic pH in the regulation of macrophage lysosomal enzyme secretion', *Biochem J*, 272: 407-14.

Tournier, N., B. Stieger, and O. Langer. 2018. 'Imaging techniques to study drug transporter function in vivo', *Pharmacol Ther*, 189: 104-22.

Tronde, A., B. Norden, A. B. Jeppsson, P. Brunmark, E. Nilsson, H. Lennernas, and U. H. Bengtsson. 2003. 'Drug absorption from the isolated perfused rat lung--correlations with drug physicochemical properties and epithelial permeability', *J Drug Target*, 11: 61-74.

Tronde, A., B. Norden, H. Marchner, A. K. Wendel, H. Lennernas, and U. H. Bengtsson. 2003. 'Pulmonary absorption rate and bioavailability of drugs in vivo in rats: structure-absorption relationships and physicochemical profiling of inhaled drugs', *J Pharm Sci*, 92: 1216-33.

Tsuda, M., T. Terada, T. Mizuno, T. Katsura, J. Shimakura, and K. Inui. 2009. 'Targeted disruption of the multidrug and toxin extrusion 1 (mate1) gene in mice reduces renal secretion of metformin', *Mol Pharmacol*, 75: 1280-6.

Turck, D., W. Weber, R. Sigmund, K. Budde, H. H. Neumayer, L. Fritsche, K. L. Rominger, U. Feifel, and T. Slowinski. 2004. 'Pharmacokinetics of intravenous, single-dose tiotropium in subjects with different degrees of renal impairment', *J Clin Pharmacol*, 44: 163-72.

Ufuk, A., F. Assmus, L. Francis, J. Plumb, V. Damian, M. Gertz, J. B. Houston, and A. Galetin. 2017. 'In Vitro and in Silico Tools To Assess Extent of Cellular Uptake and Lysosomal Sequestration of Respiratory Drugs in Human Alveolar Macrophages', *Mol Pharm*, 14: 1033-46.

Ufuk, A., G. Somers, J. B. Houston, and A. Galetin. 2015. 'In Vitro Assessment of Uptake and Lysosomal Sequestration of Respiratory Drugs in Alveolar Macrophage Cell Line NR8383', *Pharm Res*, 32: 3937-51.

Upton, R. N., and D. J. Doolette. 1999. 'Kinetic aspects of drug disposition in the lungs', *Clin Exp Pharmacol Physiol*, 26: 381-91.

van de Steeg, E., V. Stranecky, H. Hartmannova, L. Noskova, M. Hrebicek, E. Wagenaar, A. van Esch, D. R. de Waart, R. P. Oude Elferink, K. E. Kenworthy, E. Sticova, M. al-Edreesi, A. S. Knisely, S. Kmoch, M. Jirsa, and A. H. Schinkel.

2012. 'Complete OATP1B1 and OATP1B3 deficiency causes human Rotor syndrome by interrupting conjugated bilirubin reuptake into the liver', *J Clin Invest*, 122: 519-28.

van den Brink, K. I., M. Boorsma, A. J. Staal-van den Brekel, S. Edsbacker, E. F. Wouters, and L. Thorsson. 2008. 'Evidence of the in vivo esterification of budesonide in human airways', *Br J Clin Pharmacol*, 66: 27-35.

van der Deen, M., E. G. de Vries, W. Timens, R. J. Scheper, H. Timmer-Bosscha, and D. S. Postma. 2005. 'ATP-binding cassette (ABC) transporters in normal and pathological lung', *Respir Res*, 6: 59.

Volk, Christopher. 2014. 'OCTs, OATs, and OCTNs: structure and function of the polyspecific organic ion transporters of the SLC22 family', *Wiley Interdisciplinary Reviews: Membrane Transport and Signaling*, 3: 1-13.

Wagner, D. J., T. Hu, and J. Wang. 2016. 'Polyspecific organic cation transporters and their impact on drug intracellular levels and pharmacodynamics', *Pharmacol Res*, 111: 237-46.

Wijeweera, J. B., A. J. Gandolfi, A. Parrish, and R. C. Lantz. 2001. 'Sodium arsenite enhances AP-1 and NFkappaB DNA binding and induces stress protein expression in precision-cut rat lung slices', *Toxicol Sci*, 61: 283-94.

Wu, X., R. L. George, W. Huang, H. Wang, S. J. Conway, F. H. Leibach, and V. Ganapathy. 2000. 'Structural and functional characteristics and tissue distribution pattern of rat OCTN1, an organic cation transporter, cloned from placenta', *Biochim Biophys Acta*, 1466: 315-27.

Wu, X., W. Huang, P. D. Prasad, P. Seth, D. P. Rajan, F. H. Leibach, J. Chen, S. J. Conway, and V. Ganapathy. 1999. 'Functional characteristics and tissue distribution pattern of organic cation transporter 2 (OCTN2), an organic cation/carnitine transporter', *J Pharmacol Exp Ther*, 290: 1482-92.

Xiong, J., J. Feng, D. Yuan, J. Zhou, and W. Miao. 2015. 'Tracing the structural evolution of eukaryotic ATP binding cassette transporter superfamily', *Sci Rep*, 5: 16724.

Yabuuchi, H., I. Tamai, J. Nezu, K. Sakamoto, A. Oku, M. Shimane, Y. Sai, and A. Tsuji. 1999. 'Novel membrane transporter OCTN1 mediates multispecific, bidirectional, and pH-dependent transport of organic cations', *J Pharmacol Exp Ther*, 289: 768-73.

Yokogawa, K., J. Ishizaki, S. Ohkuma, and K. Miyamoto. 2002. 'Influence of lipophilicity and lysosomal accumulation on tissue distribution kinetics of basic drugs: a physiologically based pharmacokinetic model', *Methods Find Exp Clin Pharmacol*, 24: 81-93.

Yoshimori, T., A. Yamamoto, Y. Moriyama, M. Futai, and Y. Tashiro. 1991. 'Bafilomycin A1, a specific inhibitor of vacuolar-type H(+)-ATPase, inhibits acidification and protein degradation in lysosomes of cultured cells', *J Biol Chem*, 266: 17707-12.

You, G. , and M. E. Morris. 2006. 'Overview of Drug Transporter Families.' in, *Drug Transporters*.

Yu, J. Y., and G. R. Rosania. 2010. 'Cell-based multiscale computational modeling of small molecule absorption and retention in the lungs', *Pharm Res*, 27: 457-67.

Zamek-Gliszczynski, M. J., C. A. Lee, A. Poirier, J. Bentz, X. Chu, H. Ellens, T. Ishikawa, M. Jamei, J. C. Kalvass, S. Nagar, K. S. Pang, K. Korzekwa, P. W. Swaan, M. E. Taub, P. Zhao, and A. Galetin. 2013. 'ITC recommendations for transporter kinetic parameter estimation and translational modeling of transport-mediated PK and DDIs in humans', *Clin Pharmacol Ther*, 94: 64-79.

Zhang, L., M. J. Dresser, A. T. Gray, S. C. Yost, S. Terashita, and K. M. Giacomini. 1997. 'Cloning and functional expression of a human liver organic cation transporter', *Mol Pharmacol*, 51: 913-21.

Zheng, N., H. N. Tsai, X. Zhang, and G. R. Rosania. 2011. 'The subcellular distribution of small molecules: from pharmacokinetics to synthetic biology', *Mol Pharm*, 8: 1619-28.

Zhou, S. F., L. L. Wang, Y. M. Di, C. C. Xue, W. Duan, C. G. Li, and Y. Li. 2008. 'Substrates and inhibitors of human multidrug resistance associated proteins and the implications in drug development', *Curr Med Chem*, 15: 1981-2039.